

PRECISE  $^{82}\text{RB}$  INFUSION SYSTEM FOR CARDIAC PERFUSION MEASUREMENT  
USING 3D POSITRON EMISSION TOMOGRAPHY

by

Ran Klein B.A.Sc

A thesis submitted to the  
Faculty of Graduate and Postdoctoral Studies  
in partial fulfillment of the requirements for the degree of

**Master of Applied Science**

in Electrical and Computer Engineering

Ottawa-Carleton Institute for Electrical and Computer Engineering  
School of Information Technology and Engineering (Electrical & Computer Engineering)

Faculty of Engineering  
University of Ottawa

February, 2005

©2005, Ran Klein, Ottawa, Canada

## Credits

---

I wish to extend my gratitude to Robert deKemp and Andy Adler for guiding me through this project. Their mentoring, support, and friendship have made this a memorable experience.

## Abstract

---

**Introduction:** Quantitative myocardial perfusion measurements using positron emission tomography (PET) can be improved by introducing diagnostic tracers at a constant rate of activity.  $^{82}\text{Rb}$  can be produced cost effectively by eluting a  $^{82}\text{Sr}/^{82}\text{Rb}$  generator with saline; however, it exhibits an undesirable, but reproducible, activity rate variation. Previously, a threshold-comparison algorithm controlled saline flow through either generator or bypass line using an on/off valve, to simulate constant-activity elutions. **Methods:** In this work a mechanical system and control software is developed to control tracer infusion. The valve is cycled at 5Hz and its duty-cycle controlled by a predictive-corrective algorithm in order to reduce measurable activity rate fluctuations. **Results:** Precision increases (RMS error improves from >40% to ~14%) as does the range of relative activities that can be eluted from the generator. **Conclusion:** The proposed method demonstrates superior precision and flexibility. However, further tests must be conducted to ensure that the precision of the system does not deteriorate over time.

**Key Words:** Rubidium-82,  $^{82}\text{Sr}/^{82}\text{Rb}$  generator, cardiac, perfusion, positron emission tomography, PET, predictive control.

---

## Table of Contents

---

Credits .....	ii
Abstract .....	iii
Table of Contents.....	iv
Table of Figures.....	vi
Table of Tables.....	viii
List of Acronyms .....	ix
List of Variables .....	x
Introduction .....	1
Chapter 1: Introduction to Molecular Imaging and Dynamic PET.....	4
1.1 Positron Emission Tomography.....	4
1.2 $^{82}\text{Sr}/^{82}\text{Rb}$ Generator – a Cost-effective Tracer Source.....	7
Sr Breakthrough.....	9
1.3 $^{82}\text{Rb}$ Elution Profiles .....	10
1.4 Constant-Activity Elution for Quantitative Perfusion Measurement in the Left Ventricle of the Heart ..	11
1.5 Quantitative Perfusion Measurements Using $^{82}\text{Rb}$ .....	14
Chapter 2: The Second Generation $^{82}\text{Rb}$ Infuser – a starting point.....	16
2.1 The Daily Protocol and Elution Types .....	17
2.2 Hardware Description .....	19
2.3 Prototype Performance.....	25
2.4 Further Development of the $^{82}\text{Rb}$ Elution System (RbES).....	26
Chapter 3: System Design and Conceptual Understanding .....	28
3.1 Requirements.....	28
Functional Requirements.....	28
Non-Functional Requirements.....	29
Other Requirements.....	30
3.2 Initial Design Considerations .....	32
Safety.....	32
Process Monitoring.....	33
Hardware Modifications .....	34
Software packages.....	36
3.3 Flow Hardware Layout Justification .....	39
Pump Speed Variation.....	40
Bypass Ratio Control.....	41
3.4 Design of Physical Processes .....	43
Run sequence.....	44
Calibration .....	45
Breakthrough Activity Measurement.....	50
Elution Tests.....	52
3.5 Software Design .....	53
Pre-Run Stage and the GUI-Sequence.....	53
Post-Run Stage .....	55
Real-Time Sequence.....	56
Physical Sequence .....	58
3.6 Error Detection.....	64
Pressure Errors.....	66
Pump Communication and Operation Errors.....	66
Computer Resources.....	67
Positron Detector Errors .....	67

---

Dose Calibrator Communication Errors .....	67
Maintenance.....	67
Software Errors.....	68
Warnings.....	68
Outlier Highlighting .....	68
3.7 System Refinement .....	69
Dose Calibrator Spike Removal Algorithm.....	69
3.8 Summary .....	70
Chapter 4: Elution Profile Control.....	71
4.1 Threshold Comparison Algorithm with Auto-tuning Hysteresis Correction (HC-TC).....	73
4.2 Variable Flow Control.....	74
Cycling Valve Control.....	74
Transient State Control.....	74
Implementation of the Variable Flow Control.....	75
Valve Response Measurements .....	76
Modeling of Valve Response.....	79
PWM Valve Life Span.....	80
4.3 Variable Flow Control Algorithms.....	81
PID Control.....	82
Forgetful PID Controller.....	85
Predictive Control.....	85
Predictive Corrective Control.....	88
Initial Error Removal.....	89
Setting the Saline Flow Rate.....	90
Automatic Parameter Tuning.....	91
Summary.....	96
Chapter 5: Testing and Characterization.....	98
5.1 Safety Testing.....	98
The Worst Case Scenario.....	99
5.2 Test Cases.....	100
User Interface Testing.....	102
Functional Testing .....	102
Error Handling Testing.....	103
5.3 Testing in a Routine Clinical Setting.....	103
Computer Crash Issue.....	104
5.4 Calibration Characterization.....	106
Calibration Constant vs. Flow Rate .....	107
Summary of Calibration Analysis.....	109
5.5 Analysis of the Self-Tuning Model.....	110
Variation in Valve Model Parameters with Requested Elution Parameters.....	112
Analysis of Tuned Valve Response .....	114
5.6 Elution Tests.....	116
Range of Relative Activities as a Function of Elution Duration.....	120
5.7 Generator Life Span .....	121
Breakthrough Sr Activity.....	122
Activity Curves.....	123
5.8 Benefits of $^{82}\text{Rb}$ Constant-Activity Elutions .....	124
Comparison of $^{82}\text{Rb}$ and $^{13}\text{N}$ -ammonia for Measurement of Perfusion in 3D PET .....	124
Optimized Perfusion Measurements .....	126
5.9 Critical Analysis and Future work.....	127
Chapter 6: Conclusion .....	130
List of References.....	133
Appendix A: Test Cases .....	137

---

## Table of Figures

Figure 1-1 – Positron emission tomography.....	5
Figure 1-2 – <sup>82</sup> Rb uptake images for measurement of myocardial perfusion.....	6
Figure 1-3 – <sup>82</sup> Sr/ <sup>82</sup> Rb decay sequence.....	8
Figure 1-4 – <sup>82</sup> Rb activity during recharging of a generator.....	10
Figure 1-5 – Generator activity/volume curves with different flow rates and at different times.....	11
Figure 1-6 – Dynamic <sup>82</sup> Rb imaging of a canine heart.....	12
Figure 2-1 – Daily protocol flow chart.....	19
Figure 2-2 – Hardware component diagram of RbES.....	19
Figure 2-3 – Photograph of the assembled RbES and its components.....	24
Figure 2-4 – Photograph of top cover of the RbES.....	24
Figure 2-5 – Elution of 50% bolus activity within 30 s using a simple threshold comparison algorithm.....	25
Figure 3-1 – Electro-optic level switch operation.....	35
Figure 3-2 – Response of transport of activity through a fixed volume line at a fixed flow rate.....	40
Figure 3-3 – Flow control through generator using a bypass line maintains a constant flow rate through all other lines.....	41
Figure 3-4 – Flow control through the generator using a variable pinch valve on the generator line.....	42
Figure 3-5 – Flow control through the generator using a double sided pinch valve on the bypass line and generator line.....	43
Figure 3-6 – Schematic of the activity counter relating some of the factors that contribute to its efficiency measure.....	46
Figure 3-7 – Dose calibrator chamber measurement diagram.....	47
Figure 3-8 – Sample calibration run results.....	48
Figure 3-9 – Aperture response of the dose calibrator as a function of distance along the saline line from the vial.....	49
Figure 3-10 – Example of a constant-flow test run without (top) and with (bottom) a Gaussian aperture correction.....	50
Figure 3-11 – Opening message screen.....	53
Figure 3-12 – Various screenshots.....	54
Figure 3-13 – Sequence, data, and control, flow and structure diagram of software.....	56
Figure 3-14 – The Hardware_Interface model.....	57
Figure 3-15 – Flow Chart for all elution types.....	59
Figure 3-16 – Inputs to the Physical_Sequence M-file S-Function block.....	62
Figure 3-17 – Calibration results with and without the dose calibrator peak removal algorithm.....	70
Figure 4-1 – Elution of 50% bolus activity within 30 s using a simple threshold comparison algorithm.....	72
Figure 4-2 – Pulse-width-modulation control of a solenoid valve to simulate a variable pinch valve.....	74
Figure 4-3 – Activity vs. time curves as measured with the generator valve cycling at 15 Hz at various generator valve duty-cycles.....	76
Figure 4-4 – Valve response curves at $v_{\text{valve}} = 2, 5, 15, \text{ and } 100 \text{ Hz}$ .....	77
Figure 4-5 – Elutions at valve flow ratio $\approx 50\%$ produced by cycling the generator valve at 2, 5, and 15 Hz.....	78
Figure 4-6 – Valve response ( $v_{\text{valve}} = 5 \text{ Hz}$ ) with the swapped axes, allows to determine the duty-cycle needed to achieve a desired valve flow ratio.....	79
Figure 4-7 – Closed loop controlled system using a PID controller.....	83
Figure 4-8 – Affects of PID controller parameters on system response.....	83
Figure 4-9 – Sample simulation results of a PID controlled elution.....	84
Figure 4-10 – Modified PID correction implementing a “forgetful” proportional component.....	85
Figure 4-11 – Block diagram of the predictive-corrective control of a PWM valve.....	88
Figure 4-12 – Simulation of perfect control with erroneous activity concentration prediction due to a slight volume shift.....	89
Figure 4-13 – Analyzed errors of a constant-activity elution with flow ratios spanning a large range.....	93
Figure 4-14– Analyzed errors of a constant-activity elution with flow ratios only in the lower range.....	93
Figure 4-15 – Demonstration of an elution in which the entire bolus activity has been eluted.....	95
Figure 5-1 – Sample test case layout.....	102
Figure 5-2 – Calibration constant over the course of a generator life.....	106

---

Figure 5-3 – Correlation of calibration constant to generator activity.....	107
Figure 5-4 – Calculated calibration constant over the range of flow rates. ....	108
Figure 5-5 – Calibration constant dependence on flow rate in the case of a high flow resistant generator column. ....	109
Figure 5-6 – Progress of accelerated self-tuning of the valve response model over three successive elutions at 30% over 30 s.....	111
Figure 5-7 – Evolution of parameters G and L during self-tuning through repeated runs of 30% relative activity over 30 s.....	112
Figure 5-8 – Parameters G and L evolving during a 30% relative activity over 30 s training session. ....	112
Figure 5-9 – Example activity rate error measurements used for valve response model parameter tuning that could lead to conflicting adjustments based on how the data is treated.....	113
Figure 5-10 – Adaptation of parameter L over a repeated sequence of 50% relative activity over 30 s elutions revealed that the adaptation law is flawed.....	114
Figure 5-11 – Valve response correction curve used to determine the PWM duty-cycle required to achieve a desired valve flow ratio.....	115
Figure 5-12 – Comparison of performance measures of elutions [n=10] over 30 s at 10, 30, 50, and 70% relative activity. ....	118
Figure 5-13 – Activity rate at patient outlet calculated based on the activity counter readings and dose calibrator readings. ....	119
Figure 5-14 – Range of relative activities that can be achieved using the HC-TC method and the PCC-PWM method without significantly influencing the precision. ....	121
Figure 5-15 – Breakthrough ratio progression over time.....	122
Figure 5-16 – Normalized activity rate vs. time curves measured during calibration runs over the life span of a generator.....	123
Figure 5-17 – Example of <sup>82</sup> Rb and <sup>13</sup> N-ammonia blood curves.....	126

---

## Table of Tables

---

Table 1-1 – Commonly Used Positron-Emitting Isotopes [1] .....	6
Table 2-1 – Minimum PC Requirements .....	20
Table 3-1 - Software Environment .....	38
Table 3-2 – Elution parameter values for each run type. ....	60
Table 3-3 – <i>Physical_Sequence</i> states and their termination conditions. As long as a termination condition is not met, the state is maintained unchanged.....	63
Table 3-4 - Detectable errors and their corresponding flags.....	65
Table 4-1 - Comparison of elution time accuracy using the threshold comparison algorithm with (HC-TC) and without hysteresis correction. ....	74
Table 4-2 - Parameters used by the prediction algorithm. ....	92
Table 5-1 – Canadian Standards Association (CSA) field evaluation for electro-medical equipment results for two RbES systems.....	99
Table 5-2 - Test classification codes and their descriptions. ....	101
Table 5-3 - List of global structures and their contents. ....	105
Table 5-4 – Typical constant-activity elution profiles for various relative activities and over 30 s. ....	117
Table 5-5 - Comparison of Performance measures for HC-TC and PCC-PWM 30 s Elutions [n=10].....	118
Table 5-6 - Dynamic scan time frame durations for <sup>82</sup> Rb and <sup>13</sup> N-ammonia perfusion measurements. ....	125
Table 5-7 – Rest study results comparing perfusion measurements in a dog at varied <sup>82</sup> Rb constant- activity elution time durations and activities show that similar results are obtained regardless of these elution parameters.....	127

## List of Acronyms

---

DAQ	Data Acquisition Card
DLL	Dynamically Linked Library
FDG	Fluorodeoxyglucose
FOV	Field of View
GUI	Graphical User Interface
HL	Half Life
K	Potassium
Kr	Krypton
LCD	Liquid Crystal Display
LOR	Line of Response
MSE	Mean Squared Error
MRI	Magnetic Resonance Imaging
NI	National Instruments
PET	Positron Emission Tomography
PID	Proportional Integral Derivative
PWM	Pulse Width Modulation
QA	Quality Assurance
Rb	Rubidium
Sr	Strontium
UPS	Uninterruptible Power Supply
UOHI	University of Ottawa Heart Institute

---

## List of Variables

---

$a(d)$	Dose calibrator aperture response
$A_{^{82}\text{Rb}}, A_{^{82}\text{Sr}}, A_{^{85}\text{Sr}}$	Activity of delivered $^{82}\text{Rb}$ , $^{82}\text{Sr}$ , $^{85}\text{Sr}$ (MBq)
$A_{\text{Cal}}$	Activity eluted during calibration run (MBq)
$\hat{A}_{\text{Breakthrough}}$	Activity measured at dose calibrator for breakthrough calculation (MBq)
$\hat{A}_{\text{P}}(t)$	Measured activity at point P at time t (MBq)
$A_{\text{P}}(t)$	Activity at point P at time t (MBq)
$A_{\text{Req}}$	Requested activity (MBq)
$\dot{A}_{\text{P}}$	Desired activity rate at point P (MBq/s)
$\dot{A}_{\text{C}}$	Desired activity rate at activity counter (also referred to as the set point) (MBq/s)
$\hat{A}_{\text{C}}(t)$	Measured activity rate at activity counter (MBq/s)
$\tilde{A}_{\text{C}}(t)$	Activity rate error at activity counter (MBq/s)
$C_{\text{C}}(v)$	Activity concentration vs. eluted volume curve measured at calibration (MBq/ml)
$\hat{C}_{\text{M-}}$	Measured activity concentration just prior to the merger (MBq/ml)
$C_{\text{M-}}$	Predicted activity concentration just prior to the merger (MBq/ml)
$\hat{N}_{\text{Det}}(t)$	Measured raw count rate at the activity counter (detector) (cps)
$n_{\text{Low}}, n_{\text{High}}$	Counts for low, high output of the square wave generator
$D_{\text{PQ}}$	Decay during transport between points P and Q (unitless)
$f$	Flow rate (ml/min)
$F$	Sigmoid factor for valve response model
$G$	Sigmoid horizontal factor for valve response model
$H$	Hysteresis of the generator valve
$k$	Activity counter intrinsic efficiency (cps/Bq)
$K$	Activity counter calibration constant ( $10^{-6}\text{cps/ml}\cdot\text{Bq}$ )
$K_{\text{A}}$	Average activity counter calibration constant ( $10^{-6}\text{cps/ml}\cdot\text{Bq}$ )
$L$	Linear slope of valve response model
$O$	Constant offset of valve response model
$p$	Count rate set point (counts/s)
$r(t), \hat{r}(t)$	Desired, measured flow ratio at time t
$r_t$	Threshold desire flow ratio at which $d\Pi/dr=2\cdot L$
$\Pi(t)$	Valve duty-cycle (ratio) at time t
$\Pi_{\text{min}}, \Pi_{\text{max}}$	Valve lower and upper bounds of duty-cycle
$s(t)$	Ratio of $^{85}\text{Sr}$ to $^{82}\text{Sr}$ isotopes at time t since manufacturer measurements, $s_0$
$\hat{T}_{\text{corr}}$	Measured time shift correction of dose calibrator curve (s)
$T_{\text{PQ}}$	Transport delay between points P and Q (s)
$T_{\text{Req}}$	Requested Elution Time (s)
$\hat{T}_{\text{Elution}}$	Measured Elution Time (s)
$T_{\text{ierm}}$	Time delay of initial error removal mechanism (IERM) (s)
$V_{\text{PQ}}$	Volume of lines between points P and Q (ml)
$\hat{V}_{\text{Corr}}$	Measured correction to eluted volume (ml)
$\gamma_{\text{H}}$	Hysteresis learning factor
$\gamma_{\text{R}}$	Valve response upper limit learning factor
$\gamma_{\text{L}}$	Valve response linear slope learning factor
$\gamma_{\text{S}}$	Valve response sigmoid scaling learning factor
$\alpha$	Dose calibrator aperture response time constant ( $1/\text{ml}^2$ )
$\lambda$	Decay constant (1/s) 0.0091 for $^{82}\text{Rb}$
$\phi$	Forgetting factor in modified PID controller
$u_{\text{valve}}$	Valve cycling frequency (Hz)
$u_{\text{clk}}$	Counter clock frequency (Hz)
$\Delta\zeta$	Range of correction during saturation

---

## Introduction

---

This work describes the development of a Rubidium-82 ( $^{82}\text{Rb}$ ) infusion system for use in positron emission tomography (PET). The system is based on a  $^{82}\text{Sr}/^{82}\text{Rb}$  generator, which produces  $^{82}\text{Rb}$  activity continuously. The system is aimed at administering the activity to patients in a precise and controlled manner.

$^{82}\text{Rb}$  is used as a PET tracer for measurement of myocardial perfusion (blood flow) in a non-invasive manner. Conventionally,  $^{82}\text{Rb}$  perfusion imaging has allowed measurement only of the relative perfusion, with healthy regions of the myocardium serving as the standard to which reduced perfusion can be compared. However, in cases of globally reduced perfusion, no healthy standard is available, which may lead to misdiagnosis. Quantitative perfusion measurements aim to solve this problem. It is believed that in order to improve their robustness, the  $^{82}\text{Rb}$  activity should be introduced at a constant rate of activity. The goal of this project is to develop a system that is capable of eluting  $^{82}\text{Rb}$  at a constant rate of activity from a  $^{82}\text{Sr}/^{82}\text{Rb}$  generator for use in a clinical and experimental setting.

The first chapter begins by introducing PET and its applications. In particular the chapter focuses on perfusion measurements in the left ventricle heart muscle. The focus then shifts to perfusion tracers and how they are produced. Once the need for  $^{82}\text{Rb}$  is justified, the functioning, history, and application of  $^{82}\text{Sr}/^{82}\text{Rb}$  generators are described.

The second chapter introduces the second generation  $^{82}\text{Rb}$  elution system (RbES), built as part of this thesis work, following an overview of the literature with regards to similar systems. This overview clarifies the work to date and the incremental contribution of the RbES. The main topic in this chapter is a description of the RbES prototype, which served as a starting point for this project. Final notes discuss the performance of the prototype system, and issues that needed to be addressed in order to complete its development.

The subsequent chapters discuss the contributions of this thesis. Initially, the system requirements are identified (chapter 3) as well as guidelines for the development process. A discussion of the system model follows in order to justify the layout of the elution hardware that is inherited from the RbES prototype system.

This chapter continues by describing the incremental development of the RbES. Some hardware modifications for improvement of the usability and safety of the system are discussed, but the main focus is on the new software. This includes all aspects of the software with exception of the activity rate control system, which is left for chapter 4. Special attention is given to the physical sequence that constitutes a complete elution sequence.

The fourth chapter focuses on the single topic of improving the precision of constant activity rate elutions. The use of an on/off valve as opposed to a variable flow valve is justified. The justification is partially through the ability to simulate variable flow by cycling the valve between its two states at a constant rate and modulating the duty-cycle (pulse width modulation). This leads to modelling of the valve response and developing a control algorithm.

A combination of varying activity concentrations from the  $^{82}\text{Sr}/^{82}\text{Rb}$  generator, long transport delays, and short elution times render non model based control systems inadequate. This problem is resolved using predictive-corrective control; a prediction algorithm is developed to compute the activity concentration from the generator based on the volume eluted through it. This is made possible by the good reproducibility of the activity concentration vs. volume curve from the generator which is measured using a daily calibration run. The eluted volume and any transport delays can also be computed with sufficient accuracy, making prediction of the valve control possible. A corrective mechanism driven by a conventional feedback loop is also included. The resulting control algorithm is referred to as a predictive-corrective control of a pulse width modulated valve (PCC-PWM).

Chapter five attends to two topics: testing of the complete RbES as a final product and comparing PCC-PWM performance with a simple threshold comparison (TC) control algorithm included in the prototype system. Testing of the system demonstrates that the system is matured for clinical and experimental use. Comparison of the two control algorithms indicates that PCC-PWM is better for precision elution of  $^{82}\text{Rb}$  activity at a constant rate. As a result of the comparison studied in the chapter, the system performance is well characterized.

The final chapter draws conclusions from this project. These conclusions are related to the achievements as well as to the limitations of the design. Future work is suggested in order to overcome these limitations or achieve incremental results.

This work has resulted in the following publications:

- R. Klein, A. Adler, R. S. Beanlands, R. A. deKemp, “Precision Control of Eluted Activity from a  $^{82}\text{Sr}/^{82}\text{Rb}$  Generator for Cardiac Positron Emission Tomography”, Proceedings of the IEEE EMBS 26<sup>th</sup> Annual International Conference, 2004, Vol 1, pp. 1393-96.
- R. Klein, N. Epstein, A. Benelfassi, R.S. Beanlands, R.A. deKemp, “A Rubidium-82 Infusion System for Quantitative Perfusion Imaging with 3D PET”, Proceedings of the 3<sup>rd</sup> Annual Imaging Network Ontario Symposium, pp. 98, 2004.
- R. Klein, R.A. deKemp, N. Epstein, “RBES – Rb82 Elution System”, Copyright 1016208, Unpublished, November 14, 2003.

## **Chapter 1: Introduction to Molecular Imaging and Dynamic PET**

With the ability to image the physiological distribution of specific molecules within the body in a non-invasive manner, nuclear medicine imaging has become a leading diagnostic tool. A compound labelled with a radioactive isotope is introduced to the patient, usually by injection, and its location in the body is later imaged using a scanner sensitive to the emitted radiation. The compounds, referred to as radiolabelled tracers, are designed to interact within the patient so that they collect in a region of interest by participating in a biochemical process of interest. Over time, the radioactive label in the tracer decays resulting in emission of radiation.

Given a closed system containing radioactive material, an exponential decrease of activity is observed as time progresses. The rate of decay is a characteristic property of the radioactive isotope, and is measured as a statistical average of the time that passes until half the original activity remains. This measure is referred to as one half-life,  $T_{1/2}$ , and can vary from split seconds to countless years depending on the isotope. In molecular imaging, one would like to use an isotope that lasts long enough to perform the measurement, but short enough to minimize exposure to the patient. A short half-life also carries the benefit of reducing the time between repeated scans of the same subject. Typical imaging applications use isotopes with a half-life ranging from several seconds to several hours.

When imaging the patient, objects containing a high concentration of the tracer radiate strongly, contrasting with the surroundings. A scanner that measures the radiation from the patient can reconstruct tomographic images through the region of interest. The concentration of activity is dependent on the interaction of the tracer within the body and is therefore indicative of a corresponding biochemical and physiological processes within the body, in contrast to anatomical images produced by modalities such as conventional x-ray computed tomography (CT) and magnetic resonance imaging (MRI).

### **1.1 Positron Emission Tomography**

Positron Emission Tomography (PET) is the leading nuclear imaging modality in terms of precision and ability to make quantitative measurements. The radioactive label is an isotope that decays by positron emission. In the nucleus, a proton is converted into a neutron

and excess positive charge is ejected in the form of a positron (positively charged electron). The positron travels a few mm through the surrounding medium and eventually interacts with an electron resulting in a mutual annihilation. The combined mass of the electron and positron is converted into two equal energy (511keV) collinear photons. These high energy photons travel through the body and can be detected by dense scintillating crystals coupled to photomultiplier tubes.

A typical PET scanner consists of planar rings of detectors. Since the two photons formed during a decay are created at the same time and travel in opposite directions at the speed of light, they should be detected almost simultaneously (i.e. coincidence) by detectors on opposite sides of the event. If two coincident photons are detected by the scanner it can be assumed that the decay occurred along the line of response (LOR) connecting the two detectors. These collected coincidence counts can be processed through various mathematical algorithms, such as filtered back projection, to reconstruct a tomographic image of the scanner field of view (FOV) as shown below.

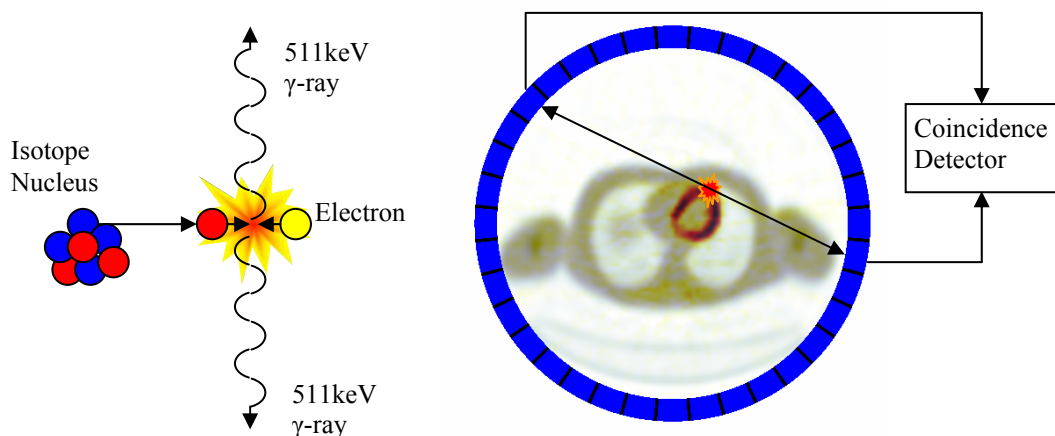


**Figure 1-1 - Positron emission tomography.** The positron discharge followed by annihilation with an electron producing two collinear photons ( $\gamma$ -rays) on the left. The projected line of response based on a detection of coincident events by the scanner is shown on the right. The image is a cross-section of the chest with red depicting tracer uptake in the heart muscle. A transmission image is fused in gray, showing the lungs and arms for anatomical reference.

PET tracers must be labelled with a positron-emitting isotope. A major advantage of PET over other molecular imaging modalities is that oxygen, carbon, and nitrogen, which are common building blocks in organic chemistry, have positron-emitting isotopes with practical half-lives (Table 1-1). These isotopes give the potential to synthesize almost any organic compound as a PET tracer.

Various tracers have been developed to image different organs and tissue. Increased glucose consumption, for example, is used for detection of cancerous tumours [2,3,4] and distinguishing between hibernating (live) and necrotic (dead) tissue in the heart using <sup>18</sup>Fluorodeoxyglucose (FDG) [5,6,7]. In neuroscience FDG has been used to locate hypoactive and hyperactive regions in the brain to diagnose disease such as epilepsy [8,9]. Another application used PET imaging to assess the integrity of the blood brain barrier [10] using <sup>82</sup>Rb as a tracer.

**Table 1-1 – Commonly Used Positron-Emitting Isotopes [1]**

Isotope		Half Life (T <sub>1/2</sub> ) [min]	Mean distance to annihilation [mm]
Cyclotron Produced	<sup>15</sup> O (oxygen-15)	2.1	1.1
	<sup>13</sup> N (nitrogen-13)	10.0	0.72
	<sup>11</sup> C (carbon-11)	20.3	0.56
	<sup>18</sup> F (fluorine-18)	110	0.35
Generator Produced	<sup>82</sup> Rb (rubidium-82)	1.27	2.4
	<sup>68</sup> Ga (gallium-62)	67.8	1.1

Blood flow (perfusion) studies are of interest in cardiac medicine as they can indicate vascular stenosis; a clogging of the arteries due to plaque build-up that restricts the flow of blood. Perfusion measurement can be achieved by introducing a cationic tracer that is similar (analogous) to potassium, K. All living cells have mechanisms that extract potassium through the cell membrane referred to as ionic pumps. If a potassium analogue is injected to a patient, the tracer will be taken up by the heart muscle cells, while the activity level in the blood reduces over time. Several minutes later the PET image shows retained activity in the heart contrasting with the low activity of the blood (as demonstrated in tomographic images in Figure 1-2).

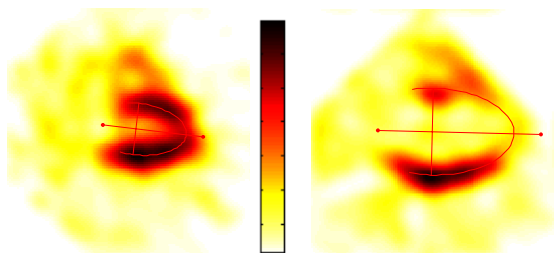


**Figure 1-2 - Sample <sup>82</sup>Rb uptake images used to measure perfusion in the myocardium. A normal heart is shown on the left depicting the elliptic shape characteristic of a long axis cross section. The image on the right reveals reduced blood flow to the septal wall and apex of the left ventricle, shown by a relatively lower concentration of activity along the upper right region of the partial ellipse.**

Although FDG scans for detection of tumours are by far the most popular application of PET today, potential applications are only limited by the available tracers. As research into the field progresses PET promises powerful new tools both for research and clinical diagnostics.

## 1.2 $^{82}\text{Sr}/^{82}\text{Rb}$ Generator – a Cost-effective Tracer Source

The half-life of the radioactive isotope dictates how much time can pass between production and scanning. After six half-lives we tend to treat the tracer as completely decayed as only 1.6% of the original activity remains. As a result, the proximity of the scanning facility to the tracer production facility is limited. If the tracer is sufficiently long lived it can be transported between facilities, however if the tracer half-life is less than several hours the tracer must be produced on-site.

Many of the PET isotopes are created using a cyclotron. This highly specialized and expensive piece of equipment accelerates protons for bombardment of a specific target. The nuclear interactions during the bombardment can form desired isotopes. In many cases these isotopes are then passed on for synthesizing the tracer molecule through a series of chemical processes. Due to the complexity and expenses involved in operation of a cyclotron, much research has focused on finding simpler and more cost effective alternatives for PET tracer production. This would be especially useful in regions of low population density (common in a country like Canada) where the cost of a cyclotron cannot be supported.

Rubidium-82 ( $^{82}\text{Rb}$ ) has been identified as a suitable tracer for perfusion measurements and can be readily produced using a  $^{82}\text{Sr}/^{82}\text{Rb}$  generator (described below). As a 1<sup>st</sup> column element in the periodic table, Rubidium is a reactive cation, which is physiologically similar to potassium (K) [11]. Potassium (and rubidium) exhibits avid uptake in certain tissues in the human body such as the myocardium. When  $^{82}\text{Rb}$  decays by positron emission it is transformed into stable Krypton ( $^{82}\text{Kr}$ ) which is a noble element and is therefore non-reactive and non-harmful (Figure 1-3). When a patient is at rest approximately 50% of the  $^{82}\text{Rb}$  is taken up from arterial blood into myocardial tissues over the course of a single blood cycle through the tissue. Observation of  $^{82}\text{Rb}$  uptake enables the assessment of myocardial perfusion. In 1989 the United States Food and Drug Administration (FDA) approved the use of rubidium-82 chloride ( $^{82}\text{RbCl}$ ) from a  $^{82}\text{Sr}/^{82}\text{Rb}$  generator system developed by Squibb Diagnostics for clinical use [12,13].

The relatively short half-life of  $^{82}\text{Rb}$  (76 seconds) is both an advantage and a disadvantage. The fast decay means a short exposure time for the patient, which thus minimizes the health risks involved with radiation exposure. In addition repeated scans can be carried out after only 10 minutes as almost no radiation remains from the previous dose.

On the other hand, the fast decay shortens the maximum scan time and thus reduces the quality of the scans. An added difficulty is that the  $^{82}\text{Rb}$  must be produced on site and directly infused into the patient [14].

$^{82}\text{Rb}$  is the product of  $^{82}\text{Sr}$  decay. In this context  $^{82}\text{Sr}$  is referred to as the parent isotope, while  $^{82}\text{Rb}$  is referred to as the daughter isotope. For this application, it implies that a batch of  $^{82}\text{Sr}$  can be used to continuously generate  $^{82}\text{Rb}$  activity. As  $^{82}\text{Rb}$  decays into stable  $^{82}\text{Kr}$  the decay process ends as is demonstrated by Figure 1-3.

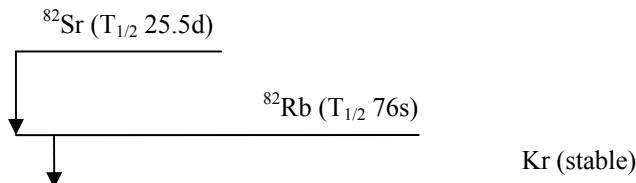


**Figure 1-3 –  $^{82}\text{Sr}/^{82}\text{Rb}$  decay sequence. Half-lives are in parentheses.**

$^{82}\text{Sr}$  is produced using large cyclotrons, capable of creating high energy protons ( $\sim 80\text{MeV}$ ), for beaming on metallic Rb or RbCl solutions [14]. Only a few specialized organizations, such as the Los Alamos Research Labs and the TRIUMF cyclotron operated by MDS Nordion, are capable of producing  $^{82}\text{Sr}$ . However, high yields and the long half-life of  $^{82}\text{Sr}$  makes the production manageable and cost-effective. As a side product  $^{85}\text{Sr}$  ( $T_{1/2}=64.8$  days) is also produced, but is not beneficial for  $^{82}\text{Rb}$  production and is difficult to separate from  $^{82}\text{Sr}$ . The manufacturer includes a measure of the ratio of  $^{85}\text{Sr}$  to  $^{82}\text{Sr}$  (typically  $\sim 1:1$  ratio) with each production.

$^{82}\text{Rb}$  can be supplied using a  $^{82}\text{Sr}/^{82}\text{Rb}$  generator at a relatively low cost, as there is no need for an onsite cyclotron. The generator consists of a tin-oxide ( $\text{SnO}_2$ ) ion-separation column which strongly binds Sr isotopes. The generator must be loaded roughly every two months with Strontium-82 ( $^{82}\text{Sr}$ ), which has a half-life of 25.5 days [15]. As the  $^{82}\text{Sr}$  decays to  $^{82}\text{Rb}$ , its chemical properties change due to the shift from a column-two element to a column-one element on the periodic table. Rb binds to the tin-oxide column much more weakly than Sr. When the column is flushed with a solution, such as 0.9% NaCl saline, the Rb is displaced by Na (sodium) and the  $^{82}\text{Rb}$  is eluted in the form of  $^{82}\text{RbCl}$  (eluate). For this reason the generator is referred to as an ion-exchange column.

Various vendors [Bracco, 2004, formerly Squibb] and research teams have manufactured  $^{82}\text{Sr}/^{82}\text{Rb}$  generators that are all similar in design. A shielding casing made of depleted uranium [TRIUMF, 1993], lead [Bracco, 2004], or tungsten is used to absorb

radiation produced by decay in the generator, thus reducing exposure to patients and personnel.

During loading,  $^{82}\text{Sr}$  (and  $^{85}\text{Sr}$  impurity) is pumped into the column through the input line, resulting in binding of most of the Sr within the first few mm of the tin-oxide column. After numerous quality assurance tests of the eluate for pyrogens, sterility, and metal breakthrough, the generator can be used clinically. In addition, these runs ensure that the  $^{82}\text{Rb}$  yield is sufficiently high.

Once the  $^{82}\text{Sr}$  decays to levels that cannot yield sufficient amounts of  $^{82}\text{Rb}$ , the generator must be reloaded or replaced. A typical life span of a generator is 1-2 months, and is primarily determined by the amount of  $^{82}\text{Sr}$  that was loaded and the  $^{82}\text{Rb}$  activity required for imaging. The activity is often measured compared to the generator production capability. If a complete generator flush will yield 2000 MBq and an injected activity of 500 MBq is desired, one would refer to 25% relative activity. Over time the relative activity needed for imaging will increase as the generator decays and the administered activity remains constant.

### *Sr Breakthrough*

As saline is flushed through the generator, some Sr detaches from the column and appears in the eluate. For this reason the column is made sufficiently long (~2cm) to bind any loose Sr [16]. Over time, migration of Sr occurs along the column.  $^{82}\text{Sr}$  and  $^{85}\text{Sr}$  “breakthrough” can result if the generator is used indefinitely. In high quantities these compounds may have ill effects on health, as Sr is absorbed in bone which surrounds the bone marrow. As cells in the bone marrow are continuously dividing to produce red blood cells, the marrow is susceptible to genetic mutation due to radiation. In severe cases this could lead to increased risk of cancer.

Although no action can be taken to reduce breakthrough once it has started, Sr levels can be monitored in the eluate. Since the half-lives of both  $^{82}\text{Sr}$  and  $^{85}\text{Sr}$  are much longer than that of  $^{82}\text{Rb}$ , a measurement of the activity of a flushed solution after sufficiently long time should yield the quantity of Sr eluted. Health Canada guidelines dictate that  $^{82}\text{Sr}$  and  $^{85}\text{Sr}$  breakthrough not exceed 20 Bq/MBq and 200 Bq/MBq respectively of the eluted  $^{82}\text{Rb}$  activity. In order to take breakthrough measurements, one should ensure that sufficient time passes for the  $^{82}\text{Rb}$  in the sample to decay below the regulation limits - approximately 20

minutes. If after 20 minutes the remaining activity is greater than the designated limit, this is an indication of excessive Sr breakthrough and elution to patients should be avoided.

### 1.3 <sup>82</sup>Rb Elution Profiles

The generator continuously produces <sup>82</sup>Rb isotopes. If saline is not flushed through the generator “recharging” occurs, as the <sup>82</sup>Sr continues to decay and the concentration of <sup>82</sup>Rb in the generator volume increases. The total <sup>82</sup>Rb activity stabilizes within approximately 10 minutes as parent-daughter equilibrium is reached as a function of <sup>82</sup>Sr and <sup>82</sup>Rb decay rates (Figure 1-4). The level of equilibrium is dependent on the amount of <sup>82</sup>Sr activity in the column.

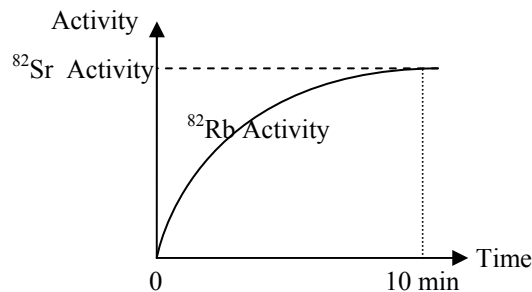


**Figure 1-4 – <sup>82</sup>Rb activity during recharging of a generator. An asymptotic rise is observed up to the level of <sup>82</sup>Sr activity.**

If saline is pumped through the generator the amount of <sup>82</sup>Rb inside the generator decreases to a new asymptote as the effect of the flushing takes its role in the equilibrium. The <sup>82</sup>Sr decay is the contributing factor, while the <sup>82</sup>Rb decay and the flushing are the reducing factors of the overall amount of <sup>82</sup>Rb of in the column.

Previous research [17,18] successfully modeled the eluted activity during constant flow rate flushing of the generator using variations of (1). The parameters  $C_1$ ,  $C_2$ ,  $C_3$  [MBq],  $R_1$ , and  $R_2$  [1/ml] are determined by fitting to empirical data. The parameter  $f$  represents the flow rate [ml/min] of the flush and  $t$  is the time since the flush start.

$$A(t) = C_1 + C_2 \exp(R_1 \cdot f \cdot t) + C_3 \exp(R_2 \cdot f \cdot t) \quad (1)$$

The curve has a characteristic peak that is reached as the <sup>82</sup>Rb from the column volume is flushed, referred to as the bolus stage. As time progresses, the activity decays to a lower asymptote as equilibrium with the saline flow is reached [19]. This is referred to as the continuous stage. The activity vs. volume curve is nearly independent of flow rate at the bolus stage [18] and the peak activity is proportional to the amount of <sup>82</sup>Sr attached to the

column. The asymptote magnitude relative to the peak activity is dependent on the saline flow rate alone.

Figure 1-5 demonstrates activity concentration (MBq/ml) curves at various constant flow rates through the generator measured ten days apart [20]. The activity was measured on the generator output line using a positron counter while the flow rate was kept constant using a peristaltic pump (Harvard Apparatus). The later curve (April 2, 2001) has a lower overall magnitude than that of March 23, 2001 due to the decay of the  $^{82}\text{Sr}$ ; however the general curve shapes are identical. The continuous stage asymptote is higher for the low flow rates (10 ml/min). Although one might expect an initial step to maximum activity, the initial rise is a result of  $^{82}\text{Rb}$  diffusion in the saline solution and the spatial response of the activity counter.

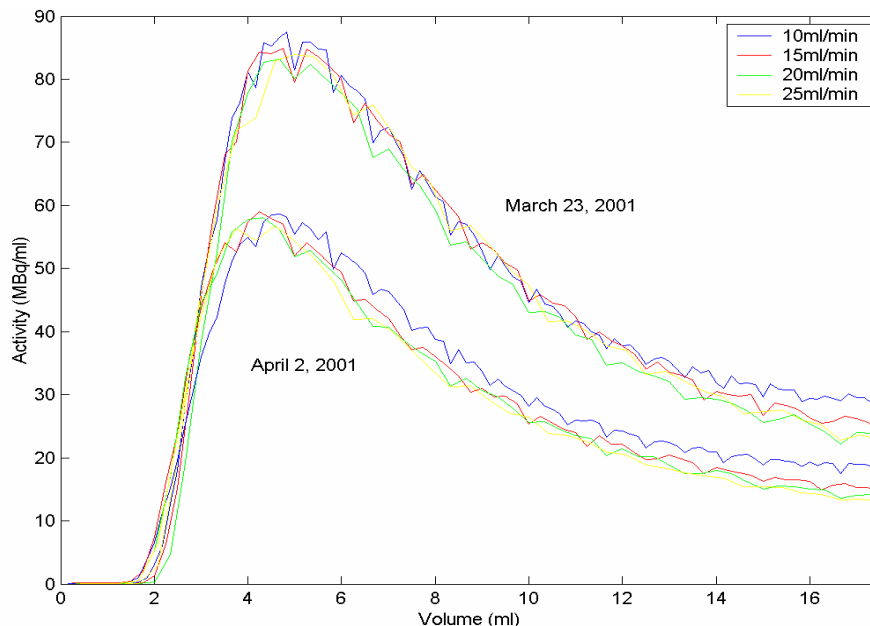


**Figure 1-5 - Representative generator activity/volume curves with different flow rates at different times [20] (from reference).**

#### **1.4 Constant-Activity Elution for Quantitative Perfusion Measurement in the Left Ventricle of the Heart**

Diagnosis of cardiac patients and optimization of their treatment is highly dependent on the measurement of perfusion in the left ventricle (LV) heart muscle. As demonstrated in Figure 1-2 the uptake images of a potassium analogue radioisotope can be used to assess perfusion. However, these images only indicate the relative perfusion with the region of highest uptake serving as the baseline to which all other regions are compared. The baseline

is assumed to be a region with normal (healthy) perfusion. Therefore a uniform uptake image is interpreted as a healthy subject.

In some cases, such as diabetes or multi-vessel coronary artery disease, the uptake may be reduced throughout the entire LV, thus resulting in uniform images. These cases can be misdiagnosed as healthy when in fact they experience a global reduction in perfusion [21]. To address this issue the need for quantitative perfusion measurements has arisen.

By dividing the imaging time into frames, one can image the tracer distribution as a function of time. This is referred to as dynamic imaging and enables to measure the rates at which a process of interest develops. In the case of quantitative perfusion measurement, dynamic images can be used to capture the rate of tracer uptake from the blood into the myocardium. A tracer kinetic model is fit to this uptake rate in order to estimate perfusion in absolute units (ml/min/g) [22].

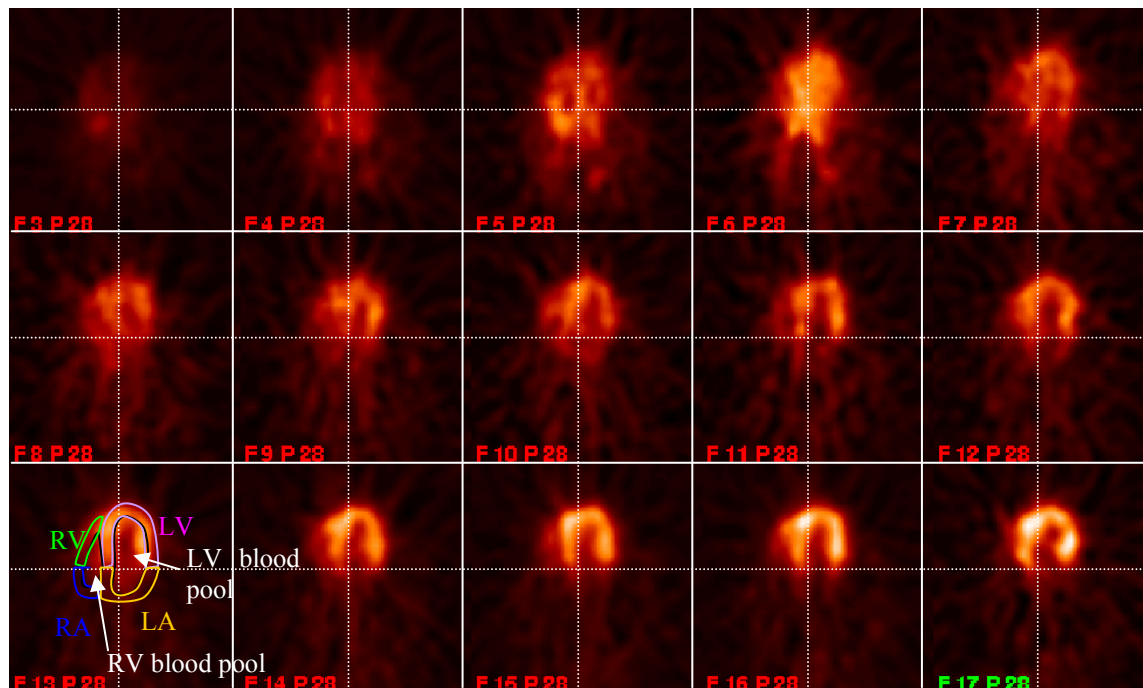


Figure 1-6 - Series of dynamic  $^{82}\text{Rb}$  images of a dog heart. Just after injection  $^{82}\text{Rb}$  is in the RV blood pool (F3,F4). Subsequent images show the LV (F4,F5) and the LV blood pool (F5,F6), dispersion through the body (F7-F11), and the resulting retention in the heart muscle (F12-F17) with most of the activity in the LV (horseshoe shape).

To demonstrate this idea, a study on a dog performed at the University of Ottawa Heart Institute (UOHI) using a  $^{82}\text{Rb}$  dynamic PET scan is shown in Figure 1-6. A series of sequential images (non-uniform time frames) shows the tracer entering the right-ventricle

blood pool (RV) (F3). The activity is then carried through the right atrium to the lungs and back to the left ventricle (LV). The LV blood pool is visible in the next frame (F6) followed by dispersion in the body and myocardial uptake and clearing of the blood pool (F7-10). Once much of the activity has been removed from the blood pool the retained activity is left visible in the LV heart muscle (P12-17). Relative perfusion non-uniformities can be easily visualized from retention images (P14-17), however in cases of diabetes and multi-vessel disease the entire region can exhibit decreased flow, which could lead to false diagnosis that perfusion is normal.

In order to achieve quantitative measurements, one must first know how much activity was introduced to the patient during the injection [20,23,24,25] and its distribution over time. The quantitative measurements that are provided by dynamic PET can be used to determine the absolute perfusion. This process is equivalent to determining a system response based on a known input function (controlled elution profile) and a measured output function (dynamic PET images). The ability to measure perfusion quantitatively implies improved diagnostic ability over other modalities [26].

The ideal tracer would be a positron-emitting isotope that is freely diffused and completely retained and with a practical half life – however none exists. <sup>13</sup>N labelled ( $T_{1/2} = 10$  min) ammonia ( $\text{NH}_3$ ) has been used as the clinical standard for quantification of myocardial perfusion, while <sup>82</sup>Rb has been recognized as a cost-effective alternative. <sup>13</sup>N-ammonia is produced using a cyclotron and is then administered using a syringe pump over a fixed interval (e.g. 30 seconds). This procedure results in a rectangular elution profile, which is well matched with PET technology [27]. The detectors on the scanner experience a significant dead-time after detection of an event. If the activity in the FOV is too high, many counts could be lost resulting in a saturation of the measurements, or even a reduction in the number of detected counts. The technologists, who administer the tracer and operate the scanner, try to maximize the activity while avoiding saturation of the detectors. To facilitate this optimization we would like to spread the activity evenly throughout the elution time, which is ideally a rectangular elution profile [18,28]. The short-coming of <sup>82</sup>Rb is that constant flow elutions (as shown in Figure 1-5) are not rectangular and therefore not ideally suited for quantitative perfusion measurement.

### **1.5 Quantitative Perfusion Measurements Using $^{82}\text{Rb}$**

Two alternative tracers for quantitative cardiac perfusion measurement in PET have been discussed;  $^{13}\text{N}$ -ammonia, which is widely accepted, and  $^{82}\text{Rb}$  as a potential substitute. The disadvantage of  $^{13}\text{N}$ -ammonia is that it must be produced using an on-site cyclotron and chemistry lab. Since it is introduced to the patient using a syringe pump, a rectangular activity vs. time profile is created during injection.  $^{82}\text{Rb}$  which can easily be obtained using a  $^{82}\text{Sr}/^{82}\text{Rb}$  generator is cheaper to produce than ammonia, but has a characteristic activity vs. volume profile that is not optimized for PET in general and quantitative perfusion measurement in particular.

To achieve the benefits of both tracers we would like to produce an elution system that can control the flow through the  $^{82}\text{Sr}/^{82}\text{Rb}$  generator to achieve a rectangular activity vs. time profile during injection to the patient. It is expected that if this is achieved, perfusion measurements using both  $^{13}\text{N}$ -ammonia and constant-activity  $^{82}\text{Rb}$  elutions could yield similar results. Constant-activity  $^{82}\text{Rb}$ , however, would serve as a cheaper solution to centers that do not have access to an on-site cyclotron.

It follows that once constant-activity  $^{82}\text{Rb}$  elutions are achieved, a comparison study of perfusion measurements with  $^{82}\text{Rb}$  and  $^{13}\text{N}$ -ammonia would precede clinical use. Constant-activity  $^{82}\text{Rb}$  elutions will serve the immediate need for such a study. It is also anticipated that constant-activity elutions are vital to achieving a reproducible quantitative perfusion measurements in a clinical setting [25]. The  $^{82}\text{Rb}$  elution system must therefore be designed to meet the strict requirements for routine clinical use.

The goal of using a  $^{82}\text{Rb}$  elution system in routine clinical PET work dictates an emphasis on accuracy, robustness, minimal maintenance, and operational simplicity. These criteria are set by the nature of a system that interacts directly with human patients and is operated by technologists that must perform multiple tasks in a timely fashion. Since this system is most suitable for centers that do not have access to a cyclotron, robustness is of utmost importance to ensure that the center is continuously productive.

In the United States, mobile PET units have been providing services to rural areas. Since a cyclotron cannot be mounted on a truck, these services have been limited to tracers with sufficiently long half-lives to be transported. This not only limits the types of diagnosis

that can be obtained, but also significantly increases the costs of operation.  $^{13}\text{N}$ -ammonia is too short-lived for transportation, therefore excluding perfusion measurements from the services offered. Generator produced isotopes such as  $^{82}\text{Rb}$  could serve as an ideal substitute as a perfusion tracer.

The price and complexity of installing, maintaining, and running a cyclotron have limited accessibility to PET to only the wealthiest regions. With the development of cost-effective radionuclide delivery systems such as a constant-activity  $^{82}\text{Rb}$  elution system, state of the art quantitative perfusion PET scans can be offered to regions of low population density as well as to less wealthy communities.

## Chapter 2: The Second Generation <sup>82</sup>Rb Infuser – a starting point

This chapter discusses previous work in the development of systems to infuse <sup>82</sup>Rb tracers, at the UOHI and elsewhere. Capabilities and limitations of these systems are discussed, and the motivation for the present work is given.

In 1981 Yano *et al.* [29] described a <sup>82</sup>Rb elution system which could be used clinically to achieve constant flow rate elutions over a prescribed time (constant-flow elution) by controlling a stepping motor coupled to a specially designed syringe pump. This system included no feedback mechanism for monitoring, data collection, or testing.

Gennaro *et al.*, 1987 [19] described the use of a positron counter mounted on the generator output to measure the activity vs. time curves. In addition, Gennaro *et al.* developed a method of automatically calibrating the positron counter for efficiency (geometric and intrinsic) based on an ion chamber dose calibrator. The positron counter readings were convolved with the <sup>82</sup>Rb decay function and corrected for time delay to simulate the elution to the dose calibrator. The ratio of the dose calibrator reading and the convolution resulted in the calibration constant. Gennaro *et al.* was then able to measure the activity vs. time curves from the generator.

The first generation <sup>82</sup>Rb elution system developed at the UOHI was described by Alvarez-Diez *et al.*, 1999 [30]. This system included a positron counter used to monitor clinical elutions as well as recording the elution profile (the rate of activity delivered during the elution sequence). A generator bypass line was added to allow flushing of the lines to the patient at the end of the elution, thus ensuring that no activity remains as background that would be detected by the PET scanner. The operator entered a desired activity dose and elution time, which the system used to estimate an elution flow rate for the peristaltic pump. The activity vs. volume curve recorded during the daily calibration run (Figure 1-5) was integrated to determine the volume that needs to be eluted from the generator in order to achieve the requested activity dose. The flow rate was determined by factoring this volume by the requested elution time. Feedback from the positron counter was used to stop the elution when the activity was reached. These elutions are referred to as constant-time elutions.

The <sup>82</sup>Rb infuser was based on an industrial PC running MS-DOS coupled to a LCD touch-screen. The software ensured that the daily protocol (discussed below) is followed and generated a recording of each elution. In addition some rudimentary error detection was included. The system contained all the necessary components in a single cart, but had to be calibrated manually at a single flow rate (same flow rate as the elutions that would follow) by monitoring an external dose calibrator during the calibration run. The system was used in a routine clinical setting over 3 years, however it proved difficult to upgrade to include new functionality.

In [18] Epstein *et al.*, 2004 simulated a feedback controlled system that varied the ratio of flow between the generator and the bypass line to achieve a constant-activity rate (constant-activity elutions). A prototype was constructed based on the same proven design as the first generation system, which was intended to add constant-activity functionality and improve usability. A simple threshold comparison algorithm was used to compare the instantaneous activity rate to a set point. Although the simulations used a three-way variable pinch valve to control the flow between the generator and its bypass line, the prototype used a 2-way solenoid on/off pinch valve. The system was experimental and used to demonstrate the feasibility of the concept.

This system was the prototype of the second generation rubidium elution system (RbES). The RbES had to ensure the same functionality as the first generation system, while adding constant-activity elution capability, improved user interface, and additional automation to reduce radiation exposure to the operator and patients. The system was based on the hardware design of the first generation system but had an updated computer system, user interface, and operating system which enabled more advanced developments.

## **2.1 The Daily Protocol and Elution Types**

The daily protocol was first described during the development of the first generation system and is intended for routine system maintenance, system diagnostics, and clinical preparation of the system. The aim of the protocol is to ensure that the system is in full operational order, calibrated, and meets all guidelines to ensure patient and operator safety. The protocol consists of a system flush and a calibration run. Although the outline remains

unchanged, the protocol was slightly modified to remove operator intervention where automation was introduced.

The daily protocol begins with replacement of the saline supply and of the patient line and emptying of the waste container. A flush run is initiated by the operator to flush and prime all lines with 0.9% NaCl saline. The generator is then flushed with 50 ml saline in order to remove air bubbles and any Sr breakthrough from the system. The generator is then allowed to completely recharge by stopping saline flow for at least 10 minutes.

A calibration run follows to recalculate the calibration constant of the activity detector and measure the activity vs. volume curve of the generator. Calibration is performed by eluting at a constant flow rate (15ml/min) over 60 seconds to an external dose calibrator, which serves as a reference. The activity in the dose calibrator is registered 30 minutes after the end of the elution to compute the breakthrough <sup>82</sup>Sr and <sup>85</sup>Sr activity. Only after a calibration run with low Sr breakthrough has been successfully completed can patient elutions be carried out. The calibration constant is a measure of the positron counter's efficiency and is therefore not expected to change significantly. Monitoring of the calibration constant can be used to detect problems in the system.

Once the daily protocol has been completed successfully, patient elutions are enabled until the end of the day. Refer to Figure 2-1 for a flow chart of the daily protocol. Three patient elution modes are of interest:

**Constant-Flow** elutions allow the user to specify the flow rate and duration of the elution. This elution is identical to early elutions as described by Yano [29].

**Constant-Time** elutions allow the user to specify the desired activity and time for the elution. The flow rate is automatically calculated based on the activity vs. volume curve measured during calibration. This mode offers the same functionality as the first generation system [30].

**Constant-Activity** elutions allow the user to enter the desired activity and duration of the elution. The system automatically estimates a flow rate and controls flow through the generator or a bypass line by a threshold comparison algorithm to achieve fluctuations around the desired set point.

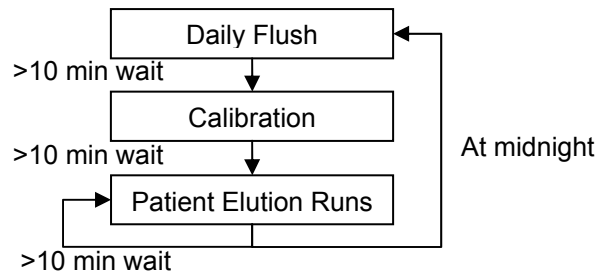


**Figure 2-1 - Daily protocol flow chart.** At the start of each day a flush and calibration run must be performed prior to patient elution runs. At midnight the calibration and flush expire. A minimum of 10 minutes must pass between elutions.

## 2.2 Hardware Description

The second generation elution system focused on improving usability, automation, and precision. The primary goal was implementation of a constant-activity elution mode. Since the first generation elution system has been proven as a reliable design, it served as a basis for the second-generation infuser. The hardware remained almost unchanged, while the software was completely rewritten using Matlab/Simulink.

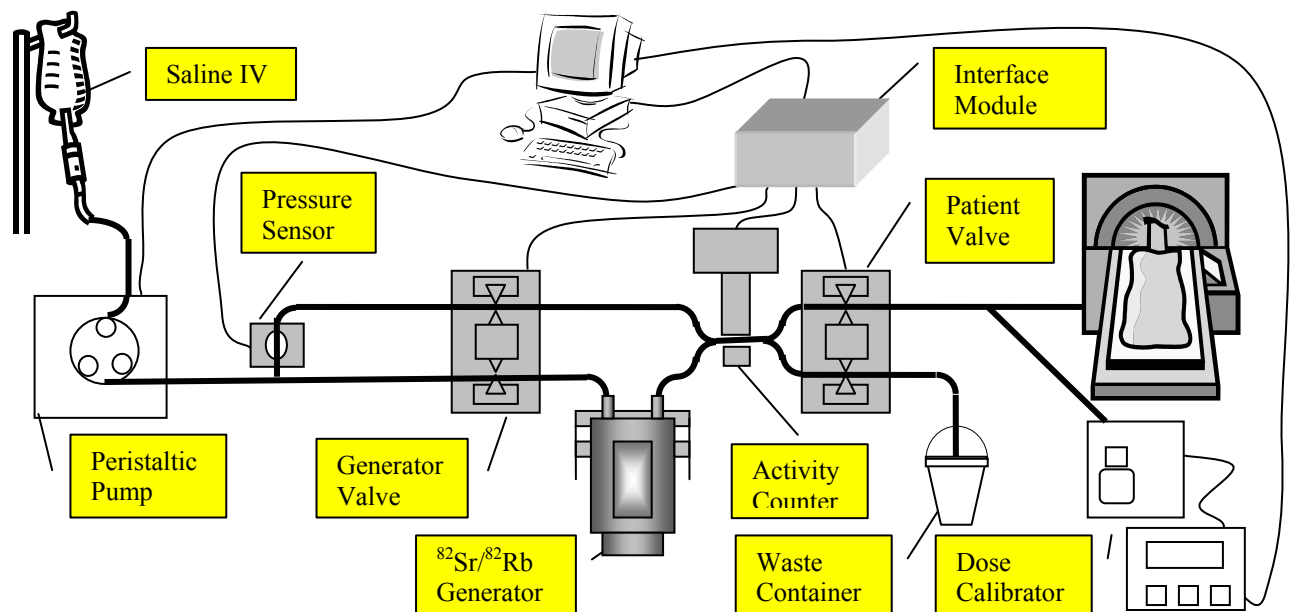


**Figure 2-2 – Hardware component diagram of the RbES prototype [18] was not altered.**

The system is based around a PC which interfaces with the various sensors and actuators. Based on the mode of operation and measured data, the real-time software controls the pumps and valves. These in turn affect the flow of saline through the generator or its bypass line to the patient, dose calibrator, or waste container. The system acquires data from a pressure sensor, activity counter, pump, and the dose calibrator which is used to monitor the process and control the elution. Figure 2-2 shows the overall design of the second-generation  $^{82}\text{Rb}$  infuser.

### *Computer*

The PC was modified to allow interfacing with other system components. An additional RS232 serial port was added through a PCI board. The data acquisition card was installed on a second PCI slot. In order to power the buffer board, a 12VDC power cord was spliced from the floppy drive power cable. Table 2-1 lists the specifications of the PC that was installed. A mini-tower case was selected due to the physical restrictions of the cart.

**Table 2-1 – Minimum PC Requirements**

<b>Component</b>	<b>Specification</b>
CPU	Intel Pentium III 1200 MHz
RAM	256 MB
Hard Drive	40 GB
CD-ROM Drive	1
USB Ports	4
RS232 Serial Ports	1 + 2 added with a PCI interface board
Case	Mini-tower
PCI slots	2 – serial port and data acquisition board
Power Supply	350 W

An important advantage of using a PC to control the system is the wide range of applications and devices that are readily supported. This included off-the-shelf user interface devices, as well as machine interfaces and data acquisition devices. In addition a wide range of operating systems and development environments could be chosen from. Simply said, PCs offer a good performance to price ratio in a flexible package.

### *User Interface Medium*

The user interface was designed to meet the following requirements:

- Interface with the user must to be simple and intuitive.
- The technologists must be able to monitor the progress of the elution even from a distance, so as to reduce radiation exposure.
- The technologist must be able to operate the system with a single gloved hand.
- The input device must be resistant to small amounts of liquid and easy to clean.

A 17-inch liquid crystal display (LCD) resistive touch screen was chosen (3M M/50). Large buttons as part of the graphical user interface (GUI) allow easy operation, while a simple display allows viewing from across a room. Connections to a PC through a standard VGA cable for display and a D-type 9 pin RS232 serial cable for touch screen inputs. Included in the package are the drivers required for manipulating the mouse cursor via the touch screen. Although the screen is not waterproof, it will withstand a few droplets.

#### *Data Acquisition Board (DAQ)*

The National Instruments PCI-6035E data acquisition board is used to both acquire readings from sensors and control actuators. National Instruments has a good reputation in the field of data acquisition and is widely supported by development platforms. Both Matlab/Simulink and Labview have drivers integrated into their packages without the need of further purchase. The PCI-6035E boasts a variety of input and output capabilities including:

- 8 Digital I/O Channels
- 8 Analog Inputs, 16 bit, 160 kHz A/D converter
- 2 Analog Outputs, 16 bit, 160 kHz D/A converter
- 2 General Purpose 24 bit Counters/Timers

#### *Flow Control Valves*

The flow control valves are solenoid-powered pinchers that squeeze the silicon tubing to a seal. They are controlled by an operating signal of 0 or 12 VDC (polarity does not matter). Each valve is a double pincher allowing flow through one tube, while blocking flow through a second. These valves are manufactured by Angar Scientific and were chosen for their proven reliability.

#### *Buffers*

To supply the required current to the flow control valves the need for buffers arose. The control signals were fed directly from the data acquisition board digital I/O and amplified using solid-state relays (Crydom). The buffer mounting board (also manufactured by Crydom) was modified by exchanging the pull-up resistors with pull-down resistors. This modification was conducted as a safety precaution to ensure that the valves fail to a safe

position (flow through the bypass to the waste container) should control lines become inactive.

### *Activity Counter*

Some of the positrons emitted during decay are absorbed in a fluorescent optical fibre<sup>1</sup> (scintillator) and converted into photons. A photon detector (Hamamatsu H7155) coupled to the optical fibre is used to count these photons. For each recorded event a 30ns TTL pulse is sent through a coax cable to the DAQ on board general purpose counter/timer (GPCTR).

The photon counting head is a single package containing a high voltage power supply and a high-speed photon counting circuit. 5 VDC powers the photon counting head and a coax TTL cable supplies one output pulse for each photon, counting up to 1.5 million counts per second.

It is important to note that although not all the emitted positrons are captured in the fibre, and not all the photons in the fibre reach the counting head, the resulting TTL count rate is proportional to the activity and can therefore be factored by a calibration constant.

### *Pump*

An off-the-shelf peristaltic rotary pump head and control board manufactured by Harvard Apparatus were used. The control board was mounted in an interface box, while the pump head was mounted on the cart top to form an aesthetic installation. Communication between the pump and the PC is achieved through RS-232 serial communication. Control messages include setting the elution volume and flow-rate, while feedback includes the pump status. Continuous pump status-checking ensures both synchronization between the computer and the pump as well as fault detection.

### *Pressure Sensor*

A typical medical pressure sensor is attached to the saline lines immediately downstream from the pump. This pressure is continually gauged to detect blockages in the line through an increase in line pressure. Blockages are caused primarily by air-bubbles that can

block the filters and are normally fixed by replacing the filter. However, blockages can also occur as a result of crystallization in the lines and pinched lines.

The sensor is supplied with 5 VDC from the DAQ board and returns a  $\pm 0.05$  V analogue signal which is proportional to the line pressure. Since pressure in liquid is uniform, readings can be calibrated using an external pressure gauge connected to the same line. The pressure is constantly monitored and can lead to program termination if the pressure rises above a set threshold (25-30 psi) for a prolonged period of time.

### *Dose Calibrator*

A Capintec CRC-15 (Ramsey, New-Jersey) series<sup>2</sup> dose calibrator is supported as an external device for calibration purposes. This dose calibrator is the gold standard throughout the nuclear medicine industry and is a common tool in medical radiation labs. The CRC-15 is composed of an ionization chamber, which is used to detect ionizing radiation, and a console, which powers and monitors the chamber as well as provided a user interface. Communication between the PC and the dose calibrator is achieved through RS-232 polling by the PC.

The dose calibrator is utilized in the system for both calibration and testing. During calibration the dose calibrator readings are used as a reference to which activity counter readings are compared. During test runs the calibrator readings are used to verify the expected results.

### *Assembly*

All the components are assembled in a stainless steel cart shown in Figure 2-3. The generator was placed in the cart and surrounded by lead rings to provide maximum radiation shielding. All the saline lines were mounted on a modified top cover for easy access and monitoring (Figure 2-4). A high density plastic lid covers the lines to reduce positron exposure. Finally the LCD touch screen was mounted on an adjustable support arm, so that the operators can adjust its angle for ideal height and visibility.

---

<sup>1</sup> Bicon BCF-10, blue scintillator optimized for diameters  $> 250\mu\text{m}$

<sup>2</sup> Both the CRC-15R and CRC-15PET models were tested and used during this research.

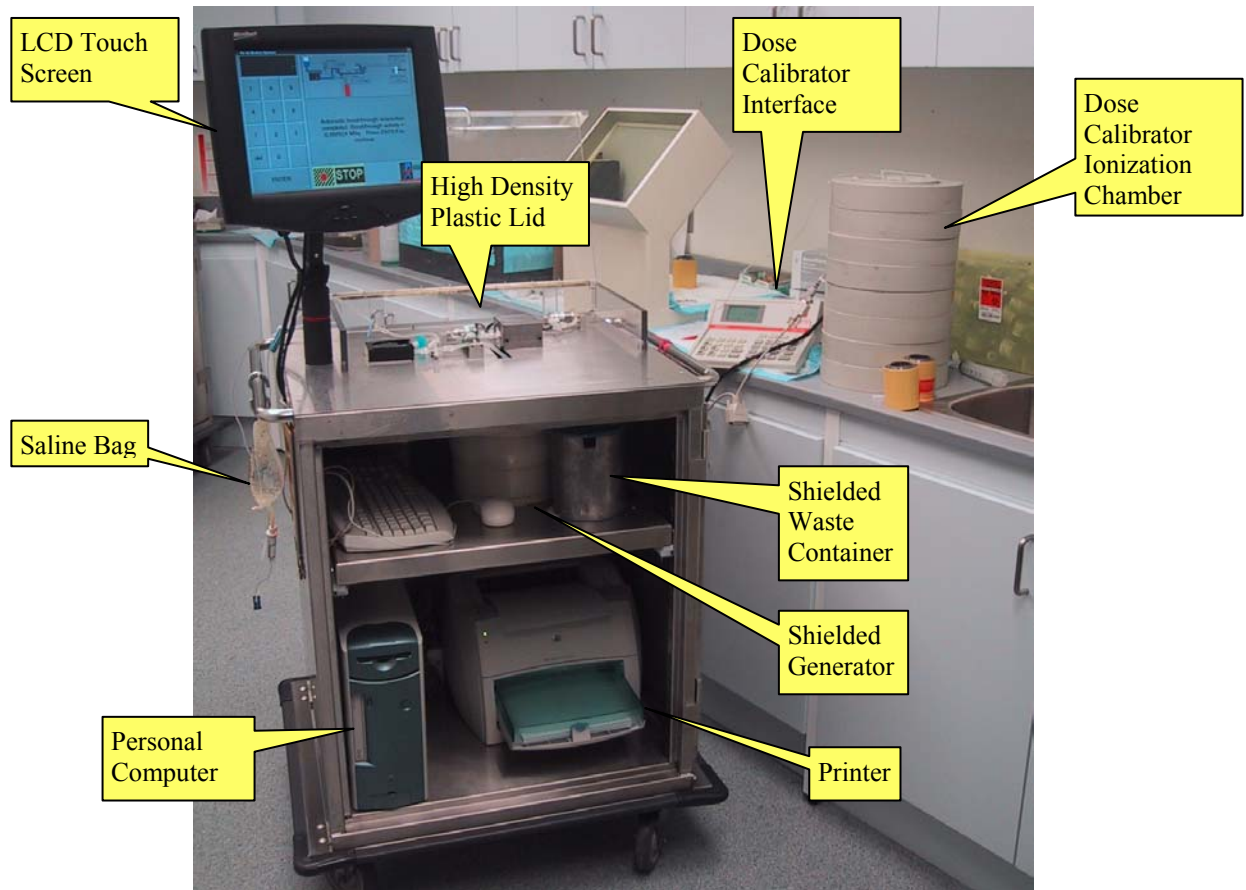


Figure 2-3 - Photograph of the assembled  $^{82}\text{Rb}$  elution system and its components.

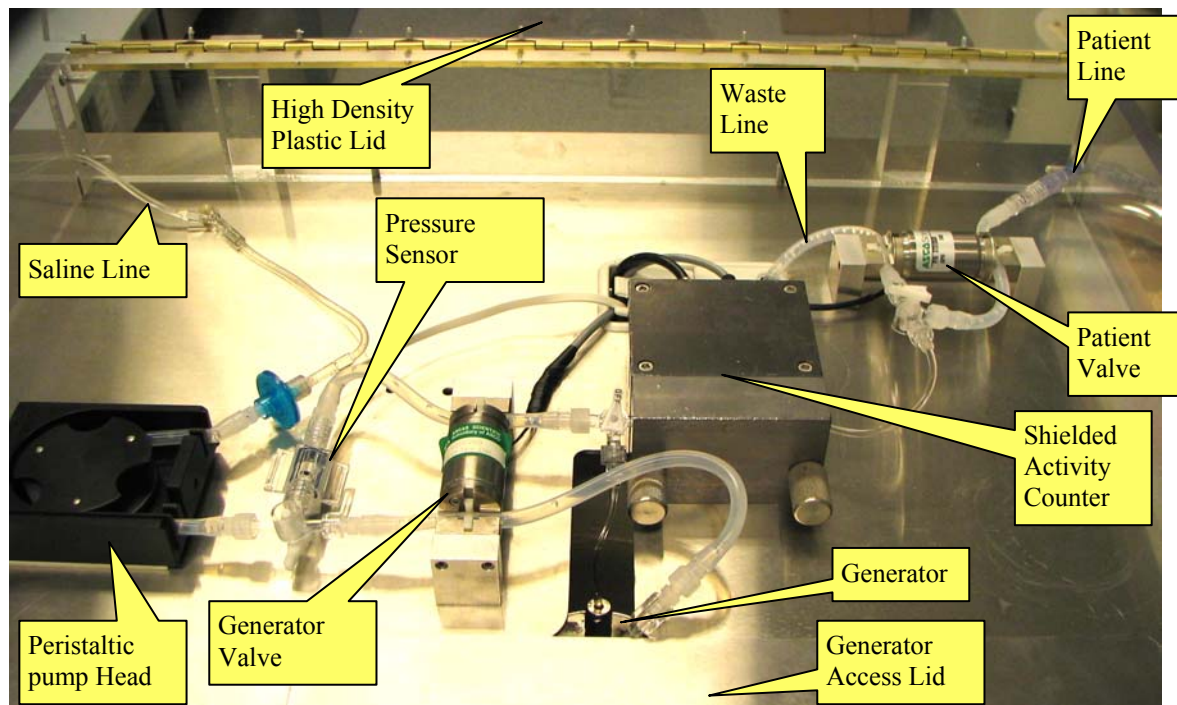
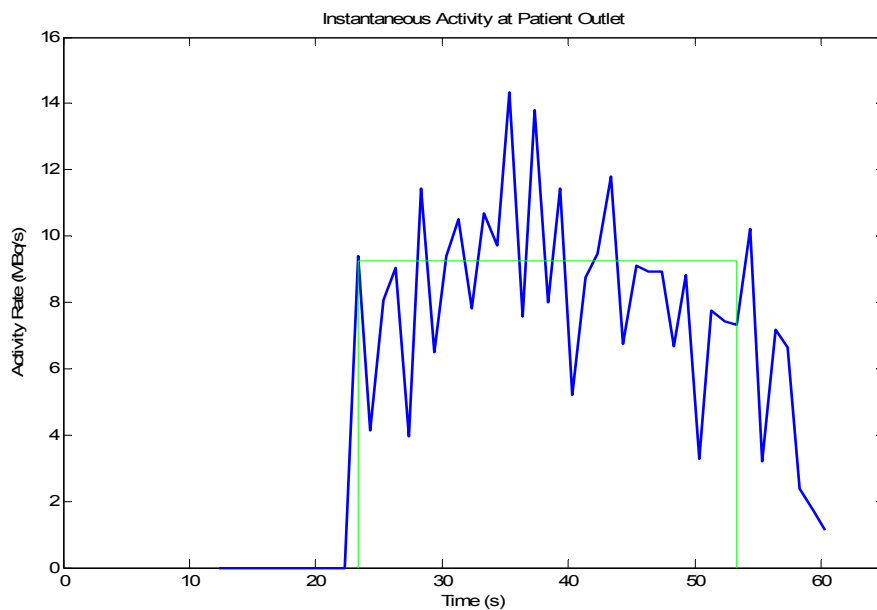


Figure 2-4 - Photograph of top cover of the  $^{82}\text{Rb}$  elution system.

The PC, printer, and power isolation transformer were mounted on the lower tray. An interface box was constructed for mounting below the top cover and included the pump interface board, valve driver circuitry, and DAQ I/O connector block. Finally the waste container was mounted on the top shelf inside a lead container with a lid.

### 2.3 Prototype Performance

In [18] Epstien *et al.* presented initial results with the RbES. The reported results include simulation data as well as elution measurements. Elutions in the range of 10-70% generator bolus activity (relative activity) were justified as a reasonable range for clinical applications. A newly loaded “hot” generator should have about 2000 MBq<sup>3</sup> bolus activity (first 15 ml eluted) and would decay to approximately 785 MBq within 5 weeks. At the UOHI Cardiac PET Center, a typical dose is 550 MBq while a small dose is 200 MBq. A small dose on a hot generator corresponds to 10% activity while a cold generator and a large dose corresponds to approximately 70% generator activity. Typical elutions are 30 seconds long and were therefore used in these measurements.



**Figure 2-5 - Elution of 50% bolus activity within 30 s using a simple threshold comparison algorithm as described in [18]. The actual activity rate at the patient outlet (blue) since the beginning of the elution is compared to the desired result (green).**

<sup>3</sup> Bq are physical units that measure the number of nuclear disintegrations per second. In our case, we use MBq referring to one million positron emissions per second.

Using a threshold comparison approach, Epstein *et al.* reported fluctuations around the set activity rate of about 40% (as demonstrated in Figure 2-5). These fluctuations were believed to be caused by a delay in the activity measurement due to the real-time system refresh rate 50 ms and some activity spill over. However, we believe that most of the overshoot is a result of transport delay between the merge point (of the generator and bypass line), and the activity counter.

#### **2.4 Further Development of the $^{82}\text{Rb}$ Elution System (RbES)**

The primary motivation for developing the RbES is to develop an infusion system capable of eluting a given activity at constant rate over a prescribed time period from a  $^{82}\text{Sr}/^{82}\text{Rb}$  generator independent of generator age, so long as sufficient amounts of activity can be provided by the generator. The system is required to operate in a clinical setting and therefore must be reliable, easy to operate, and above all, safe. The prototype that was developed prior to the work of this thesis was incomplete with the following issues still needing attention:

- Precise constant-activity elutions were not achieved. Fluctuations around the set point needed to be significantly reduced through an improved control of flow through the generator.
- Only a few error detection mechanisms were implemented. Of those that were implemented, the report to the user was uninformative.
- There was no means for the operator to manually terminate an elution if a problem was noticed during the elution.
- A key requirement of this system is to reduce radiation exposure to the technologists by automating the system and allowing monitoring from a distance. Although this goal was mostly achieved in the prototype system, breakthrough activity measurement remained a manual function.
- The interface lacked sufficient real-time feedback to the technologists about the state of the system.
- Although the electronic reports and logs of the elutions were mature, a paper report which is needed to be filed in patient charts was not available.

- The system contained no measures to avoid electrical ground leakage. This issue had to be addressed especially since the cart is made of stainless steel, contains electrical equipment, and connects to the patient with saline, which is conductive.
- No protection against overflow of the waste container was implemented in the prototype system. If overflow was to occur, this could potentially lead to damaging of the system components, or developing of a shock and fire hazard.

The hardware design of the prototype system addressed many of the prototype system requirements and could therefore be used as a platform for further work. The software, on the other hand, was in an incomplete state with many requirements left unaddressed. The prototype system served as a starting point from which the state of the art could be understood, and as a reference to which future developments could be compared. The remainder of this document describes the research, development, and testing that was carried out to bring the system from a prototype stage to a mature system fully ready for clinical use.

## Chapter 3: System Design and Conceptual Understanding

Development of the RbES described in this work was started from the research prototype that was already partially functional (as described in the previous chapter). Although this meant less flexibility in the overall design of the system, it provided a starting point that could save much time and effort in the development process. The hardware was based on the first generation elution system [30], which had been routinely used over three years in a clinical setting and had proved to be reliable.

The software, on the other hand, was in an unfinished state and proved to be unstable. The constant-activity control algorithm, described in [18], was simplistic and left much room for further improvement. Therefore, it is the software that would undergo the most development, with few minor additions/revisions to the hardware. Before commencing the development the prototype design had to be understood and the project had to be defined.

### 3.1 Requirements

The  $^{82}\text{Rb}$  infuser was destined for human use from the start. This dictated tight safety requirements that must be considered throughout the design process. Safety considerations focused both on the patient and the system operator and included mechanical, electrical, and radiation exposure risks. The main goal of this project was to design and implement a system capable of providing a constant and controlled rate of  $^{82}\text{Rb}$  activity over elution times in the range of 15 to 60 seconds for clinical PET scans in humans. In addition, the system had to be capable of reproducing elution profiles that were tested and understood in the literature – the constant-flow and constant-time elutions.

#### *Functional Requirements*

Functional requirements relate to the functionality and features that the system must provide in order to justify its existence.

- The system must identify faults during run-time and provide meaningful messages to the operator.
- Once an elution from the generator is started, the system must be fully automated so as to minimize exposure to the operator.

- The system must at all times display the status to the operator in a fashion that is readable from at least three meters from the device.
- The system must be capable of producing constant-flow, constant-time, and constant-activity elutions as well as respective tests with respect to an external standard.
- A record must be kept of all completed elutions for analysis and filing.
- The system must ensure compliance with the daily protocol described in the previous chapter. A flush followed by a calibration run and successful breakthrough measurement must be completed in order to enable patient elutions for the remainder of the day. The system should delay at least 10 min between runs.

### *Non-Functional Requirements*

The non-functional requirements are additional constraints on the design that define desirable behaviour or design of the system. These requirements do not define the functionality that the system must provide.

- The system must not pose a health risk to patient, operator, or any other person under any circumstance.
- The system must react in a predictable and controlled manner at all times.
- Any detectable error will result in a controlled termination of the elution with all actuators in a safe mode:
  - Patient valve set to waste
  - Generator valve set to bypass
  - Pump stopped
- Between each run the application will be completely re-initialized so as to prevent the chance of any data being carried over to the next run.
- The system must be self contained with an interface to an external activity measurement standard for calibration and testing purposes.

## *Other Requirements*

### *Performance*

Since the  $^{82}\text{Rb}$  elution system is designed as a real-time application, it must meet performance requirements that are suited for the task at hand.

As with the prototype system, the most crucial sensor for the control algorithm is the activity counter as it is the sole sensor participating in the feedback loop. In order to measure activity in the line, positron counts must be collected over sufficiently long time. However, one must account for the limited counter capacity (24 bits) to avoid counter overflow. Assuming a detector efficiency of 1 and a measurement of 30 MBq the counter would overflow in just over half a second. To avoid counter overflow readings are taken at 20 Hz. Jitter must be avoided in order to ensure that the activity measurements are accurate. This frequency provides the base refresh rate of the real-time application.

The real-time user interface and the physical sequence state machine could run at a slower refresh rate, but not less than 1 Hz. A refresh rate of 1 Hz was chosen to reduce processing overhead as much as possible, while still maintaining a reasonable refresh rate of the GUI.

In order to meet these criteria both hardware and software performance and services should be considered. An operating system capable of providing real-time scheduling services must be chosen. The combination of software packages and hardware must ensure that the processes can be executed within a reasonable time and minimal jitter to the real-time scheduling.

### *User Interface*

The user interface must be informative, allow the operator to control all the features of the elution system, but also limit the user input to ensure validity. The elution system software may run as an application leaving access to all other features of the operating system so as to enable the system manager to conduct maintenance and collect data. The interface must be solely through the touch screen which will display a keypad and exit button. Other buttons and radio-buttons must be added only at relevant states and

immediately removed at the end of each state. Prior to initiating an elution, all the parameters set by the user must be displayed for confirmation.

The real-time graphics display must include a system diagram with updated information about the state of the system. This includes the current activity rate reading, flow rate, valve status, and expected accumulated activity at the patient outlet. In addition, progress bars must be included for each stage of the elution so as to facilitate monitoring of the system. An emergency stop button must be enabled throughout the elution and take immediate effect to bring the system to the safe mode.

At the end of an elution, reports must be generated based on the type of elution and its mode of completion. If an error is detected, a red screen including details of the error and recommendations to resolve the issue must be displayed. If the emergency stop button is pressed, a yellow screen must contain an appropriate message. On successful completion a grey screen must list statistics relevant to the elution. In addition, a separate window must list a comprehensive display of all statistics in addition to activity curves relating to the activity rate, and the integrated activity at the patient outlet.

### *Test Runs*

For each of the patient elution types (constant-flow, constant-time, and constant-activity) a test mode must be offered as well. These modes are identical to the patient elution modes but include data logging from the external dose calibrator. These data are used to confirm that the actual activity as delivered to the patient outlet is similar to the expected activity. These modes can be used to test the system.

### *Elution Recording and Reports*

Data logging for analysis and recording is at 1 Hz regardless of other measures and will include a log from the start of the elution until its termination. For all elutions the elapsed time, activity counts, line pressure, and generator valve open-time must be logged. In the case of calibration runs and elution tests, the dose calibrator reading and the serial communication delay must also be logged. In addition the elution settings and event times must be recorded.

### **3.2 Initial Design Considerations**

#### **Safety**

A first concern with any system that interacts with humans is safety, and even more so when the system is used clinically and interacts directly with the patient's body. The design must have multiple robust mechanisms to ensure that in any case of failure, the patient is not at risk. The following safety requirements were set and tightly followed:

1) Under no circumstances may any electric current leak through the saline line. Saline is essentially water with dissolved salts to ensure pH and salinity similar to that of the blood. Due to these solutes, saline conducts electricity quite well. Even the smallest current directly through the body can cause discomfort or pain. It is for this reason that the saline in the system is electrically isolated. Throughout the system, saline is enclosed in silicon or PVC tubing with plastic connectors.

2) Only a limited amount of saline may be infused to the patient, and at a limited rate. Even in the case of a software crash the flow and quantity must be controlled and limited. The off-the-shelf and reliability proven peristaltic pump is programmed with a desired (maximum) volume and flow rate, and runs autonomously. However, the computer monitors the pump's status and issues a stop command if the pump does not terminate within the prescribed time limit.

3) The pressure in the line must not exceed 20 PSI (138 kPa). This is to ensure the accuracy of the effective flow rate and to reduce the risk of line bursting. The pump head is rated to 30 PSI (207 kPa). In the event that the pressure limit is exceeded for more than 3 seconds, the elution is immediately terminated.

4) The activity delivered to the patient must not exceed the requested dose as to reduce saturation of the PET scanner sensors and needless exposure to the patient. The activity readings from the counter are used to monitor the progress of the elution. The elution is terminated once the requested dose is reached regardless of how much time has elapsed.

5) The activity delivered to the patient should not exceed the dose set by Health Canada guidelines (2200 MBq). This issue is handled in part by safety issue 4, but is also ensured by the limited activity in the generator (~2000MBq) and the use of an autonomous pump that is programmed with a finite elution volume. The worst case scenario is thus the

possibility where the elution system software does not respond, the valves do not fail to a safe mode, the autonomous pump continues running indefinitely, and a hot generator is being used. In assessing the worst case scenario we have concluded that no more than the total generator activity, could be eluted. In such a case it is expected that the technologist monitoring the elution system would notice that the PC no longer responds and would take action by resetting the system.

6) The amount of Sr breakthrough activity must be strictly limited to the Health Canada guidelines. This issue is addressed by daily breakthrough tests as part of the daily protocol ensured by the system.

These safety concerns are of utmost importance and were addressed at all levels of the development and testing.

### *Process Monitoring*

Monitoring of the flow of activity to the patient is critical as a safety feature as well as a means of precision control. The delivered activity is dependent on the activity leaving the generator, and on the flow rate to the patient outlet. The flow rate is set by the software and controlled by the autonomous peristaltic pump. However pressure in the lines must remain within pump manufacturer specifications to ensure that the flow rate is accurate. If the pressure is above 30 PSI (207 kPa) backwash of fluid through the rotor head can result leading to an effective flow rate that is lower than expected.

The pressure sensor is used to sense high pressure in the saline lines due to blockage. This mechanism also prevents bursting of the lines as pressure increases. The pressure sensor is located downstream of the pump head and before the generator valve. This position allows monitoring the pressure in the lines regardless of the state of the valves. Since the lines are filled with liquid the pressure is equal in all parts of the line. If pressure above 20 PSI (138 kPa) is measured for 3 seconds, the elution is stopped and an appropriate message is displayed to the user.

Activity measurements are vital for monitoring the delivery to the patient. The accumulated activity is used to stop the elution when the requested dose is reached. In addition, the activity counter can be used as feedback to the controller to achieve constant-

activity elutions. The activity counter measures the activity in the volume in its field-of-view. Since the volume is flowing, these measurements represent activity delivery rate (MBq/s). Equation (2) relates the measured counts,  $\hat{N}_{\text{Det}}(t)$ , and flow rate,  $f$  (ml/min), to the activity rate at the detector  $\hat{A}_c(t)$  (MBq/s) where  $V$  is the volume in the FOV and  $k$  (cps/Bq) is an efficiency measure of the detector [19]. The efficiency and volume are combined into a single constant,  $K$ , which is measured during the calibration process as explained later.

$$\begin{aligned} \hat{A}_c \left[ \frac{\text{MBq}}{\text{s}} \right] &= \frac{1}{k[\text{cps} / \text{Bq}] \cdot V[\text{ml}]} \cdot \frac{f[\text{ml} / \text{min}]}{60[\text{s} / \text{min}]} \cdot \frac{\hat{N}_{\text{det}}[\text{cps}]}{10^6} \\ &= K \left[ \frac{\text{MBq}}{\text{ml} \cdot \text{cps}} \right] \cdot \frac{f[\text{ml} / \text{min}]}{60[\text{s} / \text{min}]} \cdot \hat{N}_{\text{det}}[\text{cps}] \end{aligned} \quad (2)$$

Accurate activity counting and accurate flow rate generation are vital to ensure that the measurement of activity rate is accurate.

### *Hardware Modifications*

#### *Waste Overflow Level Switch*

The waste container is located on the top shelf inside the cart and is contained within lead shielding to minimize exposure to the operator. The prototype system did not include a mechanism to avoid overflow. If overflow occurs the saline could drip to the lower shelf which contains electronic devices such as the UPS, PC, and printer. Therefore it is desirable to incorporate an overflow prevention mechanism.

It was decided to include a level switch that could be used to prevent further elutions and generate a warning to the user. A wide variety of level switches are available based on various technologies. However, our requirements eliminated many of these technologies.

- The sensor must be completely electrically isolated from the saline to avoid shock hazard
- The sensor should not have any mechanically moving parts as the saline can leave crystallization which could interfere with the mechanism
- The sensor should be easy to clean to keep the system sterile.

- The sensor must be small enough to fit in the lead shielding and permit a large enough amount of volume to accumulate in the waste container before being activated.
- The sensor must fail in a way that would indicate overflow.
- The total purchasing and integration cost should be kept low.

With these considerations the ELS-1100 (Gems Sensors, Connecticut, USA) Electro-optic Level Switch was chosen from a wide range of possibilities. It uses an optical transceiver to determine the existence of a surrounding liquid through a change in light refraction as is shown in Figure 3-1. The choice of an optical level switch was due to its small size, simplicity and lack of mechanical moving parts. The main disadvantage is the need to keep the lens clean from saline droplets and crystallization. However the sensor can easily be cleaned by wiping with a wet paper towel. If a droplet does form on the switch, it will signal an overflow, resulting in a fail safe system.

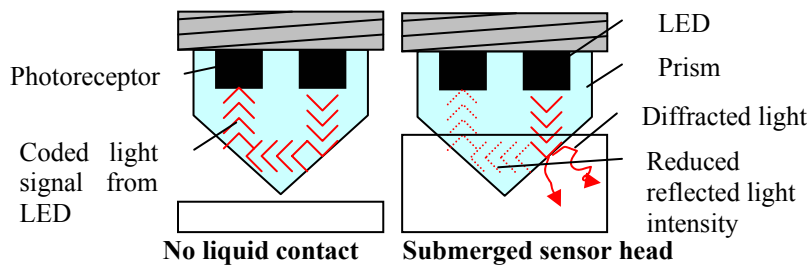


**Figure 3-1 – Electro-optic level switch operation to prevent waste overflow.**

The ELS-1100 requires 10-28 VDC operating power and returns an open collector capable of drawing up to 40mA. In the case of TTL digital logic, as is used on the DAQ board, a straight connection to a digital input line without the use of a pull-up resistor is adequate. 12 VDC were supplied directly from the PC power supply, which also powers the solenoid valve buffer board. The sensor casing is screw threaded so that it can be screwed into the lid and adjusted for height. Since no additional hardware was necessary, only the purchase cost of the sensor was incurred.

If the level switch is tripped the current elution continues to completion, but a new run is not permitted. A warning message is displayed at the end of the run. If a new run is attempted without emptying the waste container, an error is produced and the elution does not proceed until the waste container is emptied and the elution is restarted.

### *Isolation Transformer*

To meet Canadian Standards Association requirements, the equipment had to pass electrical safety tests. These include current leakage to ground tests, and surge tests. This is especially true since the stainless steel cart and the saline to the patients are both conductors. To meet these requirements, an isolation transformer through which all the electronic components in the cart are powered was added.

### *Uninterruptible Power Supply*

As the cart must be moved around the PET imaging room and time constraints can be tight, the system needed to remain powered while unplugged. This problem was easily resolved by connecting the PC, pump, and touch screen display to an uninterruptible power supply (UPS). The system is plugged into a wall socket at all times and only needs several minutes of battery power while being moved. An off the shelf UPS rated for 800 V·A was purchased (Belkin F6C800-UNV). This allows approximately 10 minutes of disconnected time with the all the components powered but no elution in process.

### *High Density Plastic Lid*

Although the generator and waste container are shielded by lead, the saline lines are a source of radiation during elutions. To minimize exposure the personnel and patients, a high density ¼ inch plastic lid was added to cover all the lines on the top of the cart. This cover absorbs most of the positrons, but only a small fraction the gamma radiation which is also of concern. Distance is the most effective shielding for gamma radiation [31] which is the reason for automation of elutions. The lid was hinged to allow access when maintaining the system and replacing the patient line.

### *Software packages*

Selection of a proper software environment is a crucial decision and should be addressed up front. Although many considerations should be taken into account, a few dominant aspects made this choice clear. We were looking for a simple and mature operating system which would be compatible with all our hardware and provide many services so as to reduce the development time. In addition we wanted to work with a flexible environment

which would allow future development as needed. Finally the realization that a familiar environment would eliminate the initial learning curve brought forth the decision to use a Microsoft Windows operating system to complement the PC platform.

Debate over the development environment (RT Rational Rose, National Instruments LabView, and Matlab/Simulink) was easily resolved based on our extensive experience with Matlab and the wide features it supports. The development environment of choice was Matlab with a real-time windows target for Simulink. Simulink allows drawing real-time applications through an extremely high level language of connecting blocks. Combined with the optional real-time windows target (RTWT) one can compile the program to executable code for optimized performance. Matlab is a high level interpreter language that provides powerful mathematical and graphical tools. The computational overhead incurred with an interpreter language could potentially be overcome by later compiling the scripts into stand alone executable programs using an optional package.

To compile the Simulink models to executable code, a supported C compiler must be provided. The Watcom C compiler is an accepted and proven compiler that is available without charge. In addition, this compiler is continually being developed and is supported by Matlab.

The RTWT runs as a CPU ring zero application (same privileges as the operating system (OS) kernel) and is driven by the PC hardware clock for accurate timing. The RTWT is triggered by a hardware timed interrupt and handles the application before triggering the OS kernel. As a result, compiled applications are guaranteed execution in a real-time fashion with the highest processing priority possible [32]. However, higher level services such as graphics rendering and higher level interpreters are still provided by the operating system.

A debate over which Windows version to use arose within our group. On the one hand, we had a long and relatively good experience with Windows 98. However, this operating system suffers from a reputation of being unstable and having poor real-time capabilities. Due to licensing issues, our alternative was windows 2000, which is based on NT™ technology and is supposed to address the above mentioned concerns. After experimenting with both operating systems and an ongoing correspondence with Mathworks' technical support team, we concluded that Matlab RTWT had a compatibility issue with

Windows 2000. It was finally decided to continue the development in a Windows 98 environment with the hope that the application would later be compatible with other operating systems.

Windows 98 was designed as a general purpose operating system that shares resources, including processor time, amongst all running tasks. As a consequence it does not meet the requirements of a real-time operating system in which tasks are handled with tight time constraints [33]. However, this is not a limitation in our case as the RTWT operates as a second kernel parallel to that of the operating system and is triggered directly by hardware events. As a result the real-time model is handled by a real-time kernel while higher level services are handled in a less timely constrained fashion by the operating system.

During the development cycle Matlab and Simulink were used as a development environment. The Simulink model was compiled to run on the RTWT. The remaining components were implemented in Matlab, including the interface and high-level control of the real time functionality. In this manner the real time components were guaranteed proper time management, while the less critical higher layers could be developed with less consideration for system resources.

**Table 3-1 - Software Environment**

<b>Software Type</b>	<b>Company and Product</b>	<b>Components and Version</b>
Operating System	Microsoft Windows 98	Windows 98 SE
Development Environment and Emulator	Mathworks Matlab 6.5.1 (Release 13)	Matlab 6.5.1 Simulink 5.0 Real-Time Workshop 5.0 Real-Time Windows Target 2.2
C++ Compiler	Watcom C++ Compiler	Watcom C++ Compiler 11.0c

#### *Minimum PC requirements*

As with any computer controlled real-time application it is a combination of software and hardware that determine the overall performance. Although the application does not initially indicate the need for much processing power, further inspection reveals some issues of concern. Matlab versions 6 and above are implemented in Java, and therefore are executed by a real-time interpreter (Java Virtual Machine). This interpreter translates Java code into machine code and therefore entails a processing overhead. Similarly, Matlab is an interpreted language as well, and therefore adds an even larger overhead of its own.

Although the option of later compiling the application into machine code exists, initial development was in Matlab. It was determined that the existing PC (refer to Table 2-1) will remain unchanged for the time being as processing power did not seem to be an issue with the prototype system.

### *Intellectual Property*

Another consideration when choosing a software development package is protection of the invested work. With an exposed interpreter language such as Matlab, it is quite simple for any person to view the software code and make modification and copies. The investment in the design of the code although protected by copyright contains intellectual information that is the property of the developer. However, in practice it is difficult to prove the theft of intellectual property. One means of protecting intellectual property in the form of software is to compile it into machine code. Although reverse engineering could potentially be used to decode the software, the inherent difficulty is enough to deter most. This reason in itself is sufficient to justify compiling of the software prior to providing the system to a third party; however, it was decided to defer this problem to a later stage if wider interest in the RbES is expressed.

### **3.3 Flow Hardware Layout Justification**

At the heart of the <sup>82</sup>Rb elution system are the saline lines that transport the activity from the generator to the patient. The layout of the saline lines, sensors and actuators is crucial to implementing a physical system that is easy to control. During flow of a radioactive volume through the lines, both a transport delay and a radioactive decay take place. Therefore the activity at the output is delayed and reduced in relation to the activity at the input. If the line volume,  $V$ , and flow rate,  $f$ , are known and fixed, one can compute the delay time,  $T$ , and the radioactive decay,  $D$  as shown below.

$$T = \frac{V}{f} \quad (3)$$

$$D = e^{-\lambda T} \quad (4)$$

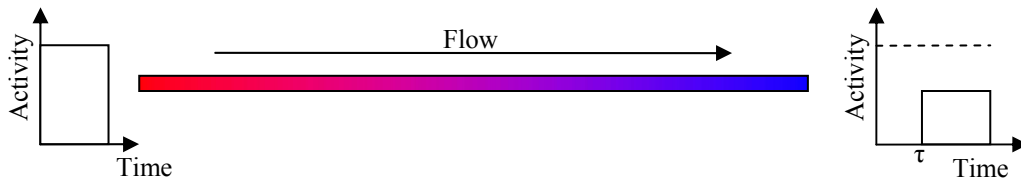


**Figure 3-2 – Response of transport of activity through a fixed volume line at a fixed flow rate.**

However, if the flow rate is not constant, computation of the delay time becomes more difficult, as one must integrate the flow rate over time to determine the transport delay,  $T$ . For each infinitely small slice of the radioactive liquid in the line, a different delay would result and therefore a different amount of decay. This can be expressed in a closed form integral as in (5) which can be solved numerically based on discrete time measurements. One could numerically integrate finite products of flow rate and time slice duration backwards in time until achieving the line volume. The sum of the corresponding time slices would represent  $T$ .

$$V = \int_0^T f(t - \phi) d\phi \quad (5)$$

Variation of flow rate would make prediction of activity at the end of a line difficult and potentially inaccurate. To avoid computational errors and increase simplicity, one would like to have a constant and known flow rate throughout the entire delivery time. This concept serves as the key to choosing the ideal saline hardware layout from the following possible solutions.

### *Pump Speed Variation*

The flow through the generator could be varied by control of the flow rate via the pump. Although this would seem like a simple and effective design, there are two main complications involved. This would make computation and control of activity at the patient output complicated as the exact time delay to the outlet must be solved based on the varying flow rate, (5). This is further complicated by the chosen pump module (Harvard Apparatus model 66 peristaltic pump) which does not support changing of flow rate on the fly. A stop command must be issued and a new start command must follow resulting in finite and varying pauses in the flow.

### Bypass Ratio Control

The above problems can be resolved by setting a constant flow rate at the start of the elution process and controlling the ratio of the saline that flows through the generator (point G in Figure 3-3). The remaining portion of the saline would flow through the generator bypass line. The two lines would then be merged (point M) upstream from the activity counter (point C). Thus, the flow in the combined line remains constant. This allows computing of the transport delay from the counter to the patient outlet (point O). The flow rate only varies in the line volume connecting the generator to the merger,  $V_{GM}$ , based on flow ratio,  $r$ . In order to reduce the variability in transport delay and decay this line volume must be kept to a minimum.

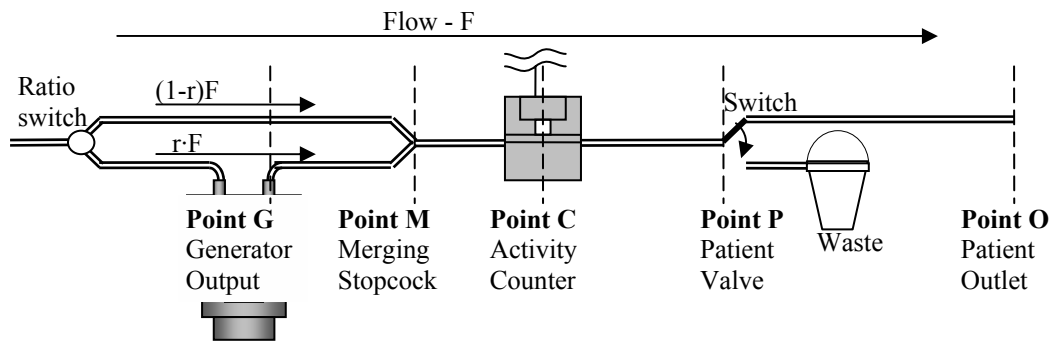


**Figure 3-3 - Flow control through generator using a bypass line maintains a constant flow rate through the other lines (M-O). Variation in flow rate is only in section G-M**

As a result of the layout an overshoot of activity may be expected due to the volume between point M and point C. If the elution is terminated based on accumulated activity measured by the activity counter, this overshoot of activity must be taken into account. Therefore the stopping threshold should be reduced to the requested dose minus the expected overshoot. The overshoot of activity can be derived from the activity curve measured during the day's calibration run and is dependent on the eluted volume and the overshoot volume,  $V_{MC}$ .

The ratio between the two lines can be controlled through various valve types.

#### Variable Pinch Valve

It is expected that with a variable pinch valve an exact flow ratio through the generator can be controlled. Ideally this would allow absolute control of the amount of activity that can be extracted from the generator. Similar to Kirchoff's law in electricity, the

pinch on one line increases the resistance, thus forcing more current through the alternative route.

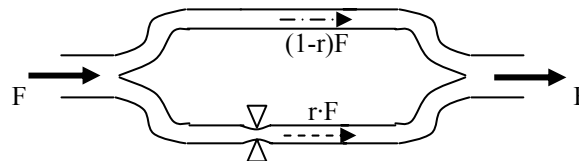
Various implementations of such valves exist. A common valve implementation includes a stepping motor coupled to a screw thread which moves the pinchers. In order to vary the pinch to a large extent, the motor must be rotated over many steps. This results in a long response time. In addition, steps can be missed necessitating a feedback mechanism.

Early experimentation in our lab [18,20] was conducted with a variable pinch valve with a one-sided pincher and position feedback. The problems mentioned above did surface, leading us to conclude that a variable valve (at least of this type) was not suitable for our application. As a result, other alternatives were sought.

#### On/Off Pinch Valve

The use of a solenoid on/off valve overcomes the complications involved with the variable pinch valve. In addition the solenoid mechanism is far simpler, leading to a lower price, simpler implementation, faster response, and increased reliability. These benefits come at the expense of precision as the solenoid can only achieve two positions – fully open and fully closed.

**Figure 3-4 – Flow control through the generator using a variable pinch valve on the generator line.**



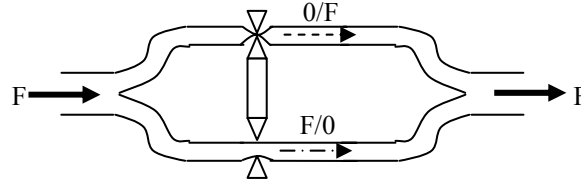
One must place a pinch valve on the generator line, with the spring set to stop flow. This is intended to achieve a fail safe state where the generator flow is blocked if no power is supplied to the solenoid. When the valve is open, saline flows through both the generator and the bypass line at rates that are dependent on the relative resistance in each path (Figure 3-4). When the valve is open, it is hoped that the majority of the flow will be through the generator line. This assumption, however, is unrealistic since the compressed tin-oxide column of the generator resists the flow of saline. A more advanced solution is necessary.

#### Double Sided On/Off Pinch Valve

Flow ratio control was achieved using a single two sided solenoid actuated pinch valve on the bypass line and generator line (Figure 3-5). The valve allows flow through one line at a time. This is equivalent to having an on/off pinch valves on each line operating

opposite to one another. The valve is spring loaded to ensure failure to the bypass open/generator closed position. This valve is referred to as the generator valve and is the liquid flow control equivalent of a selector or demultiplexer.

**Figure 3-5 – Flow control through the generator using a double sided pinch valve on the bypass line and generator line.**



### 3.4 Design of Physical Processes

Prior to the daily clinical use of the system, certain maintenance measures must be carried out as dictated by the daily protocol. These include flushing of all the lines in order to remove Sr breakthrough and air bubbles that could accumulate during hours of standby. In addition, the Sr breakthrough must be measured and a complete system test must follow. The daily protocol was designed to include the following elutions with a minimum of 10 min period between runs for the generator to recharge.

1. *Flush Run* – flushing of all the lines in the system as well as a 50 ml flush of the generator at 15ml/min. Ensures flushing of air bubbles in the saline and Sr breakthrough from the generator.
2. *Calibration Run* – flushing of the generator at 15 ml/min over 60 seconds into the dose calibrator. The integral activity recorded from the dose calibrator is used to calibrate the activity counter and verify that the calibration constant is within tolerance from previous records. If the dose calibrator sensitivity is sufficiently high, breakthrough measurements are conducted after 20 minutes from completion of the elution. If the dose calibrator is not sufficiently sensitive to measure breakthrough, the activity can be entered manually after measurement in a more sensitive device. In addition, the pump flow rate (ml/revolution) can be calibrated by manually entering the actual eluted volume.
3. *Patient Elutions* – Over the remainder of the day elutions to the patients can be carried out in three modes:

- a. *Constant-Activity* – a prescribed dose is eluted over a prescribed time at a constant-activity rate.
- b. *Constant-Time* – The generator is flushed at a constant rate to achieve a prescribed dose within a prescribed time.
- c. *Constant-Flow* – The generator is flushed at a prescribed flow rate until a prescribed dose is reached.

The <sup>82</sup>Rb infusion system software must ensure that the protocol is followed (i.e. that each run is enabled only after the prerequisites have been completed successfully). All the above elutions are similar in sequence and only vary in parameters, therefore a single physical process was implemented.

### ***Run sequence***

All elution types follow the same general set of events. These events are designed to keep the lines primed at all times and to ensure flushing of all activity in the lines to either the waste container or the patient outlet. No activity should remain in the patient line at the end of an elution, in order to provide the prescribed dose to the patient and reduce background activity. The following sequence is common to most elutions.

1. *Flush Bypass-to-Waste* - The volume in the lines from the pump head to the patient valve (Point P) is flushed through the bypass to the waste container in order to remove air bubbles and activity that may remain from a previous run.
2. *Priming of the Patient Line* - When a new patient line is connected, it must be primed prior to elution to the patient. This is done by eluting the volume of the line, filter and needle with saline through the bypass. A slow drip session follows, allowing completion of the priming and connection of the line to the patient. The dripping state is performed at a low flow rate to avoid squirting of excess saline from the open ended needle.
3. *Waiting for Threshold Activity* - The generator flush is commenced while the activity counter readings are monitored. If a minimum threshold activity is not reached within a given time, the elution sequence is aborted and an error

instructing to check for blockage is reported. Once the threshold activity is reached, the elution follows.

4. *Elution* - This state is the actual elution of activity from the generator to the patient. Two types of elution states are used, depending on the elution run type:

*Wait for Cumulative Activity* – Elution until the requested dose minus an anticipated overshoot activity is reached, or the allowed time expires.

*Wait for Cumulative Time* – Elution for a given time, regardless of the amount of activity eluted.

At this stage the patient valve is switched to the patient outlet as needed. This switch is delayed in time to account for the transport delay from the counter to the patient valve. As a result, only the volume past the threshold activity is eluted to the patient outlet, while the initial rise is sent to the waste container.

5. *Bypass-to-Patient Flush* - The final state flushes saline through the bypass to the patient outlet in order to push the activity in the lines to the patient outlet. The volume of the patient line plus an extra volume (2 ml) are flushed to ensure that no activity remains in the line. The extra flush volume can be modified to simulate more closely the sequence followed during injection of <sup>13</sup>N-ammonia.
6. *Dose Calibrator Recording* - In the case of calibration or test runs, additional readings must be recorded from the dose calibrator. These reading must be over at least the duration of the elution (2 x elution times in total). To ensure that sufficient readings are always taken, data logging continues for 360 seconds following the elution stage.

### **Calibration**

The calibration procedure is primarily intended to calculate the calibration constant, K in (2), for the activity counter. This constant gives physical meaning to the events that are counted by the detector. Since this number is dependent on many parameters which cannot all be calculated, an alternative has been proposed to calibrate the counter to an external

standard [19,20]. The use of a dose calibrator as a reference calls for conversion of units and accounting for decay during the calibration process. In addition, the dose calibrator acts as an integrator, as activity accumulates in the vial. Transport delay from the activity counter to the dose calibrator,  $T_{CO}$ , and its associated decay must be accounted for as well. The calibration constant is an overall measure of the counter's efficiency incorporating geometric and intrinsic factors (Figure 3-6).

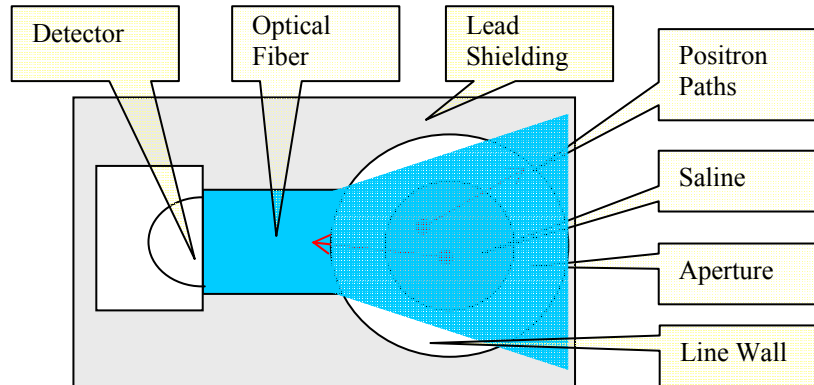


**Figure 3-6 - Schematic diagram of the activity counter illustrating some factors that contribute to its efficiency. Not all positrons in the FOV are captured by the scintillator and not all the tubing cross section is necessarily in the FOV.**

The dose calibrator is composed of an ionization chamber that is sensitive to ionizing radiation in the form of high energy photons. Although shielding from external radiation is included in the design, and is typically added in the form of lead rings, radiation from the surroundings is also detected to varying degrees. The exact region of measurement of the dose calibrator is unknown, and dependent on its geometry. Measurements are taken not only of the contents in the vial, but also of a portion of the line leading to the vial. The exact portion of the line that is measured by the calibrator cannot be easily determined theoretically. Empirically the transport delay from the activity counter to the calibrator can be determined through shifting of the measurements for optimal alignment.

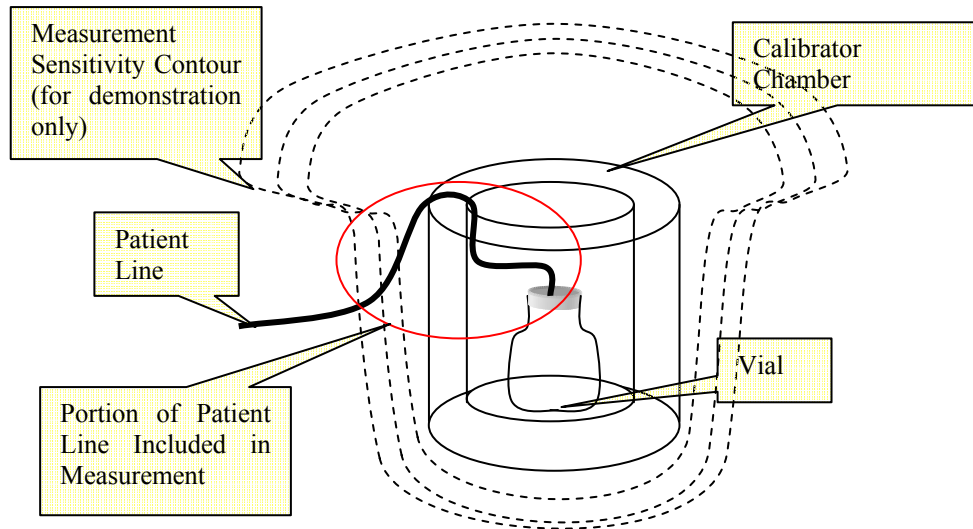


**Figure 3-7 - Dose calibrator chamber measurement diagram.**

The integral activity curve referring to the dose at the patient outlet,  $A_O(t)$ , can be obtained by convolving the instantaneous count rate from the activity counter,  $\hat{N}_{\text{Det}}(t)$ , with the  $^{82}\text{Rb}$  decay curve,  $e^{-\lambda t}$ . The convolution function accounts for the accumulation in the vial and simultaneous  $^{82}\text{Rb}$  decay. The transport delay between the activity counter and the patient outlet,  $T_{\text{CO}}$ , and its associated delivery decay, are also accounted for. Finally, the flow rate is factored to convert the units as shown in the denominator of (6).

Early detection of activity by the dose calibrator has been noted and results from detection of activity in the line prior to reaching the vial as demonstrated in Figure 3-7. This is corrected for by time shifting (with the respective decay correction) of the dose calibrator readings,  $\hat{A}_O(t)$ , to correspond with the expected activity curves at the patient outlet. The shift time,  $\hat{T}_{\text{corr}}$ , is solved for by minimizing the mean-squared-error (MSE) between the activity curves measured by the dose calibrator and calculated from the activity counter readings. The shifted and decay corrected dose calibrator readings are symbolized by  $\hat{A}_{\text{cal}}(t)$  in (6).

The calibration constant can be most reliably computed by factoring the integral of the measured doses over the time that activity is contributed to the vial as shown in (6). Using the integral activity accounts for all available data and therefore decreases the effect of noise.

$$K = \frac{\sum \hat{A}_{cal}(t)}{\sum A_O(t)} = \frac{\sum \hat{A}_O(t - \hat{T}_{corr}) \cdot e^{-\lambda \hat{T}_{corr}}}{\sum (\hat{N}_{Det}(t - T_{CO}) \otimes e^{-\lambda \tau}) \cdot f \cdot e^{-\lambda T_{CO}}} \quad (6)$$

A complimentary approach can be carried out to compute the activity counts,  $N_{det}(t)$ , based on the dose calibrator measurements,  $A_{cal}$ . This requires deconvolution ( $\otimes^{-1}$ ) of the dose calibrator measurements with <sup>82</sup>Rb decay function and shift/decay correction for time  $-T_{CO} + \hat{T}_{corr}$  as shown in (7). Although this curve can be useful for verification of results, it is undesired for calibration calculation as the deconvolution is inherently noisy.

$$N_{det}(t) = \frac{A_{cal}(t - (T_{corr} - T_{CO})) \otimes^{-1} e^{-\lambda \tau}}{K \cdot f} e^{-\lambda(T_{corr} - T_{CO})} \quad (7)$$

Both calibrator and detector readings are recorded over the course of a one minute flush at 15ml/min and an additional two minutes following. The detector readings are converted to the calibrator readings and vice versa. As a result, four, curves are obtained as is demonstrated in Figure 3-8. The pairs can be compared to calculate the calibration constant. Calculation of the calibration constant based on the area under the calibrator readings and their estimate from the detector improves accuracy through the use of all available data. These areas can be calculated by integrating the activity over the interval that activity is being eluted.

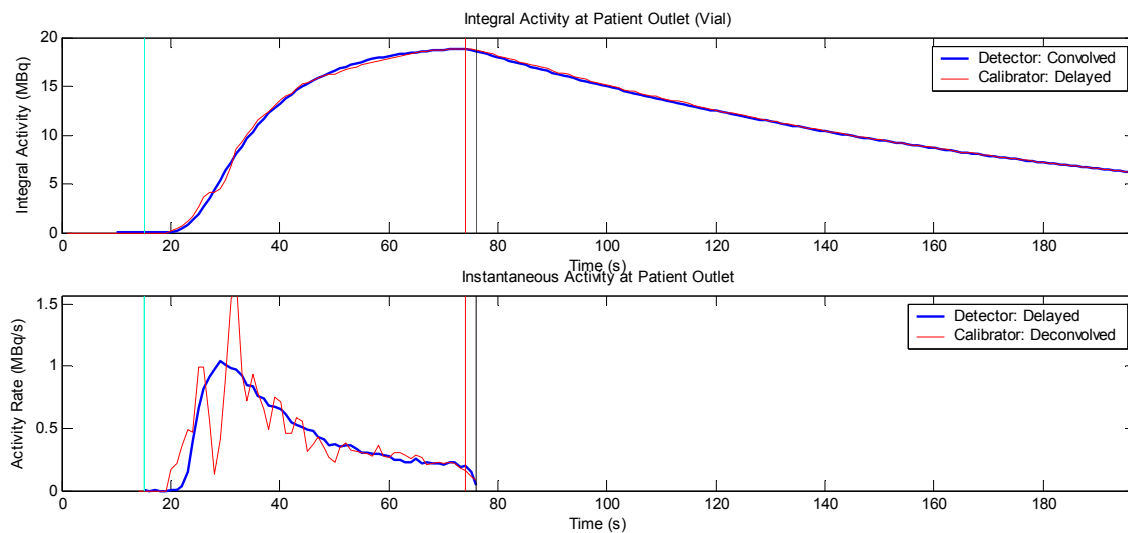


**Figure 3-8 - Sample calibration run results. The top graph demonstrates the recorded and estimated activity at the dose calibrator after calibration. The bottom graph shows the actual and estimated activity rate at the activity counter. The cyan line refers to the beginning of elution (threshold activity = 0MBq/s is passed). The red line indicates the end of the elution (generator valve is closed) while the black line indicates the overshoot volume that is flushed to the calibrator.**

The calibration process was validated over various flow rates and showed close correlation of the integral activity curves. However, at low flow-rates larger variations were noticed. This is partially explained by the aperture response of the dose calibrator demonstrated in Figure 3-7. As activity enters the aperture, the sensitivity increases. The shape of the response is unknown, but was estimated to be Gaussian at the edges as demonstrated by Figure 3-9b. The prototype system assumed the aperture to be a step response to the line distance (Figure 3-9a). Once the activity is in the chamber the sensitivity is highest and is assumed equal throughout. The undetermined distance that relates to the region of full sensitivity is depicted by the flat portion of Figure 3-9a and right and is accounted for by solving for  $\hat{T}_{\text{corr}}$ .

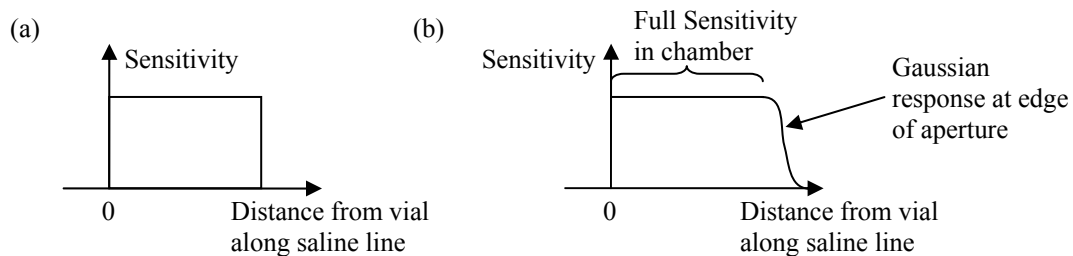


**Figure 3-9 - Aperture response of the dose calibrator as a function of distance along the saline line from the vial as assumed initially (a) and corrected for aperture response with an estimated Gaussian edge (b).**

The chamber aperture sensitivity is estimated as a Gaussian of the line distance as shown in (8). Since the line cross-section is uniform and the flow rate,  $f$  (ml/s), is constant, distance is proportional to time,  $t$  (s), for any given elution. A single constant,  $\alpha$  ( $1/\text{ml}^2$ ), was used to describe the sensitivity response of the chamber over distance. The response does not need to be normalized as at distance zero it represents a sensitivity of 1 while it decreases to an asymptote of zero as the distance from the chamber increases. This is an accurate description of the assumed aperture sensitivity response.

$$a(t) = e^{-\alpha(ft)^2} \text{ where } t \geq 0 \quad (8)$$

The parameter  $\alpha$  was determined empirically from calibration runs at flow rates ranging from 5 to 25 ml/min. Parameter  $\alpha$  was set to 0.7 ( $1/\text{ml}^2$ ) which corresponds to a 50% drop in sensitivity over 1.17 ml line volume. This volume translates to several centimetres from the dose calibrator's point of maximum sensitivity. As can be seen from (8) the aperture correction becomes closer to a step response (in time) as the flow rate increases,

which explains why this effect is more noticeable at low flow rates. An example of constant-flow test run at 5ml/min is included in Figure 3-10 depicting the integral activity with and without aperture correction. This improved modeling of the dose calibrator aperture response allows more accurate comparison of the expected activity profile to those measured by the calibrator.

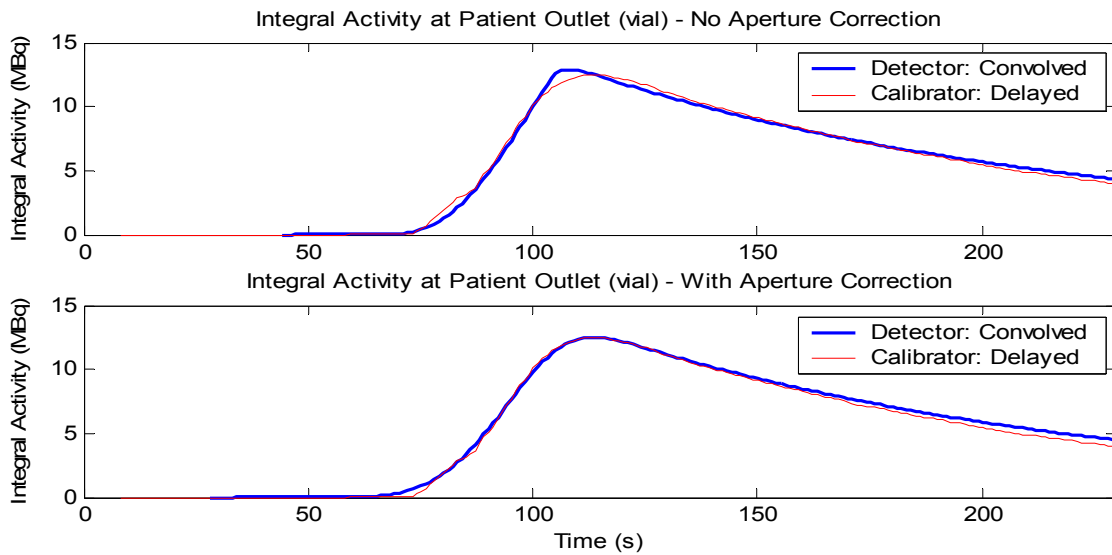


**Figure 3-10 - Example of a constant-flow test run without (top) and with (bottom) a Gaussian aperture correction ( $\alpha=0.7$ ).**

The calibration process must be carried out daily as part of the daily protocol. This is intended to not only to fine tune the system, but also to ensure a complete system test. Some variation is expected in the calibration constant as a result of errors and noise. If the variation is above 10% from a cumulative average, the calibration run does not pass and a warning is generated to the operator. The average, as is calculated in (9), may gradually adapt to accommodate long term changes in the system while rejecting random errors. The average is used as the actual calibration constant for successive runs.

$$K_A = 0.9 \cdot K_A + 0.1 \cdot K \quad (9)$$

### *Breakthrough Activity Measurement*

The dose calibrator is used to detect the breakthrough activity as part of the calibration test through measurement of <sup>82</sup>Rb activity. Once elution to a vial is complete, a high proportion of <sup>82</sup>Rb isotopes are present. This activity decays exponentially over time. After ten minutes approximately 0.42% of the activity should remain in the vial. However, as

time progresses, an asymptotic equilibrium of activity that is greater than zero may result due to the contribution of <sup>82</sup>Rb isotopes from <sup>82</sup>Sr decay in the vial.

The Sr solution that is loaded onto the generator column is composed of mostly <sup>82</sup>Sr, but also contains a large amount of <sup>85</sup>Sr. The manufacturer provides the ratio of <sup>82</sup>Sr to <sup>85</sup>Sr in the sample as was measured in the factory,  $s_0$ . The half-lives of <sup>82</sup>Sr and <sup>85</sup>Sr are 25.5 and 64.8 days respectively allowing calculation of their ratios,  $s(t)$ , at the elapsed time,  $t$ , since measurement by the manufacturer using (10).

$$s(t) = s_0 \frac{e^{-\ln(2)t/25.5}}{e^{-\ln(2)t/64.8}} = s_0 e^{\ln(2)t(1/64.8 - 1/25.5)} \quad (10)$$

The breakthrough of each isotope,  $A_{82Sr}/A_{82Rb}$  and  $A_{85Sr}/A_{82Rb}$ , is calculated as a relative activity ratio of Sr activity to <sup>82</sup>Rb activity delivered as demonstrated in (11), below.

$$\frac{A_{82Sr}}{A_{82Rb}} = \frac{\hat{A}_{Breakthrough}}{1 + 0.48s(t)} \quad \text{and} \quad \frac{A_{85Sr}}{A_{82Rb}} = s(t) \cdot A_{82Sr} \quad (11)$$

The dose calibrator is sensitive to the radiation of <sup>82</sup>Rb decay which is a consequence of <sup>82</sup>Sr decay. The <sup>82</sup>Sr activity is not measured directly.  $\hat{A}_{Breakthrough}$  is the measured breakthrough activity by the dose calibrator after sufficient time has passed for the initial <sup>82</sup>Rb activity,  $A_{82Rb}$ , to decay. The equation corrects for the dose calibrator sensitivity to the different isotopes, their decay sequence and their abundance.

If the generator is reloaded with Sr, the <sup>82</sup>Sr/<sup>85</sup>Sr ratio,  $s(t)$ , becomes unknown, since there is contribution from both the remaining Sr isotopes on the column, and the new amount that is loaded. The breakthrough is calculated based on the assumption that all the breakthrough activity measured is contributed by <sup>82</sup>Sr. The <sup>85</sup>Sr breakthrough is calculated as a ratio of the calibrator sensitivity. This implicitly assumes is that all the activity is resulting from <sup>82</sup>Sr activity and that a corresponding amount of <sup>85</sup>Sr isotopes are also present. The bias in this estimate is intended to err on the safe side.

$$\frac{A_{82Sr}}{A_{82Rb}} = \frac{S}{R} \quad \text{and} \quad \frac{A_{85Sr}}{A_{82Rb}} = \frac{A_{82Sr}}{0.48 \cdot A_{82Rb}} \quad (12)$$

Health Canada guidelines dictate that breakthrough ratios must be less than  $2 \times 10^{-4}$  and  $2 \times 10^{-5}$  for  $^{85}\text{Sr}$  and  $^{82}\text{Sr}$  respectively [34]. In order to confirm that the breakthrough is less than these ratios, the  $^{82}\text{Rb}$  dose must be given enough time to decay below these levels, which corresponds to 19.8 minutes of decay to reach  $2 \times 10^{-5}$  of the original activity. This is the minimum time that must pass until the breakthrough measurement can be taken.

The ability to accurately measure the breakthrough depends on the sensitivity of the dose calibrator. The Capintec CRC-15R (Capintec Inc., New-Jersey) that was used during the development of the  $^{82}\text{Rb}$  Elution System is rated to a sensitivity of 0.002 MBq [35]. In order to measure  $2 \times 10^{-5}$  of the initial activity, the flushed dose during calculation must be at least  $0.002/2 \times 10^{-5} = 100$  MBq. In a clinical setting, the generator must be capable of eluting at least 500 MBq to ensure good quality scans. If the eluted  $^{82}\text{Rb}$  activity is insufficient to accurately measure breakthrough, the automatic measurement is skipped. The operator may manually enter the breakthrough activity from a more sensitive instrument.

### *Elution Tests*

The system behaviour must be tested to confirm that the supplied activity is accurate. During routine patient elution runs, confirmation of the output activity is based at the activity counter which is upstream from the patient outlet. If modeling of the system is accurate, then the activity at the patient outlet can be precisely determined based on readings from the activity counter. The system model was confirmed through testing of elutions.

As part of the design, test runs had to be implemented for all patient elutions. These runs execute the exact sequence of the corresponding patient run but include data collection from the dose calibrator. A data analysis follows the elution by producing activity rate and integral activity graphs as is done with calibration runs. A correspondence between the sets of theoretical and measured curves is the ultimate indication of accurate modeling of the system. If the curves agree, it can be deduced that the model of the system reliably determines the activity profile injected to the patient.

Elution tests can be treated as a cross between a calibration run, and a patient elution. Data collection from the dose calibrator and analysis reports are identical to calibration, however, the calibration constant is not recalculated. The elution sequence dictated by the elution parameters should be identical to regular patient elutions.

### 3.5 Software Design

A complete run sequence is composed of three main stages; pre-run, real-time sequence, and post-run. The real-time sequence stage was the main focus of the development and therefore will be covered in greater detail, while the other two stages will be briefly explained and demonstrated.

#### *Pre-Run Stage and the GUI-Sequence*

The pre-run stage is controlled by the *GUISequence* function which runs through a series of steps to interact with the user and collect relevant information to initiate the elution. The only interaction with external hardware is to test communication and status.

The opening screen displays a timer countdown until the next elution can be started (Figure 3-11a). This accounts for the minimum 10 min interval required between elutions. The countdown can be skipped if desired by pressing the skip button. Once the countdown completes the timer is replaced with an appropriate message as shown in Figure 3-11b. The screen can then be pressed to initiate the *GUISequence* function. If errors are detected during the initial testing an appropriate message is displayed and the program is halted as is demonstrated by Figure 3-12a. The sequence will not continue until all errors are resolved. In the case of a warning to the user, a dialogue is displayed and the sequence will continue upon acknowledgement (Figure 3-12b).

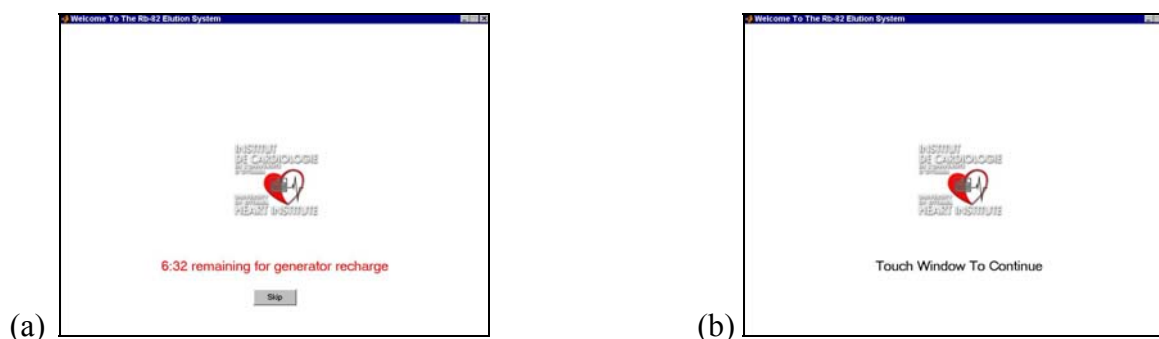


**Figure 3-11 - Opening message screen with generator recharge countdown timer (a) and without (b).**

The generator information screen is displayed first, which gives information as to the state of the generator activity and history. Following is a prompt for a user ID code, which is useful for avoiding tampering by unauthorized personnel as well as enabling test runs, which were commonly used during the development cycle, but have no clinical application. The user is then prompted to select a run type (Figure 3-12c). The options presented to the user

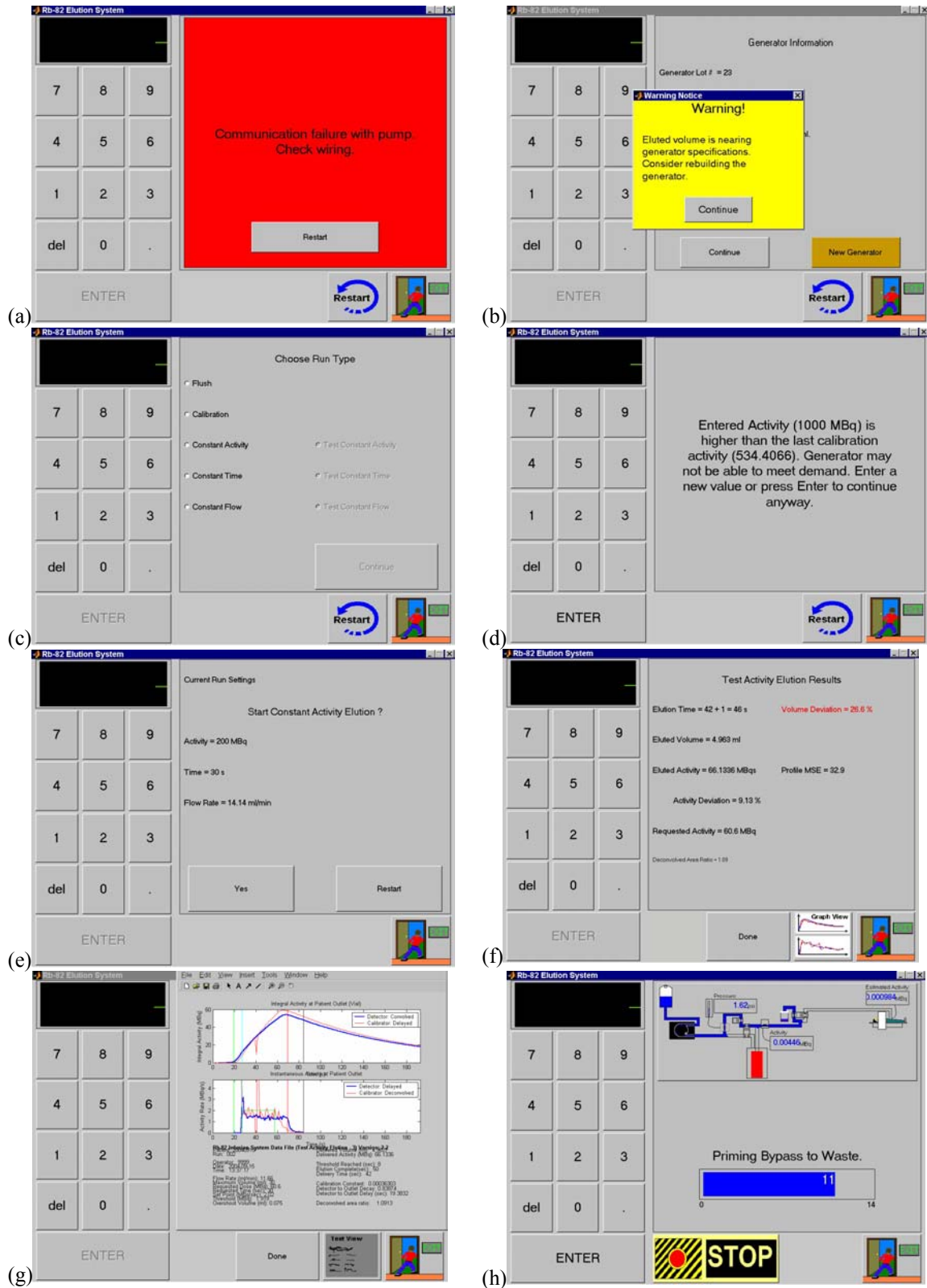


Figure 3-12 - Various screenshots of the GUI. (a) Error message. (b) Warning. (c) Data entry. (d) Out of range data. (e) Confirmation. (f) Elution results. (g) Elution graphs. (h) Elution stage and progress.

vary depending on the user ID, expiry of the generator, time since last flush, and time since last calibration. These considerations are aimed at ensuring that the generator is not used for clinical applications if it has expired. In addition it ensures that the daily protocol is followed, including a flush and calibration (including a test of breakthrough activity) at the start of each day.

Depending on the chosen run-type, the user is prompted for additional information such as patient number, dose activity, elution time, flow rate, priming of the patient line, etc. At all stages the input is checked for validity and warnings are presented to the user with detailed explanations (Figure 3-12d). If a calibration or test run is chosen, the Capintec dose calibrator is tested for communication and proper settings. Finally a confirmation screen (Figure 3-12e) is displayed with all the inputs for the user to review. After confirmation the real-time sequence is initiated with the proper settings set as global variables.

### *Post-Run Stage*

Although chronologically the real-time sequence follows, the post-run stage is discussed first due its relative simplicity. On termination of the real-time sequence one of three possible scenarios exists:

1. A successful run has terminated and the elution results must be presented.
2. An error has occurred during the real-time process and a proper message must be reported to the user.
3. The elution was aborted by the user using the *Emergency Stop* button, in which case an appropriate message screen should be displayed.

In the case of a successful run, the information presented to the user will vary based on the run-type (Figure 3-12f). With the exception of daily-flush runs, a view toggle button is presented on the bottom bar which enables to toggle between text results and a graphical report (Figure 3-12g). Two graphs are included of the instantaneous activity rate at the patient outlet and of the integral activity at the patient outlet as discussed in the calibration section.

If the termination of the real-time sequence was a result of an error or an emergency stop a window coloured red (Figure 3-12a) or yellow respectively is displayed. Error messages are as specific as possible given the available information. The messages include a description of the error and suggestions on how to resolve the issue.

After the post-run message has been displayed to the user the option of restarting the program is displayed. The program is completely restarted after each run through a call-back function which clears the entire workspace and restarts the software for the next operation.

### Real-Time Sequence

The real-time process is started by confirming the elution settings by the user. The *Hardware\_Interface* model is loaded to the RTWT, initialized with all the relevant parameters, and started. Once the start command is issued to the RTWT, the *GUISequence* terminates. On completion of the real-time process, a termination function is called which executes the post-run operations.

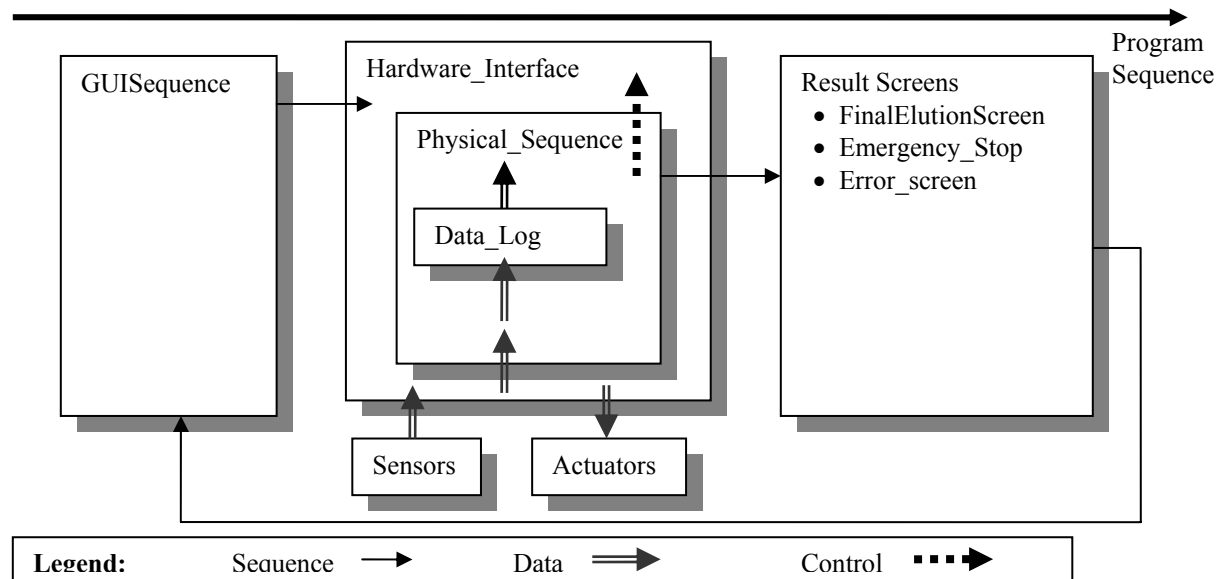


Figure 3-13 - Sequence, data, and control, flow and structure diagram of software.

The *Hardware\_Interface* model consists of several layers. At the lowest layer the *Hardware\_Interface* itself communicates with the hardware sensors and actuators. At the next layer the *Physical\_Sequence* model controls the sequence of elution steps acting as a state machine. At the topmost layer, the *Data\_Log* stores data from the *Hardware\_Interface* to global variables. These data are used for computations in the *Physical\_Sequence*, saving

of records to file, producing elution reports as part of the post-run stage, and calibration of the system. Figure 3-13 demonstrates the flow of control, data, and sequence of a full elution sequence.

### Hardware Interface

The *Hardware\_Interface* (shown in Figure 3-14) is a wrapper for the entire Simulink model which runs the real-time sequence. The model collects readings from the activity counter, pressure sensor, overflow switch, and elapsed time (green blocks). These readings are processed to control the actuators such as valves (magenta blocks), pump, and GUI. Internal variables (light blue blocks) are used for control of the *Hardware\_Interface* by the *Physical\_Sequence* block. In addition to the *Hardware\_Interface* models, the model consists of the *Software\_Interface* model and the *Valve\_Control* model. The *Valve\_Control* block controls the valves through real-time control to achieve constant-activity elutions, and is discussed in depth in Chapter 4:Elution Profile Control. The *Software\_Interface* block is a wrapper of the *Physical\_Sequence* block and collects the input data to a structured array.

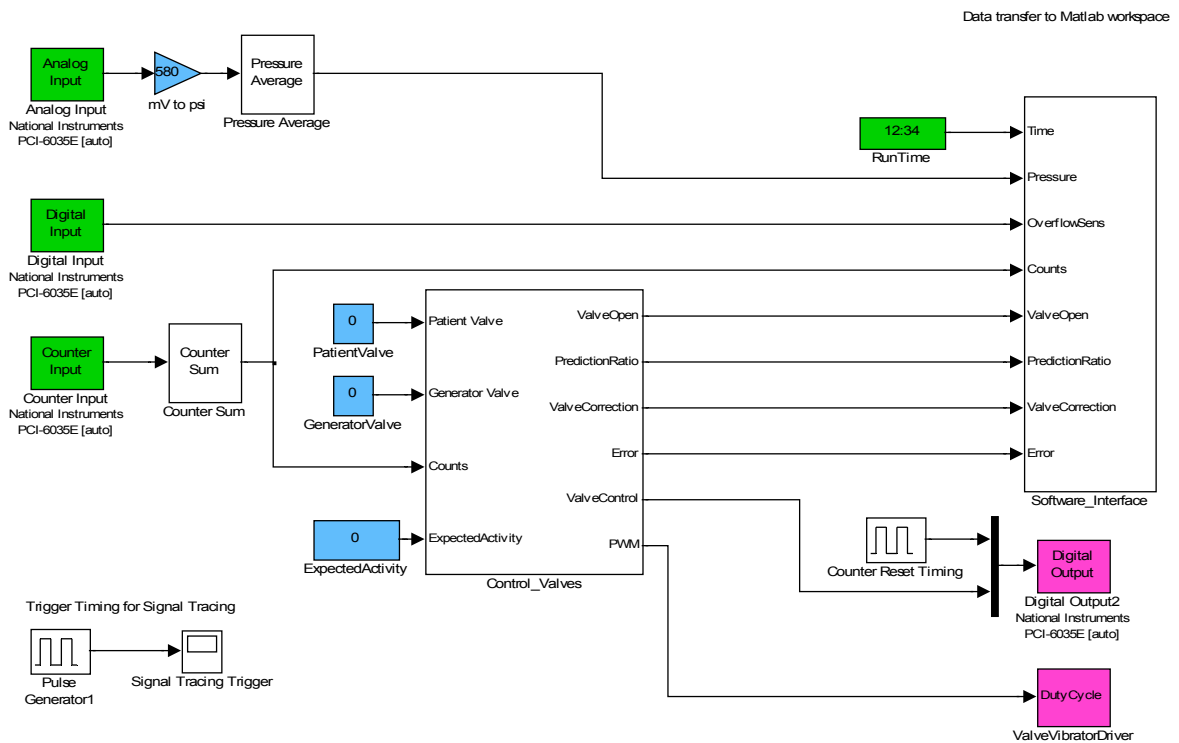


Figure 3-14 - The *Hardware\_Interface* model.

The DAQ general counter 1 (GPCTR1) is configured to accumulate on each input rise. This input is connected to the activity counter through TTL over coax cable. Over a typical elution the 24 bit counter can easily overflow, leading to data errors. To avoid this problem it is desirable to reset the counter after each reading by the software; a feature that is not supported by the Simulink drivers. In the prototype system this issue was elegantly solved by connecting the counter external reset to a digital output on the DAQ. The *Hardware\_Interface* periodically resets the counter in synch with reading of the counter value.

Other sensors are straightforward to interface; the pressure sensor is read by an A/D converter and the overflow switch is a binary input. The pressure and counter readings are both conditioned through an averaging filter. This is achieved through a simple delay line and averaging of all the readings over the past second. Since each is read at 20 samples per second, the averaging is over 20 samples. The pressure sensor readings are converted to PSI units through multiplication by a calibration constant (determined to be 580 through empirical calibration with an external gauge). Recalibration after 1 year showed no significant change in this calibration constant.

### *Physical Sequence*

All the elution types comprising the daily protocol are composed of similar physical steps as shown in Figure 3-15. A single physical sequence that is controlled by the parameters of each elution is desirable. The parameters in Table 3-2 dictate the physical sequence of the elution.

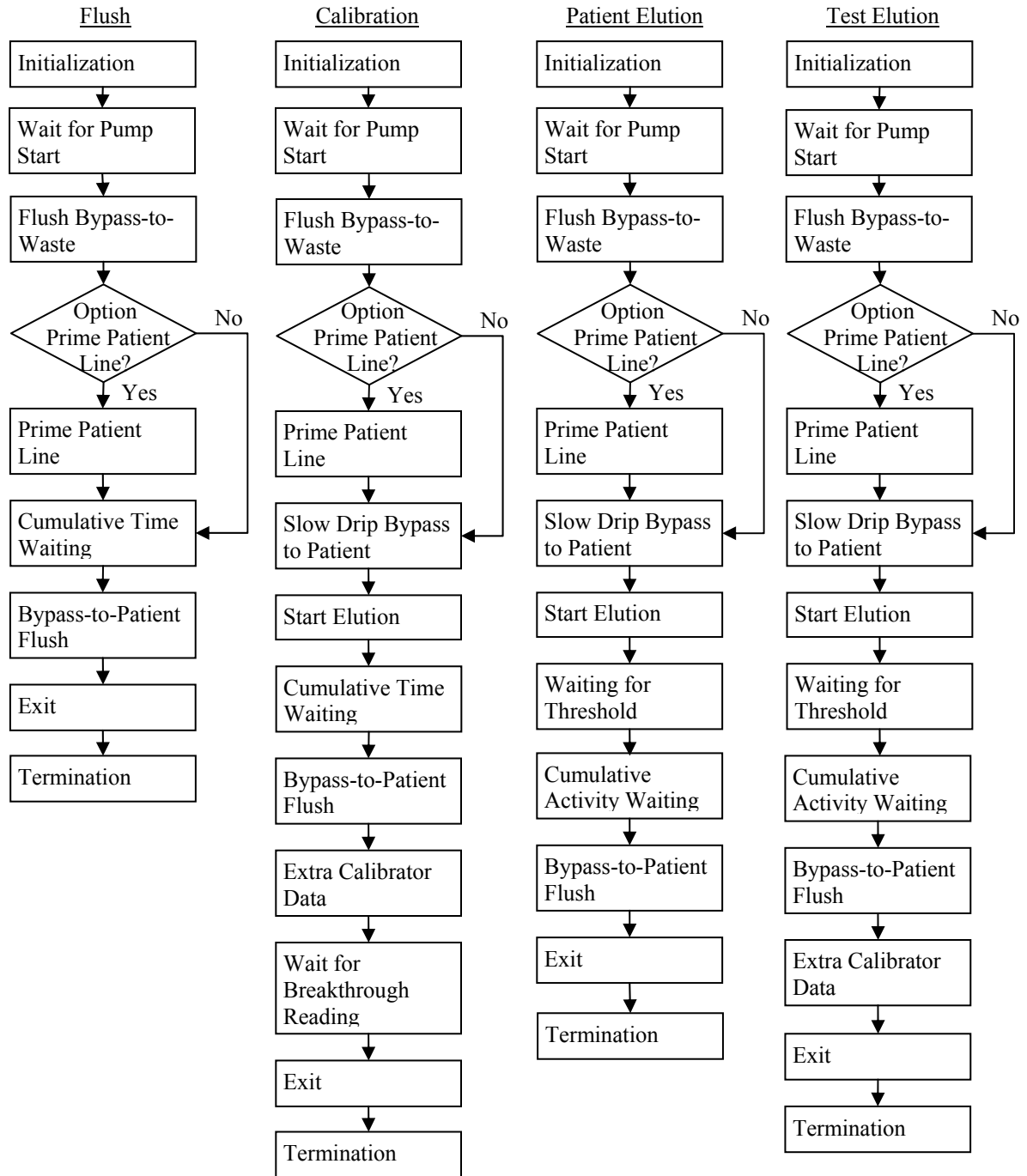


Figure 3-15 - Flow Chart for all elution types. The similarity in form justifies the implementation of a single physical sequence state machine.

**Table 3-2 – Elution parameter values for each run type.**

Parameter	Flush	Calibration	Constant-Activity	Constant-Time	Constant-Flow	Constant-Activity Test	Constant-Time Test	Constant-Flow Test
Prime patient line	U.D.	U.D.	U.D.	U.D.	U.D.	U.D.	U.D.	U.D.
Elution Activity	∞	∞	U.D.	U.D.	U.D.	U.D.	U.D.	U.D.
Elution Flow Rate	15 ml/min	15ml/min	Calc.	Calc.	U.D.	Calc.	Calc.	U.D.
Maximum Elution Volume	50 ml	15 ml	30 ml	15 ml	30 ml	30 ml	15 ml	30 ml
Elution Time	200 s	60 s	U.D.	U.D.	60 s	U.D.	U.D.	60 s
Elution Set Point	∞	∞	Calc.	∞	∞	Calc.	∞	∞
Threshold Activity Rate	0	0	Calc.	0.5 MBq/s	0	Calc.	0.5 MBq/s	0
Overshoot Volume	0	0	0.075 ml	0.25 ml	0.25 ml	0.075 ml	0.25 ml	0.25 ml
Calibrated run	'no'	'yes'	'no'	'no'	'no'	'yes'	'yes'	'yes'
Calculate Calibration Constant	'no'	'yes'	'no'	'no'	'no'	'no'	'no'	'no'
Legend: Calc. – Calculated U.D. – User Defined								

The real-time sequence is based on a state machine composed of eleven discrete states (Figure 3-15), not including the initialization and termination of the component. The *Physical\_Sequence* was implemented as an M-file S-function, which is a Simulink block that is implemented in Matlab code. Although execution requires an interpreter at real-time (adding a significant processing overhead), it greatly simplifies development. Matlab provides services to compile the M-file S-function into executable code (DLL file), providing improved performance and better protection of intellectual property. Compilation, however, requires some customization of the Matlab code and is a fairly involved process. It was therefore decided to use the interpreter during the development stage.

### *M-file S-functions*

The Matlab and Simulink framework dictates a strict yet flexible template for all Simulink blocks implemented through Matlab code. The framework describes a complete

state machine through two main stages that are executed each iteration. The Update stage checks conditions to change state and is also used to initialize the upcoming state. The Output stage conducts the operations associated with the current state, such as recalculating outputs and updating a display. In addition, an initialize stage is called when the object is loaded and a terminate stage is executed just prior to closing the object. The RTWT manages the current stage (Initialize, Update, Output, or Terminate) to the M-file S-function by passing a stage parameter on each S-function call.

Parameters are passed to the physical sequence through global variables, while the real-time collected data are passed through the Simulink block inputs. These inputs include the various sensor data, elapsed run time, accumulated generated flush time, and other measures of the valve control block. The simplicity through which this block can be integrated in the Simulink implementation raises an important question: which functionality should be implemented in Simulink, and which should be programmed as part of the S-function? As a general guideline it was decided to leave only the sensors data, real-time clock, and any results of the real-time valve control block as inputs to the *Physical\_Sequence* block for the sake of simplicity. All the computational, graphical, and data collection functionality is implemented through the *Physical\_Sequence* S-function.

The inputs to the *Physical\_Sequence* function were collected and structured by the *Software\_Interface* block within the *Hardware\_Interface*. The *Physical\_Sequence* function is called through the use of a function call block within the Simulink model. The implementation is shown in Figure 3-16 where the long vertical bar acts as a multiplexer and combines all the inputs into a single array. The zero-order holds are all run at the same rate, which is set by a local parameter  $T_s = 1$  s, and are intended to convert all inputs to the function's sampling rate.

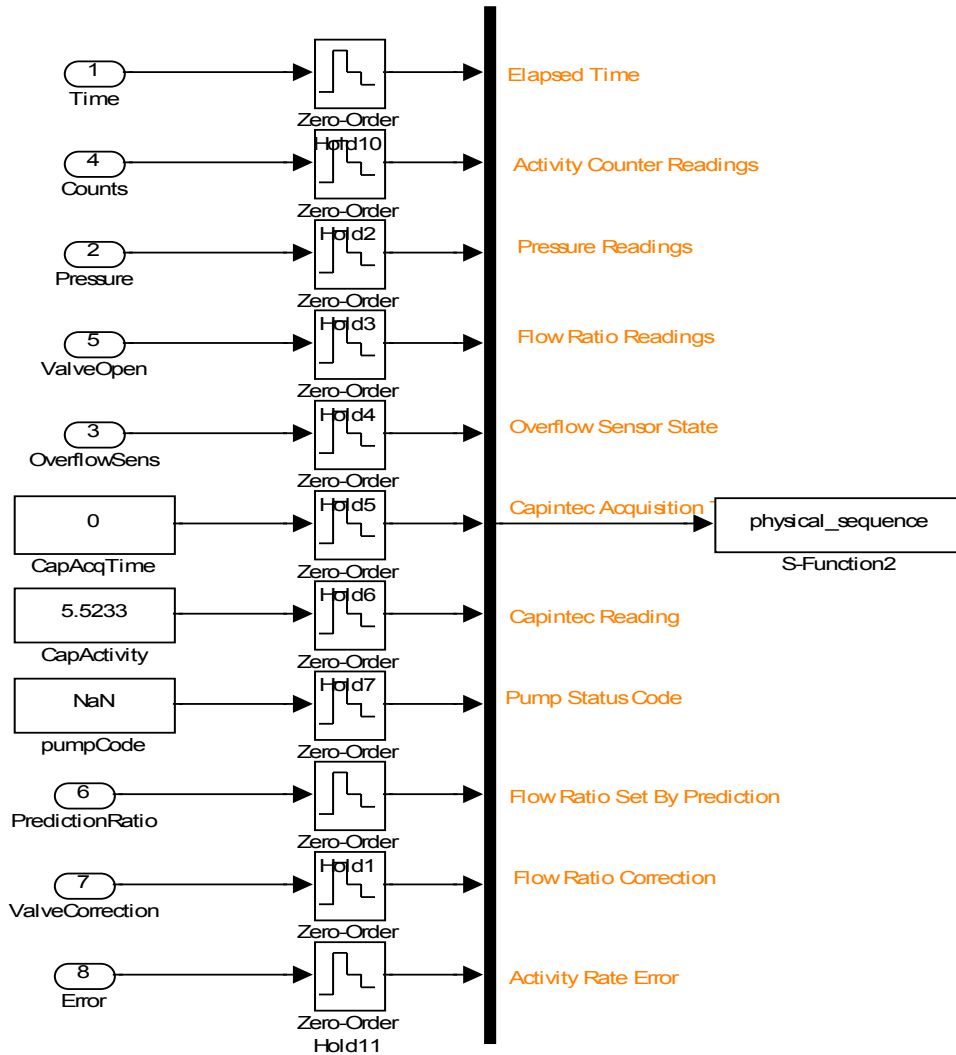


Figure 3-16 - Inputs to the *Physical\_Sequence* M-file S-Function block.

*The Physical Sequence*

The *Physical\_Sequence* code utilized the Update and the Output stages of the M-file S-function for separate tasks. The Update stage determined the state for the next iteration based on the current state, the type of elution run, and the accumulated data. When a state transition is initiated, the next state is initialized by preparing the GUI for the next state, computation of variables, and sending commands to the actuators. The *Output* stage performs updating operations within the current state. This includes updating the actuators and GUI while performing real-time data gathering and computations. The Update and Output stage tasks overlap only in the sense that the Update stage performs Output tasks only as an initialization of a stage that should occur at a single instance of stage transition. In

summary, the Update stage updates the state of the state machine and initializes the next step (routines that are carried out a single time at the beginning of a state), while the Output state maintains the actuator states and GUI during the state.

The Update stage is composed of a large switch-case statement for each of the sequence states and condition statements for transition to subsequent states. If the transition condition is met for the current state an initialization of the next state is executed and the function return value is set to the next state code. The states and their termination conditions are listed in Table 3-3.

**Table 3-3 – *Physical\_Sequence* states and their termination conditions. As long as a termination condition is not met, the state is maintained unchanged.**

State Name	State Description	Termination Condition		Next State	
Wait for Pump Start	Wait until pump driver is loaded and pump starts.	Pump is running after less than 2 restart tries		Flush Bypass to Waste	
		Else		Error is set (Termination follows)	
Flush Bypass-to-Waste	Bypass route (from pump to patient stopcock) is flushed to the waste.	Enough time has elapsed to prime lines	Prime Patient Line?	Option Prime Patient Line	
			Else	Flush run?	Slow Drip Bypass to Patient
			Else		Cumulative Time Waiting
Prime Patient Line	Patient line (from patient cock-stop to patient) is flushed to the patient.	Enough time has elapsed to prime patient line	Flush run?	Cumulative Time Waiting	
			Else	Slow Drip Bypass to Patient	
Slow Drip Bypass to Patient	A slow drip to the patient line until the continue button is pressed.	Continue button is pressed	Threshold activity exists	Calibration or flush run	Cumulative Time Waiting
				Else	Cumulative Activity Waiting
			Else		Waiting for Threshold
Waiting for Threshold	Elutes from generator to waste until the threshold activity is reached, or the time has expired.	Threshold activity rate is reached	Calibration or flush run?	Cumulative Time Waiting	
			Else (elution or test)	Cumulative Activity Waiting	
		Threshold not reached – timed out		Error is set (Termination follows)	
Cumulative	Elute activity	Requested time has passed		Bypass Patient	

Time Waiting	from the generator for a given time.			Flush
Cumulative Activity Waiting	Elute the activity until the required dose is reached or time expires.	Requested dose reached		Bypass Patient Flush
		Requested dose not reached – timed out		Error is set (Termination follows)
Bypass-to - Patient Flush	Flush the remaining activity in the line to the patient.	Enough time has elapsed to flush activity from lines	Flush or patient run	Exit
			Else (calibration or elution test)	Extra Calibrator Data
Extra Calibrator Data	Gather additional data from dose calibrator for convolution comparison.	Enough measurement time has elapsed	Calibration run	Wait for Breakthrough Reading
			Else	Exit
Wait for Breakthrough Reading	Wait for decay to read breakthrough from dose calibrator.	Enough time has elapsed or user has aborted measurement		Exit
Exit	Dummy State indicating that sequence was gracefully completed.			<i>Physical_Sequ</i> <i>ence</i> termination function

The Output is implemented using an identical switch-case statement determining the operations during the current state. However, there are additional functions that are carried out regardless of the current state. One such task is error detection, which is carried out through a series of tests on the input data. Another common task is data logging (implemented by *Data\_Log* function), which is enabled once actual elution from the generator is started. Finally, the real-time system diagram is updated by rewriting the current measurements and calculations to the GUI fields.

### 3.6 Error Detection

A variety of error detection mechanisms have been included in the software to handle hardware malfunctions as well as software errors. Error trapping is included in all phases of the program and leads to immediate termination of an elution with an error message which guides the operator towards resolution of the error. Table 3-4 lists the errors that the system may detect and their corresponding internal error flag. At the beginning of the application the

error flag is set to zero. If at any point the flag changes to a value other than zero, the elution will terminate with the error message screen.

**Table 3-4 - Detectable errors and their corresponding flags.**

<b>Error Code</b>	<b>Message</b>
<b>Pressure</b>	
10001	High pressure encountered. Check bypass and waste lines.
10002	High pressure encountered. Check bypass and patient lines.
10003	High pressure encountered. Check generator and waste lines.
10004	High pressure encountered. Check generator and patient lines.
10005	High pressure encountered while pump should be stopped. If the problem persists contact the developer.
<b>Pump – communication</b>	
20001	Pump communication error. Check pump control cable and power and restart the elution.
20002	Pump version mismatch detected. Contact the developer.
<b>Pump – operation</b>	
30001	Pump stalled. Check proper line position in pump head and ensure that there are no obstructions.
30002	Pump should be running and is not. Restart the elution. If the problem persists contact the developer.
30003	Pump should be stopped and is running. Restart the elution. If the problem persists contact the developer.
30004	Pump failed to start. Restart the elution. If the problem persists contact the developer.
<b>Computer Resources</b>	
40001	Time has stalled during run. Contact the developer if problem persists.
40002	Error while backing up calibration file. Restart the system.
40003	Error while writing calibration file. Restart the system.
40004	Error while writing elution file – extension exceeds limit. Use a new patient number.
40005	Error while writing elution file. Restart the system.
40006	Error while loading INI file. Restart the system.
40007	Error while loading CAL file. Restart the system.
40008	Error while loading elution file. Restart the system.
40009	No calibration file found for today. Conduct calibration run before proceeding.
<b>Positron Detector</b>	
50001	No counts read by positron detector. Check wiring to interface box.
50002	Threshold activity not reached. Check plumping for air bubbles and blockage and ensure that the generator is properly connected.
50003	Threshold activity could not be found in calibration curve. Recalibration may be necessary.
<b>Capintec Dose Calibrator</b>	
60001	Communication error with Capintec dose calibrator encountered during elution. Check connection between computer and calibrator and restart the elution.
<b>Maintenance</b>	
70001	Waste container full. Empty container and restart elution.
<b>Software</b>	
90000	Unexpected procedure step encountered. Contact the developer.
90001	Unpredicted termination of Physical Sequence. Contact the developer.
90002	Unexpected Run Type value detected. Contact the developer.
90003	Real-time processes not responding on clean up. Contact the developer.
90004	Illegal desired pump state passed. Contact the developer.
Otherwise	Unknown error code reported. Contact the developer.
<b>User Intervention</b>	
<b>Error Code</b>	<b>Meaning</b>
-1	Termination of elution and exit issued by operator
-2	Emergency stop button pressed
0	No error reported and no user intervention.

The error flag may receive two identifiers relating to user intervention. Error flag code -1 (negative one) relates to termination and exiting of the software by the operator. The software will abort the elution, set all actuators to their safe mode, and display the exit screen. Error flag code -2 (negative two) corresponds to the user pressing the emergency stop button during an elution. The program will likewise terminate and set the actuators to their safe modes, and finally present a yellow screen indicating the operator has terminated the elution.

### ***Pressure Errors***

Pressure errors are included only for cases when the pressure rises above a threshold (20 PSI, 138 kPa) for a prolonged period of time (over 3 seconds). High pressure is an indication of a blockage or pinched line and could result in backwash through the pump head or rupturing of the saline lines. When backwash occurs, the effective flow rate is lower than expected, introducing error to the transport delay and control algorithms.

Each pressure measurement at the physical sequence level corresponds to an average of 20 hardware readings over the previous one second. This mechanism is included to reduce the effect of outliers, which could lead to false error detection. An appropriate message is generated based on the state of the valves at the time of error detection. This message is intended to guide the operator to the problematic lines.

### ***Pump Communication and Operation Errors***

Pump communication is over an RS-232 serial connection with a software implemented polling algorithm (every 400 ms). Loss of communication to the pump is a critical error and it is therefore important to set the valves to their safe modes, so that elution to the patient does not continue if the pump fails to stop. The pump software version is also verified on initialization as an additional safety measure.

As the pump is polled, its status is verified to ensure that it correlates with the physical sequence stage. Timing windows of 3 seconds have been included to allow sufficient time for communication and response. The pump is also capable of reporting stalling of the pump head due to increased mechanical resistance.

### ***Computer Resources***

Errors relating to the computer and software are abundant. File access errors are checked and reported throughout the software. In addition time stamps are checked during the real-time application. If time stamps are lost, the software can no longer reliably control the real-time process. This issue has come up at the prototype system, where computer resources were over consumed. This test is still included mostly as a diagnostic tool for the developers.

### ***Positron Detector Errors***

Errors corresponding to the activity (positron) counter exist on two levels. The first ensures hardware functionality by verifying that some counts (background activity) are always being detected. Background activity is unavoidable and should result in some counts. If the counter value is unchanged over 5 consecutive seconds, an error is reported. At a higher level the software ensures that a threshold activity is reached within a given time window. This tests that sufficient activity is eluted from the generator as expected.

### ***Dose Calibrator Communication Errors***

Although the dose calibrator is tested prior to every calibration or test run for proper settings, it is also tested for communication errors during the elution. This is intended to ensure that it is not unplugged or turned off during the calibration or test resulting in false readings.

### ***Maintenance***

This test includes testing of the waste container overflow switch. If the waste container is found to be full in the first 5 seconds of the elution, the elution is aborted with a proper message. This is to avoid overflow of the waste leading to a spill inside the cart and onto the printer, PC, UPS, or power cords on the lower shelf. If overflow is detected during the elution, but after the first 5 seconds, a warning message is displayed at the end of the elution and the next elution will not start until the waste container has been emptied. However, the elution continues without interruption to avoid aborting an elution needlessly (a sufficiently large reserve is present in the waste container to complete the elution).

### ***Software Errors***

As a final measure, error mechanisms are included to test the software itself. If an invalid physical sequence stage or a run type is set, then an error code is set. If the real-time sequence stops prematurely (before the exit stage of the physical sequence), this is an indication that an error has been detected by the real-time kernel. Finally, if the pump communication driver does not terminate and clear in time (within 1.5 s) this too is reported as a software error. All these errors are intended for the developer for diagnostic purposes and are indication of errors in the software itself.

### ***Warnings***

Warning messages (Figure 3-12b) are intended as important messages that should be addressed immediately, but are not critical to the success of an elution. The list below indicates the warnings that may be generated:

- Total volume eluted through the generator is above (90%) the specification volume for clinical use.
- Calibration constant has varied more than 10% from the evolving average.

### ***Outlier Highlighting***

As the system is redundant in design, certain measurements can be tested by comparing to expected values. One such measurement is the calibration constant for the activity counter which is computed in each daily calibration run. The calibration is computed based on the daily run, but is then compared to an evolving average to ensure variations less than 10%. Similarly the activity eluted during calibration and flush runs is compared with the activities of the previous day. These activities are corrected for <sup>82</sup>Sr decay which results in lowered activity as the generator ages.

Patient elution and test runs are tested for discrepancy with the expected values of eluted activity and eluted time. Although eluted activity is monitored as a stopping criteria for all runs, variations can occur due to response time, overshoot, or if the total activity is not reached. Variation between the requested time and actual elution time for constant-time and constant-activity elutions is an indication of the accuracy of the flow rate prediction and control algorithm respectively.

If any of the above variations exceed 10% of the requested value, the variation statistic is highlighted in red. This serves as an indication to the user that the elution did not complete as expected and attention to the system may be necessary.

### 3.7 System Refinement

#### *Dose Calibrator Spike Removal Algorithm*

During experiments with the system, spikes of activity were recorded from the dose calibrator as the activity rose above 500 MBq. By monitoring the dose calibrator display during several elutions it was confirmed that the spikes arise from the dose calibrator itself and not from the RbES or the communication protocol. As the activity in the dose calibrator rises, it switches scales to avoid saturation. This scale transition is not smoothed, lasts approximately 5 seconds, and is uncontrollable. Furthermore, the peaks can be in the form of an increase or decrease in measured activity or combination of the two in the form of two consecutive peaks. These peaks can vary by many orders of magnitude from the actual measurement.

It was determined that during calibration runs, the spikes have a significant effect on the calibration constant in some, but not all cases. To accommodate this artefact, an algorithm was implemented to remove these spikes. A search window of 7 seconds was passed over the entire curve to locate the ratio,  $r_p[i]$ , between the center activity and the average of the two extreme readings. If the maximum ratio in the entire series is considered significant by (13) where  $T_p$  is a threshold ratio, all the readings in the window are deleted and interpolated from adjacent values. The process is repeated, until no more significant peaks are found.

$$\max\{\log(r_p[i])\} = \max\left\{\log\left(\frac{2 \cdot A_{cal}[i]}{A_{cal}[i-3] + A_{cal}[i+3]}\right)\right\} > T_p \quad (13)$$

With  $T_p$  set to 0.1 good results were obtained. Almost all peaks were removed, while the overall curve shape appeared to be unchanged. Figure 3-17 demonstrates the same calibration results with and without the peak removal algorithm. The corresponding MSE changed from 39,959 MBq<sup>2</sup> to 1084 MBq<sup>2</sup> and the calibration constant changed from  $3.679 \cdot 10^{-4}$  to  $3.724 \cdot 10^{-4}$  which is substantially closer to the average calibration constant ( $3.777 \cdot 10^{-4}$ ).

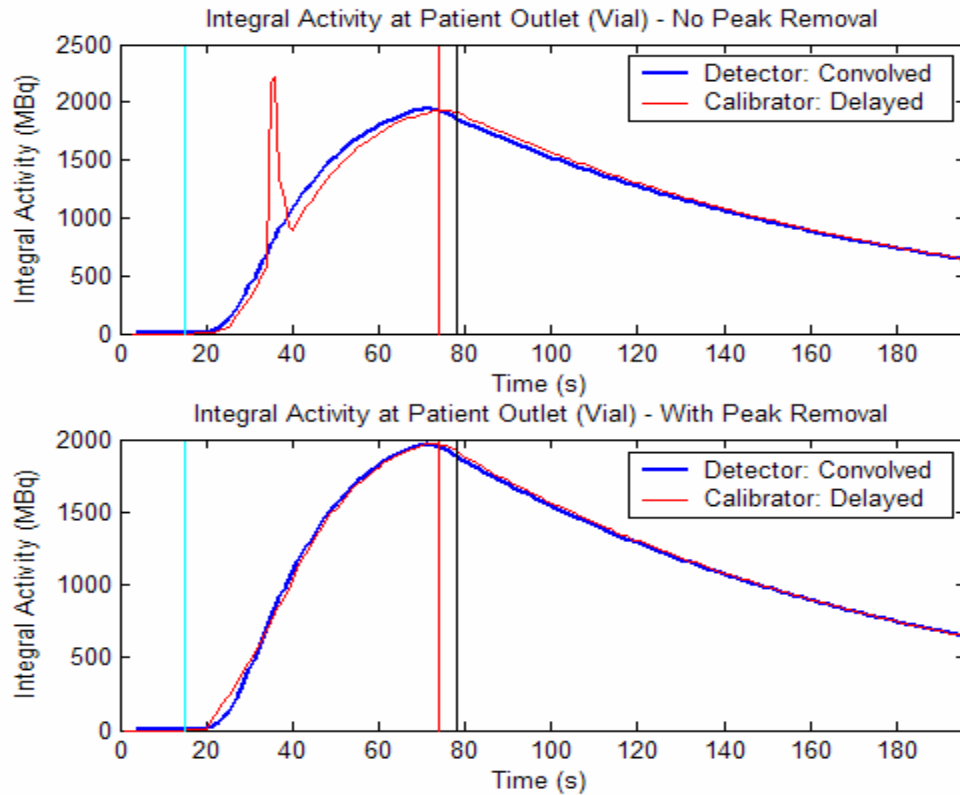


Figure 3-17 – Calibration results with and without the dose calibrator peak removal algorithm.

### 3.8 Summary

The  $^{82}\text{Rb}$  elution system (RbES) was based on experience with the first generation system and took into account decisions made when developing the prototype of the second generation system. The requirements were identified and served as a guideline throughout the development process. These requirements focused primarily on safety and reduced exposure to both the operator of the system and to the patient. The complete framework handled all aspects of the daily protocol, physical sequence, error detection, and user interface.

All requirements were met with the exception of improved constant-activity control. The design of the system ensured enough flexibility to continue development of the control system at a later stage and with no significant change to the existing infrastructure. Both the *Hardware\_Interface* and *Physical\_Sequence* models allowed for modification as necessary while maintaining the software design. The development of the constant-activity control is described in the following chapter.

## Chapter 4: Elution Profile Control

The primary motivation for developing the second generation <sup>82</sup>Rb elution system (RbES) was to introduce the tracer to the patient at a fixed rate of activity (measured in MBq/s) over a prescribed time period. When plotting the activity rate over time, in this context referred to as an elution profile, a rectangular curve is desired. As with any control system the goal is to achieve output behaviour as close as possible to a desired profile. In the case of a constant output, one can compute a set-point (detector count rate) that corresponds to an ideal output. One must then attempt to minimize the deviation between this set point and actual output. Typically output error is kept to a minimum by including feedback mechanisms which the control algorithm manipulates to control the actuators.

A generator bypass line was already included in the first generation <sup>82</sup>Rb elution system to permit flushing of activity to the patient outlet at the end of an elution. The valve in place was a two-way solenoid pinch valve that could either direct flow through the generator or the bypass line at any given time. In addition, an activity counter was included in the design to allow data collection and monitoring of the elution of activity. With these elements in place the problem was reduced to developing a controller capable of directing saline through the generator or its bypass line by actuating the generator valve in order to achieve a constant rate of activity using feedback from the activity counter.

The control algorithm presented in the prototype system [18] used a simple threshold comparison, which was only intended to demonstrate the feasibility of eluting at a constant-activity rate. If the measured activity rate was higher than the set point, saline flow would be directed through the bypass line. If activity rate dropped below the set point, flow was directed through the generator. The set point was calculated based on the desired activity rate at the patient outlet and was corrected for transport delay as is shown in (14).

$$p = \frac{1}{K} \cdot \frac{A_{Req}}{T_{Req}} \cdot e^{-\lambda \frac{V_{CO}}{f}} \quad (14)$$

The set point,  $p$ , denotes the number of counts per second to be measured by the activity counter to achieve the desired rate at the patient outlet. This rate is converted to raw detector counts, using the calibration constant  $K$ . The rate at the patient outlet is computed based on the requested activity,  $A_{Req}$ , and the requested elution duration,  $T_{Req}$ . The desired

activity rate is corrected for the  $^{82}\text{Rb}$  decay during transport delay through the volume of the lines from the activity counter to the patient outlet,  $V_{\text{CO}}$ , at a constant flow rate,  $f$ .

The threshold comparison algorithm presented by Epstein *et al.* [18] was used as a benchmark for evaluating changes in performance during this research and was therefore maintained as an optional elution mode. As expected, the threshold comparison control results in fluctuations of activity rate around the desired activity rate as is demonstrated in Figure 4-1 for 50% relative activity elution over 30 s. The fluctuations typically had a 2-4 s period depending on the flow rate and activity concentration from the generator. The relative amplitude of the fluctuations was approximately 30-40% of the set point.

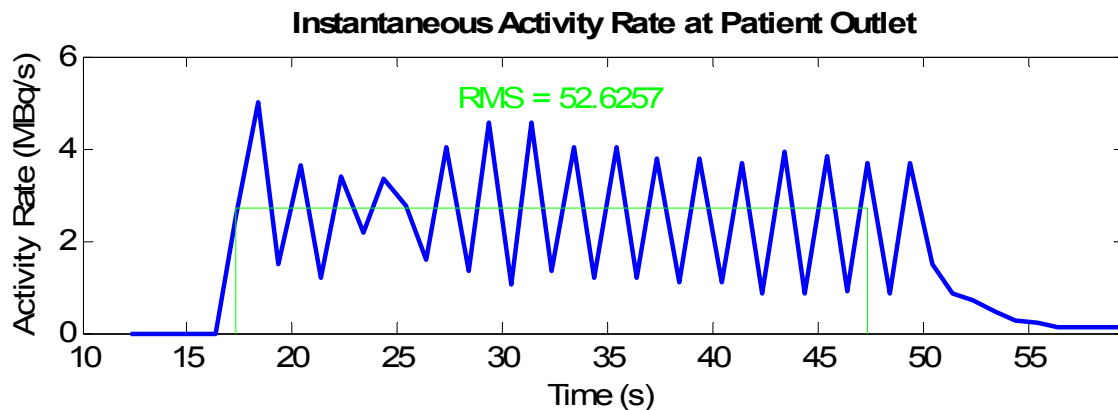


Figure 4-1 - Elution of 50% bolus activity within 30 s using a simple threshold comparison algorithm as described in [18]. The actual activity rate at the patient outlet (blue) since the beginning of the elution is compared to the desired result (green).

This chapter details the work performed on the control algorithm with the aim of improving the precision of the control algorithm while maintaining, or improving, other performance characteristics. These characteristics include maximizing the range of relative activities that can be eluted in order to maximize the useful life span of the generator. In addition, the range of elution durations should be maximized to enable experimenting with the optimal elution profile for accurate perfusion measurements. In general, the goal is to increase the flexibility of elutions while improving the precision of the elution system with the threshold comparison approach serving both as a starting point and a benchmark to which changes can be compared.

#### 4.1 **Threshold Comparison Algorithm with Auto-tuning Hysteresis Correction (HC-TC)**

Initial analysis of the threshold comparison algorithm revealed that elutions ran longer than requested indicating a reduced effective activity rate. The prolonged elution time was assumed to be a direct result of the hysteresis of the valve. Hysteresis refers to a system behaving differently depending on the direction of change of an input parameter [36] usually due to delayed response. In this case, the valve opening and closing latencies differ. The hysteresis was accommodated by factoring the set point,  $p$ , using a hysteresis factor,  $H$ .

The hysteresis correction factor,  $H$ , describes the on/off switching characteristic of the generator valve and is expected to change over time with material fatigue, tubing wear, or other factors. Therefore parameter  $H$  needs to be tuned continuously. The auto-tuning algorithm adjusts  $H$  depending on the difference between the actual and requested elution time,  $\hat{T}_{Elution}$  and  $T_{Req}$  respectively as is shown in (15). The time variation is factored with  $H$  and an adaptation constant  $\gamma_H$ . With  $\gamma_H$  chosen small enough (0.01 in our case) the system is ensured to not change significantly due to outliers but evolve slowly over time. Factoring of  $H$  is not crucial in this case where  $H \approx 1$ , but is intended to ensure incremental changes,  $\Delta H$ , that are orders of magnitude less than  $H$ . To further reduce the influence of outliers, changes to  $H$  that are larger than a tolerance interval (5%) are rejected with a proper warning to the user.

$$\Delta H = \gamma_H \cdot H \cdot (\hat{T}_{Elution} - T_{Req}) \quad (15)$$

Parameter  $H$  was manually set to 1 and over the course of 20 random 30 s elutions ranging from 10-70% relative activity,  $H$  evolved to a value of 1.09. Parameter  $H$  showed little change over the next 30 elutions, however it was noticed to vary slightly with repeated runs at extreme relative elutions (<20% or >60% relative activity). Variation of  $H$  at extreme relative activities is likely due to other limitations in the system (insufficient activity in the generator, varying activity concentrations from the generator, and others) making it difficult to achieve the requested elution; the hysteresis mechanism attempts to compensate for these limitations.

Although this hysteresis factor resulted in smaller accuracy error numbers, the t-test (p-values in Table 4-1) indicates that these are not statistically different - partly due to the large standard deviation of elution time errors.

**Table 4-1 - Comparison of elution time accuracy using the threshold comparison algorithm with (HC-TC) and without hysteresis correction.**

Relative activity [n=10]	Flow Rate (ml/min)	Time Accuracy (%)		p-value
		No hysteresis correction	Hysteresis correction (HC-TC)	
10%	5	2.3±4.2 %	-1.0±2.3	0.062
30%	11.67	-1.7±2.3 %	-1.7±2.3	1
50%	18.33	3.3±4.7 %	3.0±5.1	0.88
70%	25	11.0±4.5 %	9.0±4.7	0.37

Although the hysteresis compensation may slightly improve the elution time precision, it does not reduce the activity rate fluctuations. To overcome the fluctuations a completely different approach was investigated.

## 4.2 Variable Flow Control

To overcome the fluctuations inherent in the simple threshold comparison algorithm, the on/off valve had to be modified to a variable valve. As explained in the previous chapter the use of a variable valve was abandoned following earlier studies due to complexity, poor reliability, and mostly due to slow response characteristics. Instead, the solenoid control signal could be modified to simulate a variable valve in two ways.

### Cycling Valve Control

An on/off valve that periodically cycles between the two states can be used to simulate an analogue valve. The valve is set to open and close at a constant frequency, but the time that it is open is varied by changing the width of the control pulse. Pulse Width Modulation (PWM) can be regarded as varying the average time that that valve is open to the generator path and therefore varying the ratio of flow between the two paths (Figure 4-2). In effect, setting the pulse width varies the duty-cycle of the control signal in the range of 0-100% where 100% corresponds to a full saline flow through the generator and 0% corresponds to full flow through the bypass line.

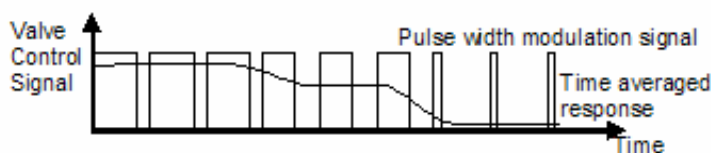


**Figure 4-2 - Pulse-width-modulation control of a solenoid valve to simulate a variable pinch valve. Flow through the generator increases as the duty-cycle is increased.**

### Transient State Control

Theoretically, by further increasing the frequency of the valve control, the valve can be forced to “hover” in a transient position [37]. The valve behaves as a low pass filter of the

control signal and the actual magnetic field generated by the solenoid is less than the full operating field strength. Precise tuning of the duty-cycle can force the solenoid and spring applied forces to cancel out with the resulting plunger position in a transient state. As with the cycling valve, varying the duty-cycle controls the valve position. The exact signal frequency is not critical, so long as it is higher than the valve's natural frequency and low enough that it can be generated by the driving circuitry.

### *Implementation of the Variable Flow Control*

Both approaches are identical in implementation and vary only in PWM frequency. While transient state actually implements a variable valve, the cycling valve only simulates variable control through time integration. Therefore, the transient state is advantageous if it can be implemented successfully.

Implementation of the PWM valve was achieved using one of two general purpose counter/timers (GPCTR) included in the DAQ. The GPCTR can be operated in several modes to serve different purposes. One such mode is an externally triggered counter as was used for the activity counter. Another mode is a continuous rectangular pulse generator. The counter is triggered by an internal 100 KHz clock while two registers are set to indicate the number of counts generating a high output and the number of counts generating a low input. The output of the counter was routed to the generator valve buffer (Crydom solid-state relay) which generates the current needed to actuate the valve.

To set the registers the counter must be stopped, initialized, and restarted using a dynamic-link library (dll) provided by National Instruments. A Matlab-Simulink driver was written that accepts the cycling frequency as a parameter and the duty-cycle as a continuous input and sets the registers whenever the duty-cycle is updated. The counter register values are computed using (16) and (17) where  $\nu_{\text{clk}}$  represents the counter clock frequency (100 KHz),  $\nu_{\text{valve}}$  is the valve cycling frequency and  $\Pi$  is the duty-cycle of the valve's actuating signal.

$$n_{\text{High}} = \nu_{\text{clk}}/\nu_{\text{valve}} \cdot \Pi \quad (16)$$

$$n_{\text{Low}} = \nu_{\text{clk}}/\nu_{\text{valve}} \cdot (1-\Pi) \quad (17)$$

### Valve Response Measurements

In order to accurately control the effective flow ratio, the valve response had to be measured for various cycling frequencies. It is desirable that the cycling be fast enough to produce undetectable fluctuations in the activity leading to smooth activity curves. In addition, the valve flow ratio response to duty-cycle should be controllable throughout the entire range (0-100% valve flow ratio). To test the transient response a frequency of 100 Hz was used, while 2, 5, and 15Hz frequencies were used to measure the response in the valve cycling range.

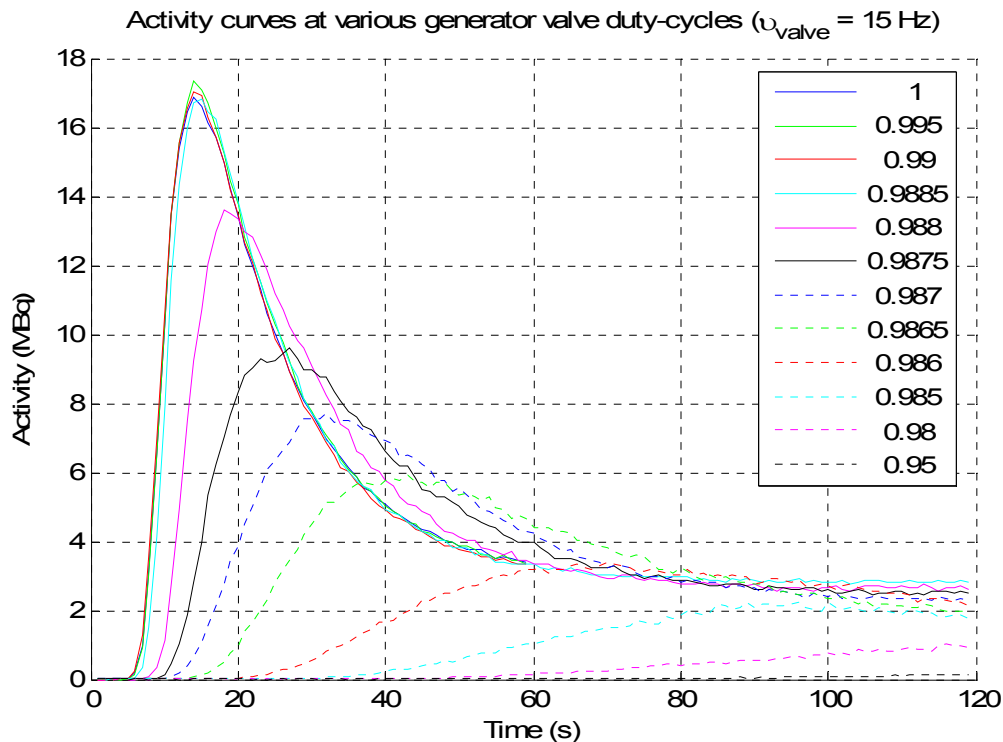


**Figure 4-3** - Activity vs. time curves as measured with the generator valve cycling at 15Hz at various generator valve duty-cycles. The rise time was estimated as the interval between initial rise and peak activity.

A series of calibration elutions was conducted for each cycling frequency with the duty-cycle,  $\Pi$ , varied to sample the dynamic range of the response (as shown in Figure 4-3 for cycling at 15 Hz). The calibration runs were identical to a regular calibration run (15 ml/min saline flow rate), except that the generator valve was set to cycle at a given frequency and duty-cycle rather than remaining fully opened. In addition, the elution was performed over 120 s instead of the standard 60 s so as to measure the longer rise times. The rise time for each elution was measured as the interval between initial rise and peak activity. The rise

time of a regular calibration run (duty-cycle set to 100%) was used as the reference to which all other rise times were compared. The ratio of rise time for a given duty-cycle and the reference rise time indicates the effective ratio of saline that flows through the generator, referred to as valve flow ratio ( $r$ ). The valve flow ratio vs. duty-cycle curves for the set of cycling frequencies were plotted in Figure 4-4. The inverse of these curves allow one to determine the duty-cycle needed to achieve an effective flow ratio.

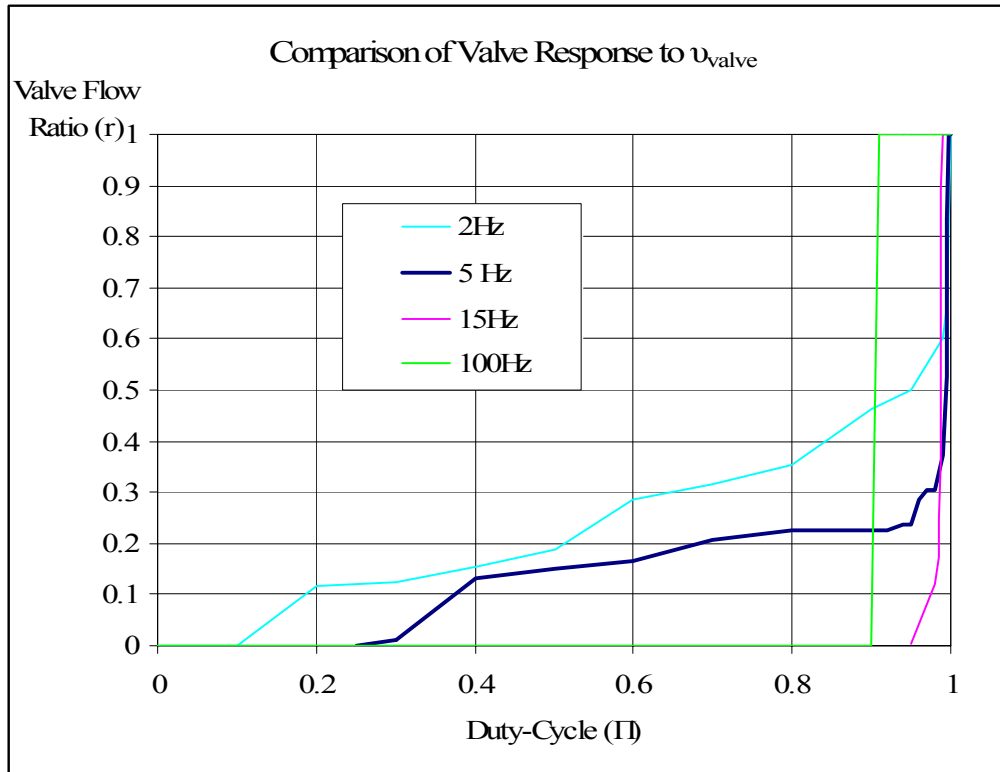


**Figure 4-4 – Valve response curves at  $v_{\text{valve}} = 2, 5, 15,$  and  $100$  Hz indicate the valve flow ratio,  $r$ , resulting from PWM duty-cycle,  $D$ .**

As the cycling frequency is increased, the valve response becomes less linear and more similar to a step function. In the case of 100Hz cycling frequency the flow ratio changed from fully opened to fully close in a very small duty-cycle interval (less than 1%). Although in [37] Imaizumi demonstrates a linear response of a solenoid valve using a transient state control, these results could not be reproduced. It is possible that the discrepancy in results is due to the valve's mechanics. In our application the return spring applies a large force so as to pinch the tubing when no current is fed through the solenoid. Imaizumi used a single pincher valve, and therefore had no need for such a powerful return spring. Due to this undesired response, the transient control approach was not explored

further, leaving the cycling valve approach as the choice alternative to emulate a variable flow valve.

The PWM response at 2 Hz seems to be the best choice of the set demonstrated in Figure 4-4 since it presents the mildest slope leading to the largest dynamic range of duty-cycles; thus small variation in duty-cycle have less effect on the effective valve flow ratio. However, examination of the activity vs. time curves at approximately 50% valve flow ratio (Figure 4-5) revealed that the low cycling frequency introduces substantial fluctuations in activity. These fluctuations are greatly reduced with the cycling frequency increased to 5 Hz while the response remains manageable. At 15 Hz cycling frequency the response is a very steep slope throughout the entire dynamic range; meaning that small errors in duty-cycle,  $\Pi$ , will result in very large errors in the valve flow ratio,  $r$ .

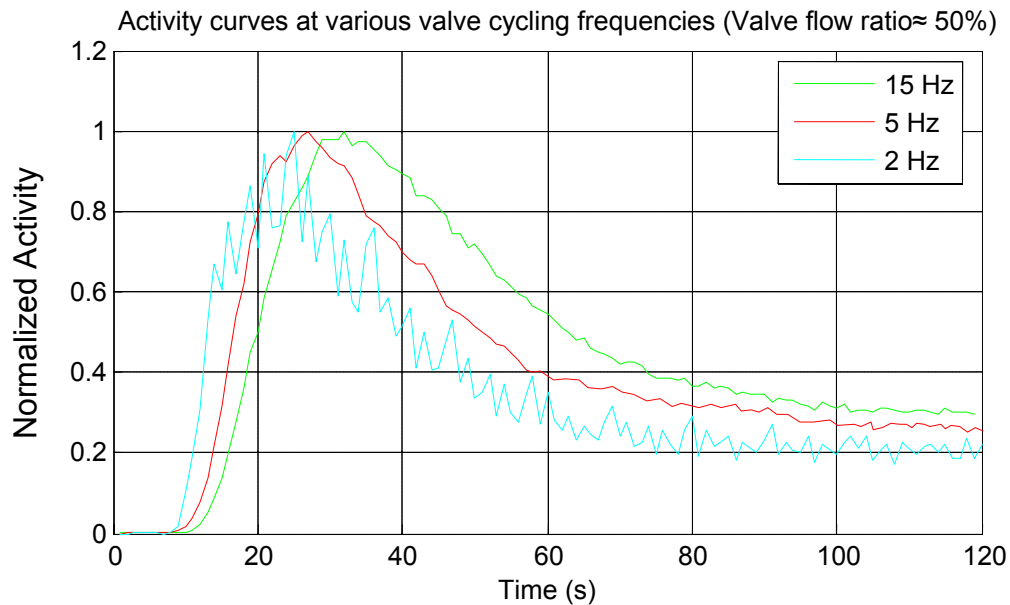


**Figure 4-5 – Elutions at valve flow ratio  $\approx$  50% produced by cycling the generator valve at 2, 5, and 15 Hz and corresponding  $\Pi$  from Figure 4-4. The activity vs. time measurements with valve cycling frequency set to 2 Hz reveal that the low cycling frequency introduces measurable fluctuations in activity.**

With all the above issues considered, it was determined that a cycling frequency of 5 Hz provided a balance between smooth activity vs. time curves and a manageable valve flow ratio response curve. Over the flow ratio range of 0-30% the slope is mildest making it the most favourable working range while the 30-100% range should be avoided due to the sharp response slope; however, this is not always possible if one wants to elute high relative activities.

### Modeling of Valve Response

The valve response is important for achieving good flow ratio control. Although the collected data demonstrated in Figure 4-4 can be used to calculate the duty-cycle needed to achieve the desired valve flow ratio, this would entail measuring of the exact valve response of each system. In addition, recalibration of the response due to changing dynamics of the valves would involve a long and complicated process. Developing a model of the response with few free parameters, would allow tuning of the valve response more easily. For flow control we show the response graph (Figure 4-4) with swapped axes (Figure 4-6), as we wish to set the duty-cycle to achieve a desired valve flow ratio.

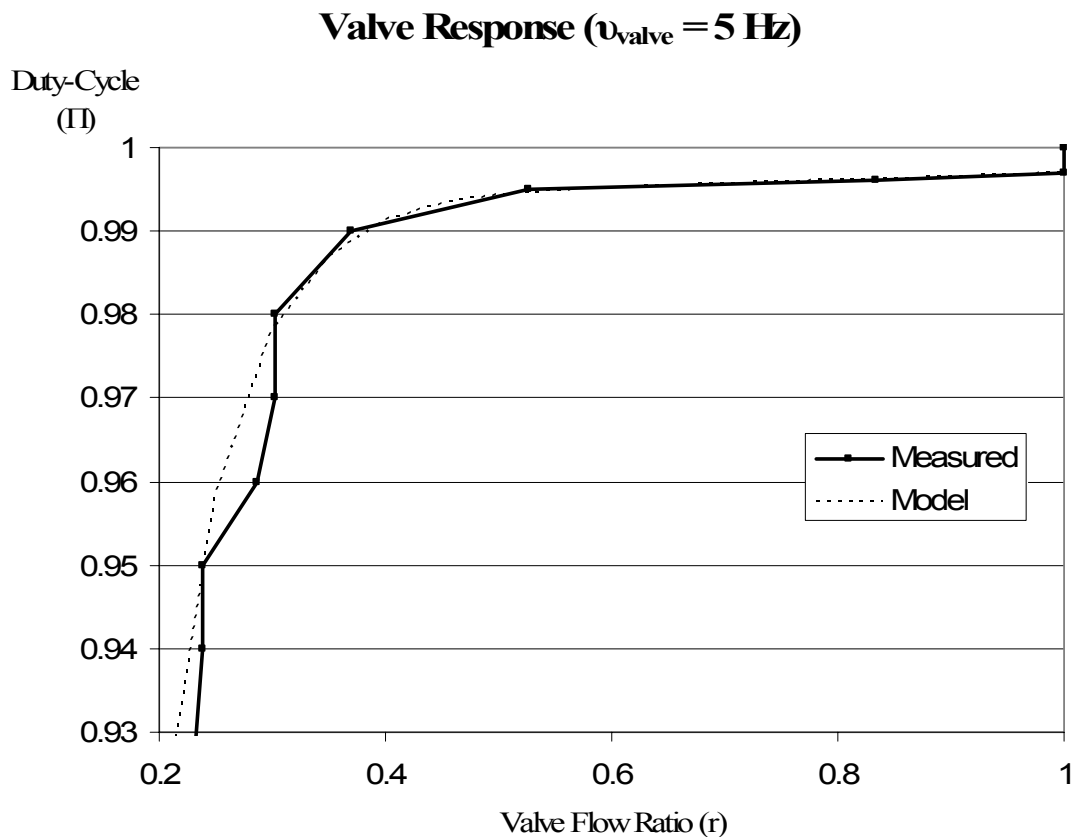


**Figure 4-6 – Valve response ( $v_{\text{valve}}=5 \text{ Hz}$ ) with the swapped axes, allows determination of the duty-cycle needed to achieve a desired valve flow ratio. Measured response (solid) and model (dashed) fitted in the useful range (20-100%) with model parameters  $\Pi_{\text{max}}=0.997$ ,  $\Pi_{\text{min}}=0$ ,  $L=0.004$ , and  $G=16$ .**

A few models were considered, leading to a combination sigmoid and linear function (18). The sigmoid accounts for the response in the lower flow ratio range (0-50%), while a line models the mild slope in the higher range (50-100%). Equation (18) converts the desired valve flow ratio,  $r$ , to valve duty-cycle,  $\Pi$ . The

parameters  $F$ ,  $G$ ,  $O$  and  $L$ , can be tuned to fit the measured response. Parameter  $G$  scales the sigmoid to match the lower ratio range, while the slope  $L$  accounts for the slope of the higher ratio range. Parameters  $F$  and  $O$  can be computed through (19) and (20) respectively based on the maximum and minimum effective duty-cycles ( $\Pi_{\max}$  and  $\Pi_{\min}$ ). The consideration for using  $\Pi_{\max}$  and  $\Pi_{\min}$  is to use measures that have physically significant meaning – upper and lower saturation duty-cycles respectively.

$$\Pi(t) = \frac{F}{1 + e^{-G \cdot r(t)}} + O + L \cdot r(t) \quad (18)$$

$$F = \frac{\Pi_{\max} - \Pi_{\min} - L}{e^{-G} - 0.5} \quad (19)$$

$$O = \Pi_{\min} - F / 2 \quad (20)$$

The measured data reveals that at duty-cycles higher than  $\Pi_{\max}=0.997$  the valve is effectively fully open to flow through the generator (upper saturation point). Similarly, at duty-cycles below  $\Pi_{\min}=0.25$  the valve is effectively closed (lower saturation point). A manual model fit of the curve was estimated with  $\Pi_{\max}=0.997$ ,  $\Pi_{\min}=0$ ,  $L=0.004$ , and  $G=16$  and plotted with dashed lines in Figure 4-6. The useful range of valve flow ratios (20-100%) is well represented by the sigmoid-linear model where the sigmoid accounts for the “knee” shape of the response curve and the line models the higher range (50-100%). The extremely low response range ( $r<20\%$ ) is not used and was ignored during the fit.

Modification of the free parameters of the model allows improving the fit in one region, potentially at the expense of other regions. Further effort on manually improving the fit proved to be difficult. It was expected that an algorithm could be developed to optimize the fit based on the actual valve flow ratio range used. Although great care was taken to estimate the effective flow ratio data in Figure 4-6, it is inevitable that manual measurements have some error. In addition, the valve response may change over time due to material fatigue, wear, and other unknown factors. An automated model parameter tuning process using measures from many elutions would be used to estimate the model parameters. However, before this could be achieved, a control algorithm based on this valve response model was developed.

### *PWM Valve Life Span*

Cycling of the valve between states may accelerate the wearing of the mechanical mechanism, thus potentially shortening its life span. The valve model chosen for the RbES

(Asco 37312830) does not have any reliability information published by the vendor. However, since elutions are short (~30 s) and the time between elutions is at least ten minutes, over heating is not a significant risk. A routine work day includes as many as twelve elutions, translating to 1800 cycles if the valve is cycled at 5 Hz. Since a typical valve reliability measure is at the very least  $10^6$  valve cycles, a life span of several years can be expected in the worst case. Asco is a reputable actuator manufacturer recognized as meeting the highest quality standards. However, only long term experience will clarify this reliability issue.

### **4.3 Variable Flow Control Algorithms**

Even with an ideal actuator in place, an appropriate controller must be designed. The goal of the controller is to monitor the progress of the process and make proper adjustments to the actuator in order to reduce the output error. Development of a controller must take into account the nature of the system being controlled, the desired results, and the limitations of the design. Several key points to be considered during the development of the RbES controller are listed below.

1. Typical elution times are short (30-60 seconds), leaving little time for conventional feedback controls to stabilize.
2. Feedback to the system has a relatively long inherited delay due to the time required for activity to flow from the generator to the activity counter and the need to accumulate counts.
3. The feedback delay is not constant due to variation in flow rates.
4. The activity concentration in the saline flowing from the generator varies as the elution progresses, but the activity concentration vs. eluted volume relationship is constant [18].
5. Most of the activity from the generator is contained in the initial bolus phase. One would like to make use of this activity (rather than pass it to the waste) to achieve high relative activity elutions.

These considerations served as guidelines throughout the control system development process. The intermediate development steps are discussed in order to clarify the difficulties involved with this control problem and to justify decisions.

### *PID Control*

Conventional approaches typically use proportional-integral-differential (PID) controllers driven by feedback measurements to drive the actuators so as to minimize the output error. The dynamics of the controller are intended to compensate for the dynamics of the mechanical system (plant) in order to achieve a more favourable overall system response. PID controllers are well established and serve as a default approach in many applications. Three scalars (P, I, and D in (21)) must be tuned to optimize the control signal,  $C$ , to the plant response. In theoretical models, controller optimization can be achieved through state-space modeling and optimal control calculation techniques. In practical situations, where modeling of the plant is either too difficult or too time consuming, the controller may be tuned through trial and error.

$$C = \underbrace{P \cdot E(t)}_{\text{Proportional}} + \underbrace{I \int_0^t E(\tau) d\tau}_{\text{Integral}} + \underbrace{D \frac{dE(t)}{dt}}_{\text{Differential}} \quad (21)$$

The three parameters of a PID controller correspond to factors of the error, its integral, and its proportional differential to produce a control signal to the actuator (Figure 4-7). The output error is the difference between the desired plant output (set point) and the actual output. Properly tuned, the controller will affect the plant actuators to reduce the output error over time. The proportional factor serves to quickly adjust the actuator based on current errors. If the proportional gain is too small, the error will decrease slowly, however, if it is too large overshoots can occur, leading to oscillations around the set point. The integral component serves to reduce steady state errors and speed up the reduction of error. The derivative component serves to reduce overshoot due to over correction by the controller. Refer to Figure 4-8 for an example of these affects.

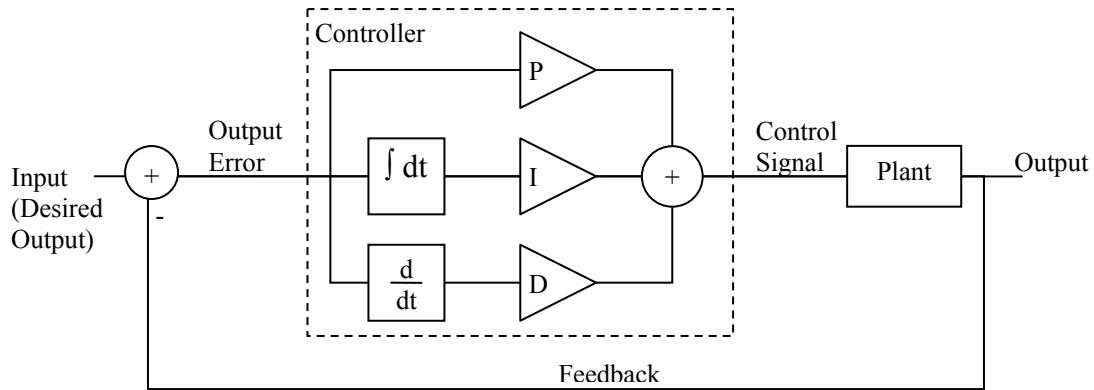


Figure 4-7 - Closed loop controlled system using a PID controller.

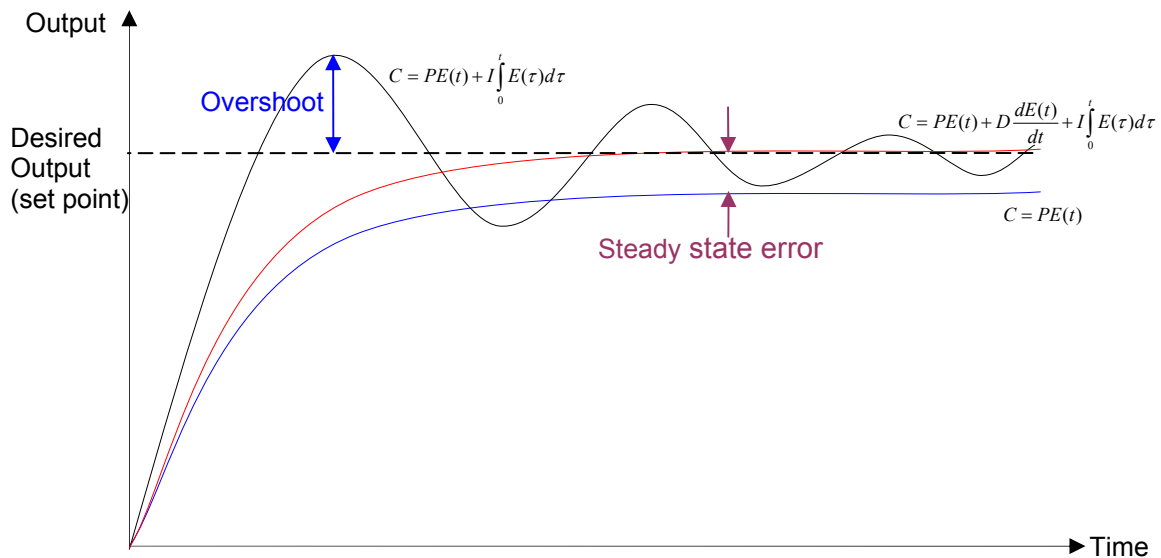


Figure 4-8 - Affects of PID controller parameters on system response.

In the case of the RbES, building of a state space model is complicated by the changing feedback delay for different flow rates. Even if this were accomplished a linear PID type controller cannot model (and therefore correct for) a pure feedback delay [38,39,40]. In addition, the activity curve continuously changes making a pure feedback control system inadequate, as it will always lag in response. These assumptions were confirmed through a series of simulations of a PID feedback loop controlling the flow ratio (ideal valve response). The transport volume from the valve to the activity counter was set to 0.13 ml and the controller rate was set to 20 Hz, which are characteristic values. The PID parameters were tuned through trial and error. Parameter D was always set to zero (PI controller) since it resulted in amplified activity fluctuations. Three sample results are included in Figure 4-9.

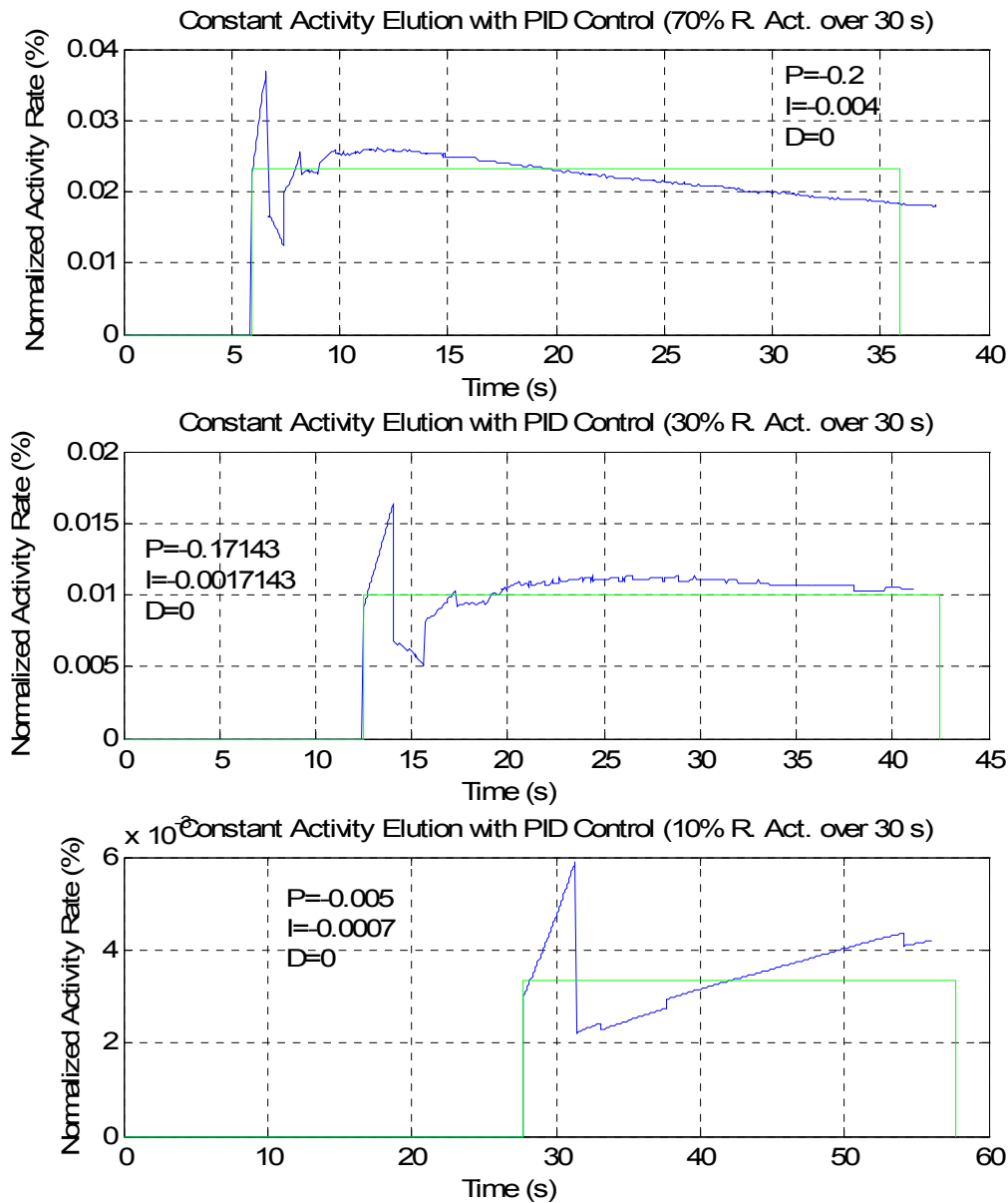


Figure 4-9 - Sample simulation results of a PID controlled elution with an activity transport delay from the valve to the activity counter (0.3 ml) and a high controller refresh rate (20 Hz).

Even in the best case scenario, the simulations demonstrate some shortcomings of using a PID controller. The activity curves vary throughout the elution due to lagging behind the change in activity concentration. This is especially noticeable in the 10% relative activity elution (bottom) where delay is longest due to the slow saline flow rate. In all the cases overshoot is noticeable in the first few seconds of the elution as the activity concentration changes fastest in the early bolus volume. Testing of this implementation on the system revealed far worse results probably due to poor modeling of the valve response at the time, slower controller refresh rates, and random noise in the feedback.

### Forgetful PID Controller

One of the drawbacks of a conventional PID is that noise in the error measurements can result in large changes in the control signal. Since noise is characterized by fast changes in measurements it is mostly amplified by the differential component and the proportional component. It is common to set the differential gain to zero in order to reduce the effect of noise, but the proportional component cannot be removed as the resulting controller will become very slow.

The conventional PID controller was modified to create a “forgetful PID” controller by converting the proportional gain into a forgetful integral with a forgetting factor  $\phi$  as is shown in (22). The proportional component depends on previous errors whose weights gradually decreased over time. With  $\phi$  set to 0.995, the current error reading,  $E[n]$ , has a weight of 1 while the previous reading,  $E[n-1]$ , has a weight of 0.995. But the weights of earlier readings, say  $E[n-100]$  (corresponding to 5 s earlier due to refresh rate of 20 Hz) have a significantly reduced weight (0.606). Most of the error correction is based on recent history which strikes a balance between the controller’s speed of response to change in error and immunity to noise. The model of the forgetful PID controller is shown in Figure 4-10.

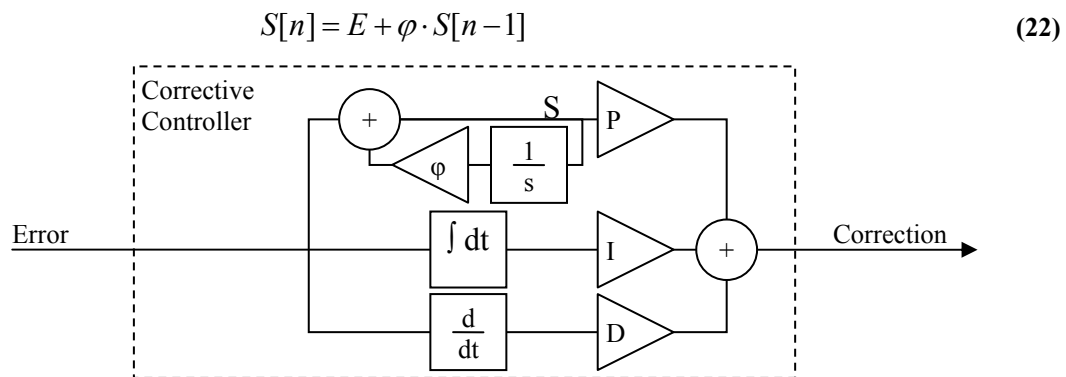


Figure 4-10 - Modified PID correction implementing a “forgetful” proportional component.

### Predictive Control

The critical disadvantage of feedback control is that the controller response is always delayed. In this case the delay is relatively long compared to the total elution time. This delay combined with the varying activity concentration from the generator makes a simple feedback controller inadequate [39,40]. To avoid delayed response, one would like to predict the activity concentration at point M (Figure 3-3) where the bypass and generator flows

merge. One option is measuring the activity in the generator line just prior to the merge using an additional activity counter, however this has the drawback of increased cost and complexity to the system and the need to know the exact flow ratio set by the generator valve.

An alternative approach capitalizes on the fact that the activity concentration is almost entirely dependent on the volume eluted from the generator. If one knows the exact volume that was eluted through the generator and the time delay to the merging point,  $M$ , one can estimate the activity concentration just upstream to the merge,  $\hat{C}_{M-}(t)$ . The main advantage of this alternative is that no hardware modifications, such as addition of another positron detector, are required.

The predicted valve ratio,  $r(t)$ , can be computed based on the predicted activity concentration just upstream from the merger,  $C_{M-}$ , and the set point,  $\dot{A}_C$  (23). Since the prediction is for point  $M$  and the set point is calculated for point  $C$ , one must account for the decay during transport,  $D_{MC}$ . The activity concentration  $C_{M-}$  is converted from activity concentration (MBq/ml) to activity rate (MBq/s) by factoring the flow (ml/s).

$$r(t) = \frac{\dot{A}_C}{D_{MC} \cdot f \cdot C_{M-}(t)} \quad (23)$$

The activity rate at the activity counter,  $\hat{A}_C$ , is equal (after a transport delay  $T_{MC}$ ) to the activity rate at the merger,  $\hat{A}_M$ , decayed during transport by  $D_{MC}$  (24). The rate of activity at the merger,  $\hat{A}_M$ , is a product of the actual activity concentration,  $\hat{C}_{M-}$ , and the flow rate through the generator path,  $f \cdot \hat{r}(t)$ .

$$\hat{A}_C(t + T_{MC}) = D_{MC} \cdot \hat{A}_M(t) = D_{MC} \cdot f \cdot \hat{C}_{M-}(t) \cdot \hat{r}(t) \quad (24)$$

With ideal valve response the actual flow ratio is equal to the predicted flow ratio,  $\hat{r}(t) = r(t)$ . Similarly, if the activity concentration just upstream from the merger is successfully predicted then  $\hat{C}_{M-} = C_{M-}$ . Substituting (23) into (24) reveals that the activity rate at the counter,  $\hat{A}_C$ , is the desired activity rate  $\dot{A}_C$  and perfect control is obtained as shown in (25).

$$\hat{A}_C(t + T_{MC}) = D_{MC} \cdot f \cdot C_{M-}(t) \cdot r(t) = \dot{A}_C \quad (25)$$

The prediction algorithm estimates  $\hat{C}_{M-}$  based on the activity vs. volume curve obtained during the calibration run of the same day,  $C_C(v)$ . The predicted activity concentration at the merger,  $C_{M-}$ , is interpolated from  $C_C(v)$  based on the volume that was eluted through the generator since the beginning of the elution as shown in (26). The eluted volume is obtained by integrating the flow ratio,  $r(t)$  from the beginning of the elution and multiplying by the saline flow rate,  $f$ . The integrated volume is corrected through a volume shift ( $V_{MC}$ ) since the measurements during calibration relate to the counter position rather than that of the merge. The activity concentration,  $\hat{C}_{M-}$ , is estimated as the mean activity concentration over the next sample period,  $S$ , using (26).

$$C_{M-}(t) = \frac{D_{GM}(t)}{{}^{cal}D_{GC}} \cdot C_C \left( f \int_{\tau=0}^t r(\tau) d\tau - V_{MC} + \hat{V}_{Corr} \right) \quad (26)$$

During the transport from the generator to the merger, significant time can pass if low flow ratios are used. The transport time from the generator to the merging stopcock,  $T_{GM}(t)$ , is calculated by integrating the flow through the generator over  $V_{GM}$  using (27). The transport time,  $T_{GM}(t)$ , is used to estimate the <sup>82</sup>Rb decay between the generator and merger,  $D_{GM}(t)$  in (26) and (27). However, the decay from the generator to the activity counter during the calibration run,  ${}^{cal}D_{GC}$  must be backwards corrected, since the generator outlet is the point of reference for the <sup>82</sup>Rb decay. To clarify the concept, one must remember that the activity in the line changes as transport time passes, therefore both the time shift and its corresponding decay must be corrected to any given reference point (the estimated generator outlet).

$$D_{GM}(t) = e^{-\lambda T_{GM}(t)} \text{ where } V_{GM} = f \cdot \int_{\tau=t-T_{GM}(t)}^t r(\tau) \cdot d\tau \quad (27)$$

The volume shift,  $\hat{V}_{Corr}$ , included in (26) improves alignment of the prediction activity curve with the actual elution curve. This adjustment is crucial for compensating for delays in pump start response time and any other introduced delays. During the beginning of the elution the valve is fully opened which allows reproducing the initial rise of the activity vs. volume curve measured during calibration. When significant activity, but less than the set point activity, is measured, the activities vs. volume curves are aligned through a volume shift to minimize the MSE. The optimized volume shift,  $\hat{V}_{Corr}$ , serves to fine tune the activity prediction in (26).

### *Predictive Corrective Control*

For accurate prediction, two conditions must be satisfied:

1. The activity concentration just prior to the merger,  $\hat{C}_{M,-}$  must be accurately predicted.
2. The valve response must be accurately modeled.

In practice, perfect prediction is impossible due to measurement errors and imperfect modeling. A corrective mechanism should be integrated to complement the prediction by driving the output error to zero. A PID loop, or variation of it, can be used for this correction. While the predictive algorithm accommodates fast changes in the activity concentration eluted from the generator, the corrective mechanism serves to refine the valve control to reduce long term errors. The corrective mechanism must compensate for all the errors and inaccuracies such as activity concentration prediction errors and imperfect actuation of the generator valve.

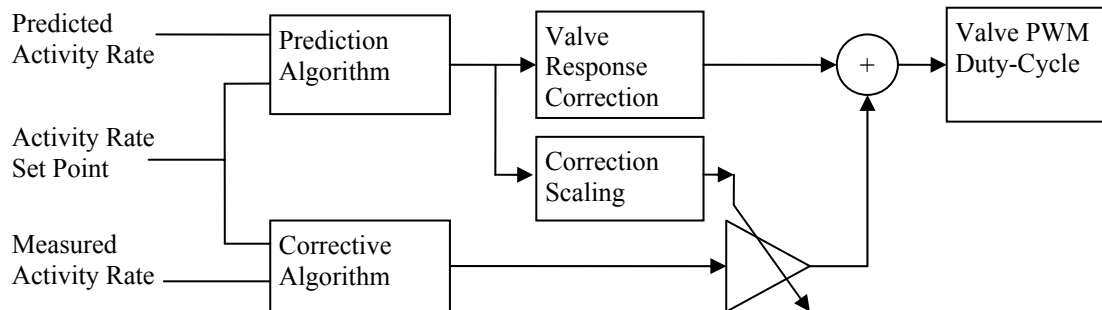


**Figure 4-11 - Block diagram of the predictive-corrective control of a PWM valve.**

The corrective mechanism included in the RbES is a modified PID loop with a forgetful proportional component as shown in Figure 4-10. In addition, the correction must be scaled to account for non-linear sensitivity of the valve in the predicted duty-cycle range (Figure 4-11). A small change in duty-cycle in the high range will result in a much larger change in flow ratio than in the lower range of duty-cycles. The scaling is performed by multiplying the correction signal from the modified PID by the differential of the valve response at the desired flow ratio ( $d\Pi(r)/dr$ ). As a result, when the valve is supposed to be wide open, the scaling is small, corresponding to the high sensitivity of the valve in this range. It is important to include this scaling since without it the correction will become over amplified as the valve is opened over the course of the elution.

### Initial Error Removal

Simulations of constant-activity elutions with slight shifts in the predicted volume eluted through the generator (Figure 4-12) revealed that the first few seconds of the elution are most susceptible to prediction errors. In cases where all the activity from the generator must be eluted to reach the requested dose, these initial errors must be tolerated. However, in cases where a much lower dose is requested, the initial errors can be avoided by diverting the elution to the waste container. The initial error removal mechanism (IERM) waits for the activity rate to reach a threshold level (90% of the desired activity rate) then begins a time delay of  $T_{ierm}$ . Once  $T_{ierm}$  has elapsed, the elution is routed to the patient rather than the waste.

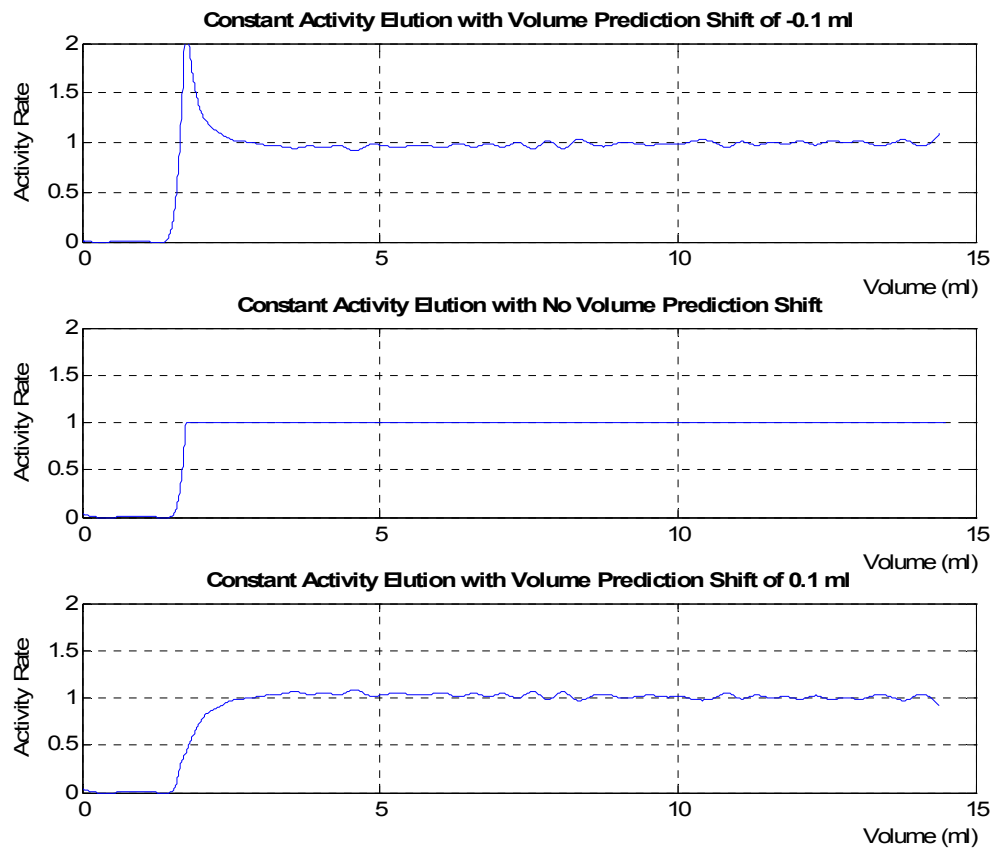


**Figure 4-12 - Simulation of perfect control with erroneous activity concentration prediction due to a slight volume shift ( $\pm 0.1$  ml). If the predicted eluted volume is less than the actual eluted volume (top) a peak of activity is expected. A slow rise is expected if the predicted volume is too large (bottom). The middle curve shows perfect alignment. Truncating the first few seconds of an elution should remove the largest prediction error regions.**

$T_{ierm}$  is calculated depending on the relative activity of the elution. For relative activities less than 10% the delay is set to 10 s. For relative activities above 70% no delay is

used. Intermediate relative activities are assigned a delay through linear interpolation between these limits. The end result is a truncation of initial errors to improve the elution profile significantly, but without affecting the range of activities that can be eluted from the generator.

### *Setting the Saline Flow Rate*

In order to minimize sensitivity to flow ratio error, one would like to use a large range of the valve flow ratios during any given elution. In addition one would like to avoid using extreme flow ratios as the valve may saturate. Finally, the lower range of flow ratios is less sensitive to control error and is therefore the preferred range to use. Since the effective activity rate is a product of activity concentration, valve flow ratio, and saline flow rate, the range of flow ratios that will be used during an elution is directly influenced by the saline flow rate. The flow rate must be set at the beginning of an elution based on the desired activity rate in relation to the generator activity, referred to as relative activity rate (%/min).

When conducting a low relative activity elution, a low flow rate is desired so that the flow ratios used during the elution are not near the lower saturation point. On the other hand, the flow rate should not be too low as to avoid long transport delay, and <sup>82</sup>Rb decay. When conducting high relative activity elutions, higher flow rates are desirable so that the generator bolus activity is eluted and minimal <sup>82</sup>Rb decay occurs en route the patient.

The reproducible flow rates in the <sup>82</sup>Rb elution system are in the range of 5-25ml/min. At the lower limit, 5 ml/min flow rates were used for 20%/min relative activity rate elutions (corresponding to 10% relative activity over 30 s). At the upper limit, 25ml/min flow rate is used for 140%/min relative activity rate elutions (corresponding to 70% relative activity over 30 s). Intermediate flow rates are obtained by linear interpolation between these limits.

The flow rate is computed prior to starting of the elution using (28) and is maintained until all the activity has been eluted and flushed from the lines.  $A_{Req}$  corresponds to the desired activity, while  $T_{Req}$  is the requested duration. The relative activity is computed using  $A_{Req}$  factored by the calibration activity,  $A_{Cal}$ , while the time ratio  $60/T_{Req}$  converts the measure into relative activity rate.

$$f = \left[ \frac{25 - 5}{1.4 - 0.2} \cdot \frac{A_{Req}}{A_{Cal}} \cdot \frac{60}{T_{Req}} + 1.667 \right] \quad (28)$$

### *Automatic Parameter Tuning*

Accurate prediction of activity concentration depends on accurate modeling of the system and accurate valve flow ratio. The prediction algorithm makes the assumption that the valve response is accurately modeled and that the desired flow ratio is always achieved. Since we have confidence in the modeling of the system, we must focus on fulfilling this assumption through good modeling of the valve response.

The valve response model parameters that were estimated manually to achieve a good fit (Figure 4-6) do not necessarily ensure the best elution performance in practice. In addition, the valve response may change over time. For these reasons one would like a self-tuning algorithm that adjusts the model parameters in order to decrease the error in elution profiles. These parameters should be adjusted through small increments in order to reduce the effects of problematic elutions on the parameters. In addition, small adjustments allow convergence to nominal values without exaggerated overshooting. On the other hand if the adjustments are too small convergence may be too slow.

The predictive corrective control of the pulse width modulated valve (PCC-PWM) was designed so that the only free parameters are in the valve response model. These parameters, listed in Table 4-2, can be tuned based on the activity rate errors measured over the course of a constant-activity elution. The algorithm for tuning these variables is detailed below.

**Table 4-2 - Parameters used by the prediction algorithm.**

Parameter	Manually tuned value	Converged value	Affects
Sigmoid scaling (G)	16	26.5	Sharpening of the “knee” in the response - Response at low valve flow ratios ( $r < r_t$ )
Linear slope (L)	0.004	0.0067	Slope of linear range - Response at high valve flow ratios ( $r_t < r$ )
Valve upper bound ( $\Pi_{max}$ )	0.997	0.9975	Threshold when valve response is equivalent to full open - If too large peaks will occur at beginning and end of elution profile
Valve lower bound ( $\Pi_{min}$ )	0	0	Overall error trend - Activity too high (elution too short) – bound needs to be lowered - Activity too low (elution too long) – bound needs to be raised

### *Sigmoid Scaling (G)*

The sigmoid component of the valve response model (18) was added to account for the increased slope in the low flow ratio range. The input to the sigmoid is scaled using parameter G which can be tuned to control the slope of the response in the lower range. Since the sigmoid function has an asymptote to 1 as the input tends to infinity, the higher range of flow ratios is almost unaffected by this parameter.

To tune parameter G the activity rate errors corresponding to valve position in the lower flow rate region ( $0 < r < r_t$ ) are selected and a linear fit to the error vs. flow ratio is conducted as shown in Figure 4-13 and Figure 4-14 by a solid line. The slope of this line is represented by  $S_L$  in (29) which computes the change to the G parameter,  $\Delta G$ . If the slope is negative for example, the activity rate error decreases as the valve is opened. This is corrected for by decreasing the scaling on the sigmoid, as a result the duty-cycle on the lower region of flow ratio will be decreased. The goal is to have no change in activity rate error as the flow ratio is modified.

$$\Delta G = \gamma_s \cdot G \cdot S_L \quad (29)$$

The upper limit of the lower flow ratio range,  $r_t$ , is computed as the flow ratio at which the slope of the valve response model (Figure 4-6) is twice the linear slope,  $d\Pi/dr = 2 \cdot L$ . At flow ratios above this point, the significance of parameter G is diminished, while at the range below this point the sigmoid shape is dominant.

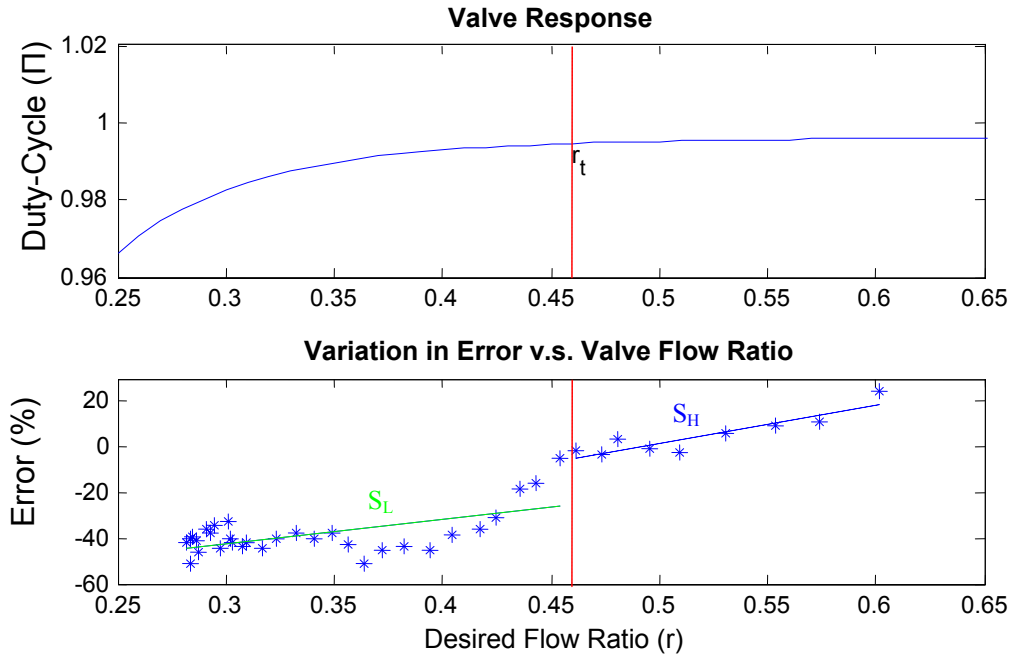


Figure 4-13 – Analyzed errors of a constant-activity elution with flow ratios spanning a large range. The slope of the error points relating to the valve flow ratio lower range ( $r < r_t$ ),  $S_L$  is used to adjust parameter  $G$ , while the slope of the error points relating to the higher valve flow ratio range ( $r_t < r < 0.95$ ),  $S_H$ , is used to adjust parameter  $L$ .

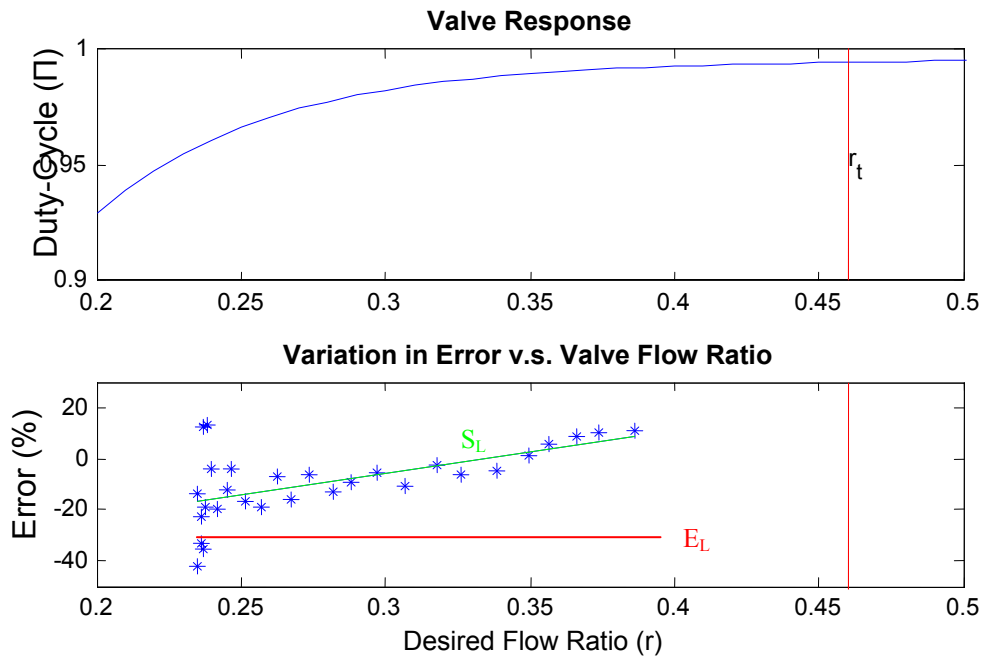


Figure 4-14 – Analyzed errors of a constant-activity elution with flow ratios in the lower range. Parameter  $G$  is tuned based on  $S_L$  in the same manner as elutions that span into the higher valve flow ratio range. The mean error across all points associated with  $r < r_t$ ,  $E_L$ , is used to adjust parameter  $L$ .

### *Linear Slope (L)*

The linear slope is corrected in one of two ways based on the available data. If sufficient error measurements are available for the region ( $r_t < r < 95\%$ ) then a linear fit is produced and its slope,  $S_H$ , serves as a correcting factor (dashed line in Figure 4-13), referred to as the slope rule. However, if not enough data points are present, as in the case of Figure 4-14, the mean error in the lower range,  $E_L$ , is used as the correcting factor, referred to as the mean error rule. This combination of corrections is expressed in (30). In the later case, the linear slope is adjusted so that the average error in the lower range ( $0 < r < r_t$ ) is driven to zero. This logic is important to include, otherwise low relative activity elutions may evolve to a state where the error in the lower range is uniform across all valve flow ration (due to adjustment of G), but this error may not be zero.

$$\Delta L = \begin{cases} \text{More than 4 data points,} & -\gamma_L \cdot L \cdot S_H \\ \text{Otherwise,} & \gamma_L \cdot L \cdot E_L \end{cases} \quad (30)$$

### *Valve Upper Bound ( $\Pi_{max}$ )*

The valve upper bound,  $\Pi_{max}$ , is defined as the duty-cycle at which the valve response saturates in an open position. For  $\Pi \geq \Pi_{max}$  the effective flow ratio,  $r$ , is 100% (i.e. complete flow through the generator). Adjusting this parameter can only be achieved if relevant error data are measured during the elution. The predicted activity concentration from the generator near the end of the elution must be insufficient to achieve the desired activity rate. Since the predicted activity rate is less than the set-point the valve flow ratio will be set to 100%. If the measured activity rate is less than the set-point the corrective algorithm will attempt to further increase the duty-cycle beyond  $\Pi_{max}$  up to duty-cycle  $\Pi=1$ . If  $\Pi_{max}$  is set too low, the activity rate may increase while the correction algorithm increases the duty-cycle. Otherwise, further correction will not result in an increased activity rate. The following algorithm is used to adjust  $\Pi_{max}$ :

- Keep all the data past the minimum flow ratio – avoid confusion with early part of elution.
- Keep all the data where predicted flow ratio was one – keep only the saturated region at the end of the elution.

- If the remaining data set is empty do not change  $\Pi_{\max}$  as there is no relevant data ( $\Delta \Pi_{\max} = 0$ ).
- Otherwise keep only the data relating to rise of activity up to the maximum point.
  - If the remaining data contains more than one data point, use the slope of a linear fit of the error vs. correction,  $S_S$ . Factor for the change in correction during this time interval,  $\Delta \zeta$ , using (31).

$$\Delta \Pi_{\max} = \gamma_R \cdot S_S \cdot (1 - \Pi_{\max}) \cdot \Delta \zeta \tag{31}$$

- Otherwise decrease the saturation point slightly ( $\Delta \Pi_{\max} = -10^{-5}$ ).

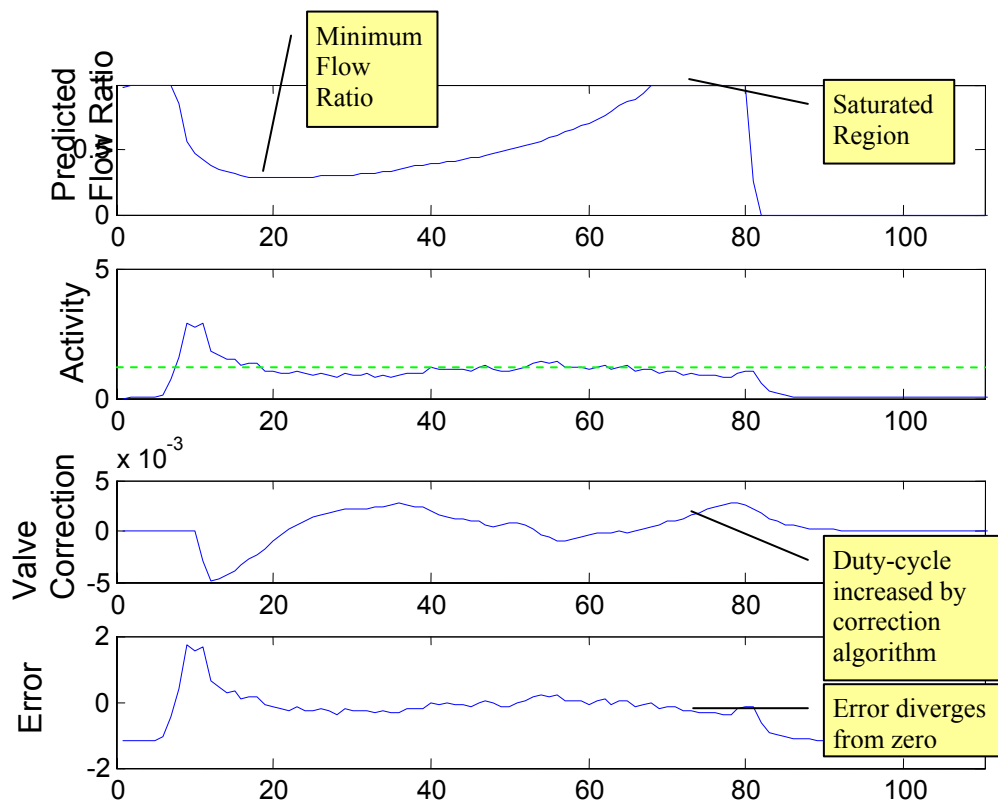


Figure 4-15 – Results from an elution in which the entire bolus activity was eluted. The valve upper bound parameter,  $\Pi_{\max}$ , can be adjusted based on the region where the valve is fully opened and the correction algorithm attempts to further increase the duty-cycle. In this case, the activity does not rise further so  $\Pi_{\max}$  will be slightly decreased.

*Valve Lower Bound ( $I_{min}$ )*

As opposed to the other model parameters, the lower bound duty-cycle was found to have little significance on measured error. This can be reasoned through observation that the predicted flow ratio never falls below 20%. As a result, modeling in the range 0-20% need not be optimized, and in fact cannot be optimized since relevant data cannot be measured. It was decided to avoid the automatic tuning of this parameter and fix it to zero. This corresponds to zero duty-cycle to achieve zero flow through the generator.

*Summary*

In an effort to develop a control system capable of delivering a constant rate of activity from a <sup>82</sup>Sr/<sup>82</sup>Rb generator various considerations had to be taken into account. These include the decay of activity during transport in the lines, the variation in activity concentration from the generator during an elution, and the slow response in feedback, especially in comparison to typical elution times. These difficulties were addressed through the development of a predictive-corrective control algorithm that attempts to predict the activity concentration at the merger of the generator and bypass lines. The predicted activity concentration is used to control the ratio of saline that flows through the generator versus to the bypass line.

The prediction algorithm uses an activity concentration vs. volume curve measured during a daily calibration run and the history of the elution to accommodate fast changes in activity concentration. A corrective feedback algorithm consisting of a modified PID loop corrects the valve control signal to drive errors in the measured activity rate to zero.

The flow ratio of saline through the generator is actuated using a solenoid two-way pinch valve cycling at a constant frequency (5Hz) with a controlled duty-cycle. As the duty-cycle is increased, a higher ratio of saline is routed through the generator, thus increasing the activity rate at the merger of the two lines. The valve flow ratio response to duty-cycle is highly non linear and was modeled using a combination sigmoid and linear function.

For the valve response model to remain accurate over time, a self-tuning algorithm was developed. This algorithm continuously adjusts the model parameters by small increments through analysis of the activity rate error as a function of the flow ratio collected

during each elution. It is expected that over many elutions, the model parameters will be adjusted so as to reduce the error in the eluted activity profiles.

With this implementation of the RbES completed, performance can be compared to the prototype system which employed a simplistic but reliable control system. The ultimate decision is whether any of the control modes (hysteresis corrected threshold comparison (HC-TC), and predictive-corrective control of PWM valve (PCC-PWM)) are sufficient for both clinical and experimental quantitative perfusion measurements using  $^{82}\text{Rb}$  in PET. The characteristics of both approaches should be compared to determine the advantages of disadvantages of each approach.

## Chapter 5: Testing and Characterization

Due to the clinical application of this system, it was important to conduct a thorough testing of the system in order to uncover any possible errors or unaddressed requirements of the system. These tests included both hardware and software aspects. Hardware safety considerations mainly concerned electrical safety, mechanical robustness, and failure to a safe mode. Although an elution is permitted to fail, it must do so gracefully without threat to the well being of the patient or the operators. The test scenarios were designed to confirm that the system behaves in a predictable manner not only in routine situations, but also when anomalies such as hardware failure and unexpected measurements occur.

Full characterization of the system's capabilities is also important. This includes confirmation of the physical model and the activity counter calibration constant. The self-tuning algorithm was scrutinized to ensure convergence to nominal values as well as stability. Finally, the constant-activity capabilities of the system were characterized. The range of relative activities that can be eluted from the system at different durations is of particular interest as it indicates the operating range of the system.

Characterization of the predictive corrective control of a pulse width modulated cycling valve (PCC-PWM) was analysed by comparison of results to the hysteresis corrected threshold comparison control (HC-TC). The testing and characterization phase allowed determination of whether PCC-PWM is a preferred alternative to HC-TC as a control method for the  $^{82}\text{Rb}$  elution system. In addition, these tests help validate the readiness of RbES for routine clinical use.

### 5.1 Safety Testing

Safety to operators and patients is the most important requirement of the design. As demonstrated in the design process of chapter 3, much emphasis was placed on reducing the chance of both current leakage and radiation exposure.

To ensure electrical safety, a CSA<sup>4</sup> certification was obtained for both the development and clinical system. Certification was obtained through testing by a third party

---

<sup>4</sup> Canadian Standards Association – a non-for-profit self-governing organization which tests and certifies equipment in order to ensure compliance with safety standards.

(Entela, Toronto, Ontario). The test includes electrical leakage, proper grounding, power isolation, and power consumption. These tests ensure general safety from electrocution, fire hazard, and surge protection. The measurements obtained for certification are listed in Table 5-1.

**Table 5-1 – Canadian Standards Association (CSA) field evaluation for electro-medical equipment results for two RbES systems.**

Test	System 1	System 2
Electrical Rating	1.19A @ 120V(60Hz)	1.19A @ 120V(60Hz)
Line to chassis surge (1000V)	Pass	Pass
Chassis to ground polarity with ground open (normal [Reverse])	<1 (Pass)	<1 (Pass)
Chassis to ground polarity with ground closed (normal [Reverse])	<1 (Pass)	<1 (Pass)

Although most of the fail-safe mechanisms were implemented in software, the hardware design also handled some of these aspects. Test cases, including hardware failure tests, are described in Appendix A. These are intended to ensure that the patient is not exposed to more than the radiation dose set in health regulation guidelines. Hardware malfunction scenarios were tested such as a computer crash, power outage, disconnected control lines, etc.

### *The Worst Case Scenario*

Even after much emphasis on developing a robust system that can identify and handle potential errors, there is always the risk of overlooking some erroneous scenarios. An additional cause for concern is that there may be situations when errors cannot be detected. In order to clarify the level of risk, the following worst-case scenario was developed:

The generator has recently been loaded with <sup>82</sup>Sr and morning flush and calibration runs pass successfully with 6800 MBq and 3400 MBq measured activities respectively. A large patient is to be imaged so an elution is started with a high dose (1500 MBq) over 30 s. The elution volume is limited by the maximum elution volume parameter (30 ml), which the autonomous pump is set to deliver. The elution begins normally, the threshold activity is passed, and patient valve is opened. As the activity concentration from the generator is still relatively low, the generator valve is set wide open. With the valve fully open, all the activity from the generator is routed to the patient. At this point, the operating system stops responding which prevents the software application from controlling the RbES. The

actuators remain in their previous state since the hardware is unaffected – the generator valve and patient valves are open and the pump is running.

Although the technologist should be monitoring the system at this point, he/she may be distracted by an urgent call of the patient. The system continues routing activity to the patient. The autonomous pump continues to run until the prescribed volume (30 ml) is reached. Although the valves remain in an open position the stopped pump prevents further flow of  $^{82}\text{Rb}$  to the patient. When the technologist returns to monitor the system, she/he notices that the user interface is not responding (or updating). In response, the computer is switched off, which cuts power to the DAQ and buffer boards and the valves return to their safe positions.

It is unlikely that the pump will continue eluting past the preset volume (30 ml). The pump chosen for this application is reputed for its reliability and accuracy due to the use of a stepping motor to actuate the peristaltic head. In terms of reliability the use of a stepping motor indicates that the pump controller must remain operational in order to actuate the pump. If the controller locks-up, the actuator by design will stall, thus limiting the deliverable volume to the prescribed dose.

This is considered the worst case scenario since it results in a maximal dose to the patient. The cycling signal is produced by a hardware counter on the DAQ, even when the computer stops responding, the signal is still generated. During this time it is expected that most of the bolus activity will be eluted to the patient, resulting in an eluted activity as high as 4000 MBq depending on the generator activity. Health regulation guidelines<sup>5</sup> permit activity doses as high as 2200 MBq per scan, but scans may be repeated as needed. Typically two scans (rest and stress) are conducted at any one session meaning that the guidelines permit routine exposure to 4400 MBq. Thus, this analysis concludes that this worst case scenario will result in radiation exposure that is within the guidelines, and thus of no significant risk to the patient's health.

## **5.2 Test Cases**

In addition to testing during general use of the system, test cases were written to validate the design requirements and test for bugs. The cases were written at an early stage of

the development process with the requirements in mind and later updated as the implementation details became finalized. No formal test approach was used, but in order to ensure thoroughness, the tests attempted to exercise as many the software branches as possible - including creating/simulating errors. As stated above, the test cases also include a hardware testing aspect in the form of malfunction detection testing and actuator response verification.

The tests were all carried out manually by the tester. Manual testing was necessary because testing included monitoring of the system display and actuators in a way that could not be easily automated. In addition, due to the real-time nature of the system, it was undesirable to further consume system resources with automated testing software. Finally, vials must be changed between elutions, which cannot be automated without the use of elaborate manipulators. Considering these complications and that the entire system could be tested within two work days, it did not seem worthwhile to set up an automated testing environment.

The tests were organized in a MS Access database for easier management and editing. Each of the 49 tests was classified under one of three groups as shown in Table 5-2. The cases are implemented in such a manner so as to test as many software branches as possible in order to shorten testing time. An example case is included in Figure 5-1 while the complete test list is included in Appendix A.

**Table 5-2 - Test classification codes and their descriptions.**

<b>Test Code</b>	<b>Test Type</b>	<b>Description</b>
E	Error Handling	Tests relating to error detection, handling, and reporting mechanisms.
F	Functionality	Tests relating to the functioning of the application – such as functionality of elutions and functions triggered by user input.
U	User Interface	Tests relating to the user interface – such as handling of invalid inputs, operation.

<sup>5</sup> University of Ottawa Heart Institute [<sup>82</sup>Rb] Rubidium Chloride Injection Investigator Brochure.

TestCode	TestName	Tester	Date
E-3a	<i>Pump Stalled Fault</i>	Ran Klein	25/08/2003
<b>Description</b>			
Test that a pump stall is detected and reported correctly.			
<b>Instructions</b>			
Start any operation. Once the real-time process has started stall the pump head. Observe that the program halts and that an appropriate error message is reported.			
<b>Pass</b>	<b>Fail</b>	<b>Repaired</b>	<b>RelatedTests</b>
<input checked="" type="checkbox"/>	<input type="checkbox"/>	<input type="checkbox"/>	E3a-c

Figure 5-1 - Sample test case layout.

### *User Interface Testing*

To reduce the chance of operator error the GUI is simple in design and all inputs are validated. An important aspect of this is limiting the user intervention to relevant functionality through a step-by-step menu. The touch screen interface displays only the information relating to the specific step in the menu, collecting a single input at any given time. Buttons that are not relevant to the specific step are disabled or removed from the screen entirely. In addition, each operator input is verified to be within a valid and reasonable range. If this is not the case, the operator is either asked to confirm the entered value or correct it. As a final measure the user is asked to confirm all the elution settings prior to starting of the automatic sequence.

To test the user interface, each software branch is executed by at least one of the 11 test cases. The tests guide the tester to perform specific actions and to observe certain behaviour of the user interface (such as disabling of buttons and appearance of messages). In addition, the final results screen, graphs, and printouts must be scrutinized for mismatches and errors.

### *Functional Testing*

This category applies to testing of the overall functionality of the system and its features. These 15 tests include ensuring the elutions proceed in correct sequence and that the hardware actuators perform correctly. During each elution sequence the cases call for visual monitoring of the display and actuators by the tester. Final elution results are analyzed to

ensure that the actual elution statistics fall within the tolerance range. Finally all record files are scrutinized for correct formatting and data.

### ***Error Handling Testing***

As a requirement, the system software was designed to detect malfunctions at the earliest possible stage and take action to avoid escalation to the worst case scenario or spoiling of the clinical test. In most cases the system copes with malfunctions by immediately stopping the elution in a controlled manner, setting the actuators to their safe mode, and generating a meaningful message to the operator. Each message includes the reason for failure and suggestions to resolve it.

The 23 error handling tests verify that errors are detected, proper action is taken by the system, and that the errors are reported in a meaningful manner. Of the 25 detectable errors, all but 3 errors are tested for proper handling. The remaining errors cannot be easily simulated and are unlikely to occur.

### ***5.3 Testing in a Routine Clinical Setting***

Monitoring of the system during routine clinical use was intended to assess the reliability of the system and to uncover any overlooked bugs and requirements. Two identical RbES were built, one of which was put into clinical use at the UOHI Cardiac PET Centre in January 2004 after passing the test cases, having obtained CSA certification, and being approved by the Medical Devices Institutional Review Committee. This system implemented all the design requirements except for the improved constant-activity control algorithm discussed in the previous chapter (PCC-PWM). The system was capable of all of the previously published elution capabilities including constant-flow, constant-time, and constant-activity using the hysteresis corrected threshold comparison algorithm (HC-TC). While the clinical system was being used routinely, development of the control system continued on the second system.

The RbES replaced the previous elution system [30] which was only capable of conducting constant-time elutions. As the technologists adopted the new system for routine use, their feedback was used to resolve issues and bugs as they were exposed. In addition, bug reports were used to assess the robustness of the system. The data collected during

clinical use were used to characterize some aspects of the RbES. The data included in this report relate to clinical trials over a nine-month period (from March 2004 to December 2004). During this time the generator was reloaded five times with 3700 MBq of  $^{82}\text{Sr}$ . The RbES was flushed and calibrated at the beginning of every work day whether or not scans were scheduled. During the trial period 667 patients underwent  $^{82}\text{Rb}$  rest and stress perfusion scans. Of those patients, 653 were scanned with the usual constant-time elutions and 14 were scanned using the HC-TC constant-activity mode.

### ***Computer Crash Issue***

During clinical use, a chronic problem of random computer crashes during the real-time sequence (2.3% of reported clinical elutions [n=925]) was observed. The crashes were manifested through total lock-up of the operating system, forcing a reboot the computer. This situation made analysis of the problem very difficult. Although the source of these crashes was not absolutely determined, it was suspected that system resources were mishandled and over-consumed. To address this possibility the software was altered with the following points of emphasis:

- Global variables – The software that was inherited from the prototype system used over one hundred global variables to communicate data between scripts and functions. The declaration of these variables in each function was carried out through the *global\_declare* script. Since Matlab is an interpreted language, the repetitive calling of this script adds significant overhead. To reduce this overhead, two concepts were enforced throughout the software:
  - Function based design – where possible, scripts were replaced with functions to which the variables could be passed as parameters during the function call. This completely removed the need to declare the global variables in the function.
  - Global variable structure – individual global variables were unified under several data structures (Table 5-3). This enabled declaring only a few global variables as needed rather than calling an entire script file.

**Table 5-3 - List of global structures and their contents.**

Structure Name	Content Description
parametersINI	Parameters loaded from the initialization file.
parametersCAL	Parameters loaded from the calibration file such as generator information, daily protocol history, and calibration parameters for the system.
runS	Parameters structure defining the current elution run (created before the elution begins)
calS	Calibration information calculated prior to the elution run.
logS	Log structure created during the elution containing all records pertaining to the actual sequence of events during the elution.
GUIS	Structure containing all parameters related to the GUI. In addition a list handles to all dynamic graphic objects is included.

- Improved graphic object management - the software was modified to better manage graphic objects through deletion of unused objects or updating of object parameters rather than overwriting them as was inherited from the prototype system.
- Pump driver – the prototype system communicated with the pump through a polling algorithm included in the *physical\_sequence* model. The communication protocol with the pump dictates a delay of 300-500 ms between the query and answer by the pump. This was handled in the prototype system through a delay loop until the query and answer was completed. Since the *physical\_sequence* is refreshed at 1 Hz this delay added significant overhead (30-50%). To reduce this overhead, a communication driver was written. The driver runs as a separate task and is triggered by an interrupt event whenever data are received on the port. The data are read, tested for errors, and updated directly in the real-time model before a new query is sent to the pump. If a reply from the pump is not received within 500 ms the query is repeated. Thus the overhead was substantially reduced leaving more system resources available.

The new implementation was not transferred to the clinical trial, but software crashes were not experienced during 6 months of use on the development system. Once the new software is subjected to routine clinical use, experience should reinforce confidence in the robustness of the new software.

#### 5.4 Calibration Characterization

Over the life-span of five generators (284 days), 189 calibration runs were conducted at 15 ml/min flow rate (Figure 5-2). The calibration constant appears unchanged with a standard deviation of 2.16%. Closer inspection revealed a small but significant correlation between the eluted activity and the calibration constant,  $K$ , ( $p=0.0044$ ,  $r^2=0.0585$ ) as is demonstrated by Figure 5-3. A linear fit revealed a small slope,  $2.59 \cdot 10^{-9}$  MBq/ml/cps/MBq (95% confidence interval [ $1.09 \cdot 10^{-9}$ ,  $4.09 \cdot 10^{-9}$ ]) in the relation between calibration constant (MBq/ml / cps) and generator activity (MBq). Over the life span of a generator the calibration activity can change by as much as 2500 MBq. This results in  $\sim 1.7\%$  change in the calibration constant over the life of a generator, which is considered a negligible effect. These results show that the calibration process is both reproducible and is relatively constant throughout the entire range of useful activities.

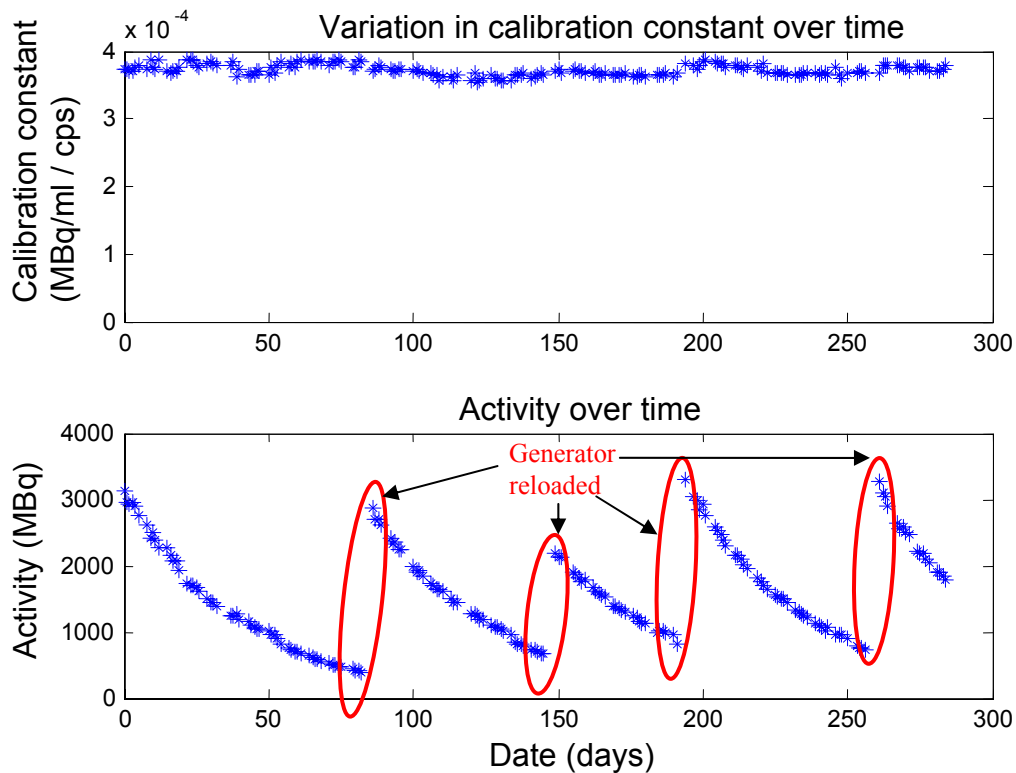


Figure 5-2 – Calibration constant over the course of a generator life (top) and the <sup>82</sup>Rb activity from the generator during calibration over the same time period (bottom).

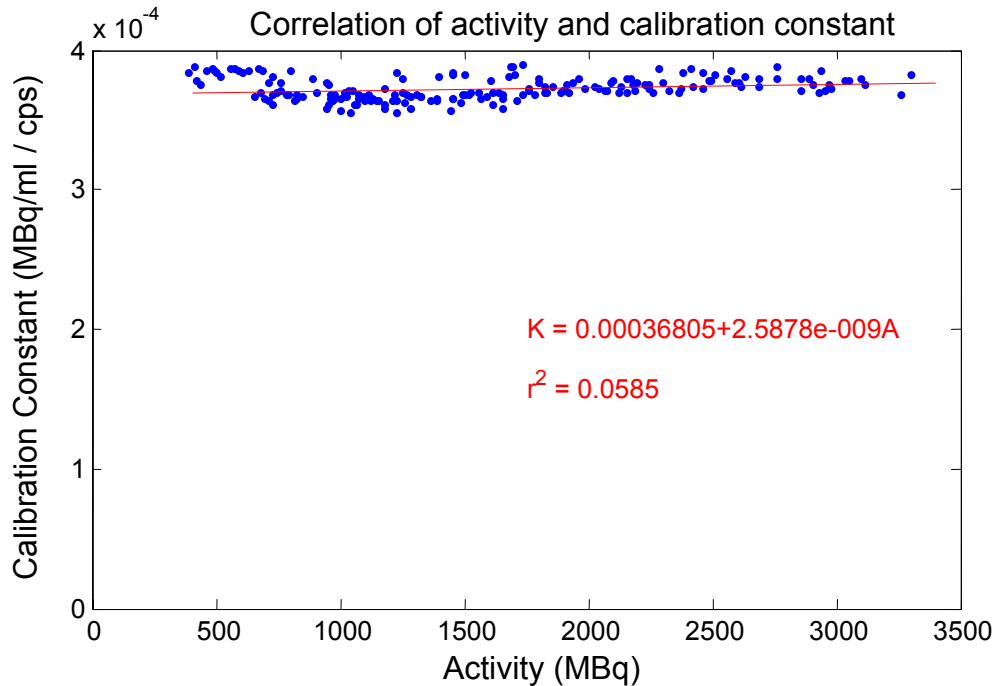
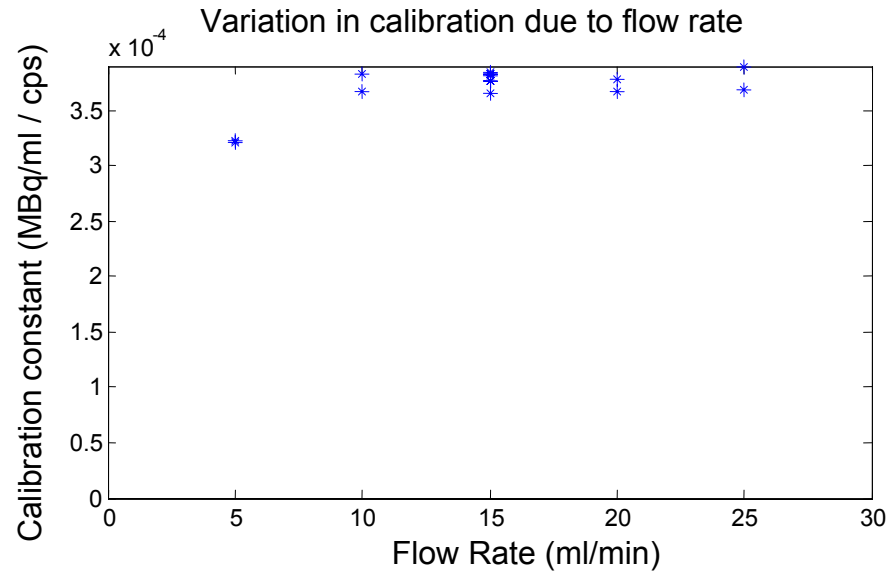


Figure 5-3 - Correlation of calibration constant to generator activity.

#### *Calibration Constant vs. Flow Rate*

Calibration elutions are performed with a saline flow rate of 15 ml/min, but elutions are performed in the range of 5-25 ml/min. Since the calibration constant is a measure of efficiency (intrinsic and geometric) of the activity counter it is expected that this constant remain valid regardless of elution flow rate. To test this assumption, five sets of calibration elutions were conducted at flow rates ranging 5-25 ml/min at increments of 5 ml/min (Figure 5-4). The value of the calibration constant did not vary significantly over the range 10-25 ml/min., however a slight decrease was noted at 5 ml/min flow rate. This reduction may be due to longer transport times to the dose calibrator than expected due to inaccuracy in the line volumes. At this low flow rate, significant <sup>82</sup>Rb decay is experienced, while at the higher flow rates the delivery time error is 2 to 5 times shorter.



**Figure 5-4 – Calculated calibration constant over the range of flow rates.**

The same test was repeated with a second generator, this time revealing a different trend in results as shown in Figure 5-5. As the flow rate increased, the calibration constant decreased almost linearly. Further investigation revealed that the line pressure was increasing linearly with the flow rate up to 20 ml/min at which point it saturated (10-25 psi compared with 7-15 psi in the previous generator). This high pressure was due to saline flow resistance imposed by the second generator. This resistance generated a high pressure resulting in backwash through the peristaltic pump head leading to a flow rate lower than expected. If calibration constants were corrected for the measured flow rate (measured through the saline volume in the vial) the calibration constant would have varied less with flow rate, demonstrated by the dashed line in Figure 5-5. However, the flow rate cannot be measured with the current hardware.

The high flow resistance introduced by the second generator is due to the tin-oxide packing of the generator column during production. Tin-oxide comes in a powder form and is filtered twice to exclude particles outside a specific size range. The filtered powder is then packed to remove large air pockets. If the packing is too tight, or the size of powder grains is too small one can expect restricted saline flow through the column. Once the generator has been loaded with <sup>82</sup>Sr and released for clinical use, the flow resistance does not seem to change over time.

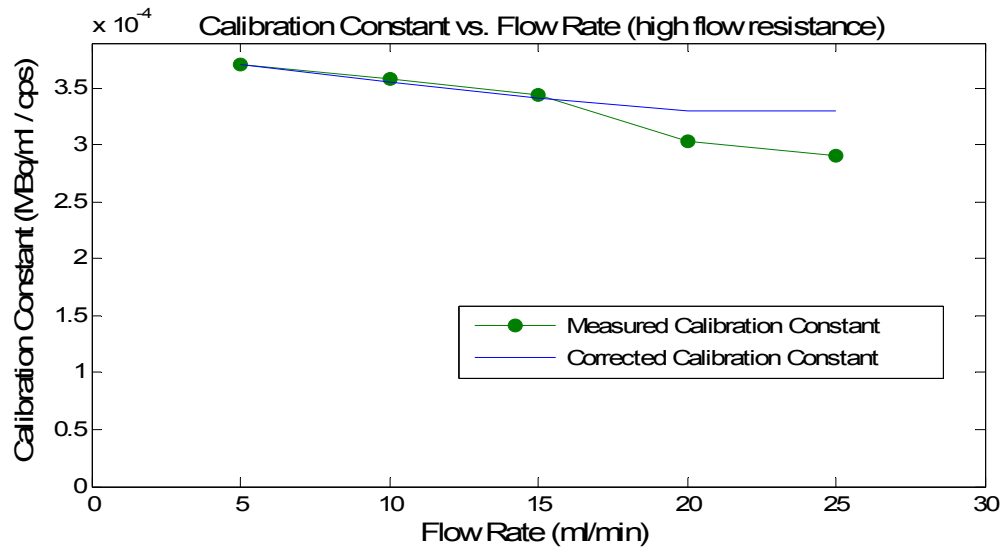


**Figure 5-5 - Calibration constant dependence on flow rate for generator column with high flow resistance.**

Variation in elution characteristics, including flow resistance, is expected between generator models. In this study two generators of the same model were used. Both were custom made at UOHI [30]. It is expected that a single generator model be used in any single facility in order to promote reliability and inter-changeability.

To address backwash through the pump-head resulting from increased flow resistance, two courses are suggested for future work. It is preferable for future applications that flow resistance be tested after the building of the column and before loading of <sup>82</sup>Sr to ensure that the saline pressure at the generator input remains below 20 psi at flow rates in the range of 5-25 ml/min. In addition it is suggested that the pump head rotor be replaced with a model that can sustain higher back pressure without backwash.

### *Summary of Calibration Analysis*

The calibration results helped validate the accuracy of the model of the physical process from the activity counter to the patient outlet. This ensures that the physical process during transport of the activity from the activity counter to the patient outlet (or dose calibrator) is well understood and can be modeled over the entire range of flow rates. This means that one can predict the activity profile at the patient outlet accurately based on measurements from the activity counter. This result is valid as long as the line pressure remains sufficiently low to avoid backwash through the pump head and a false flow rate.

## 5.5 Analysis of the Self-Tuning Model

The control algorithm was designed in such a way that manual adjustment of the system should not be needed. To achieve this, the system needs to self-tune the valve response model parameters to nominal values so as to reduce the activity rate errors over time. Although it is desirable that the valve response adapt quickly to changes in the system, it is more important that the self-tuning algorithm be robust. Poor measurements due to malfunctions or errors must not cause the model to diverge significantly from its nominal parameters. For example, if the saline supply line is pinched during an elution, no activity will be drawn from the generator, leading to low activity rate measurements, but this is not an indication that the valve response has changed. In practice the dynamics of the system are not expected to change very quickly and therefore some robustness can be maintained using small learning coefficients as demonstrated in chapter 4.

In order to assess the stability and robustness of the self-tuning algorithm, both analytical and empirical analyses were performed. The first was included in the design process and is described in the previous chapter. At the characterization stage, the performance of the self-tuning algorithm was assessed by monitoring the elution profiles and the associated model parameters.

In order to speed up the tuning process for demonstration purposes, the learning parameters,  $\gamma_L$ ,  $\gamma_S$ , and  $\gamma_R$  listed in (29), (30), and (31) respectively were increased by an order of magnitude (X10). Figure 5-6 shows the activity rate vs. time (bottom) and error vs. valve flow ratio (top) for three successive elutions (30% relative activity over 30 s). The linear slope and sigmoid scaling are adjusted based on the lower range of valve duty-cycle ( $r < r_t$ ). As the parameters converge, their adjustments decrease in magnitude. The improvement in precision can be both noticed visually as a decrease in error slope and by the gradual decrease in root-mean-square (RMS) elution error from 24.5 to 14.7.

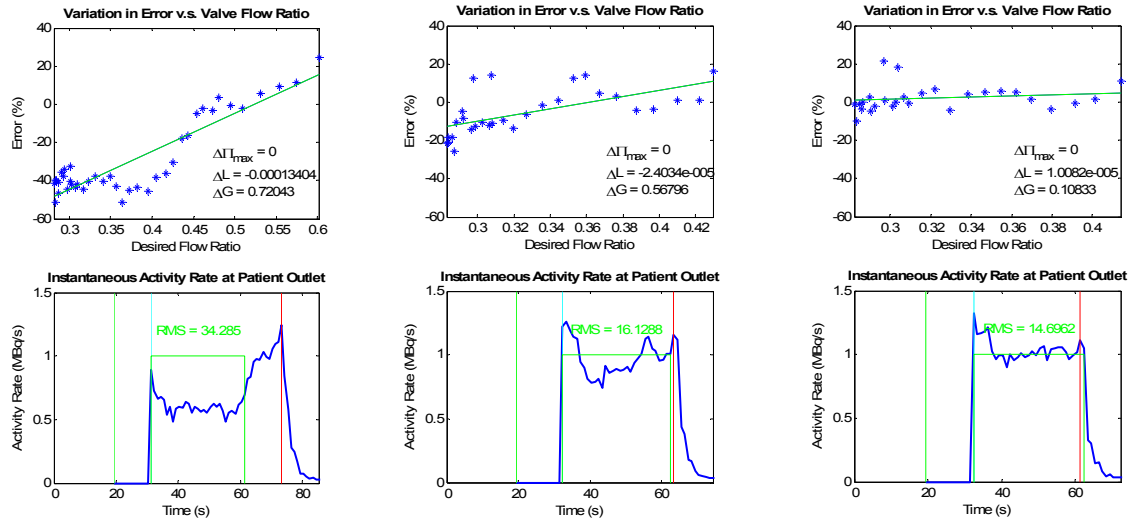


**Figure 5-6 – Illustration of the effect of accelerated self-tuning of the valve response model over three successive elutions at 30% over 30 s. The top graph represents the measured error vs. the valve duty-cycle while the bottom portion compares the eluted activity rate to the requested activity rate. As the linear slope and sigmoid scaling parameters are adjusted the RMS error decreases.**

The same process can be demonstrated over a different set of data in which 30% relative activity 30 s elutions were repeated 87 times. The evolution of parameters, and the resulting RMS error and elution time error is shown in Figure 5-7. As the valve response is self-tuned the RMS error initially increases, but then decreases as the parameters G and L converge. The elution time error increases in magnitude almost in unison with the RMS error. During the entire training session  $\Pi_{max}$  is unchanged, as the desired valve ratio does not reach the region (100% open) required for tuning  $\Pi_{max}$ .

The evolution of parameters G and L can also be viewed on the plot of the parameters (Figure 5-8). Parameter L is initially far from its nominal value, and adapts slowly. Parameter G adapts faster and overshoots its nominal value. Once L begins to converge to its nominal value, the over correction of G becomes prominent and its correction reverses. As both parameters evolve, they converge towards their nominal values and remain relatively stable in 17 subsequent runs ( $G=26.5\pm 0.65$ ,  $L=0.00677\pm 0.00017$ ).

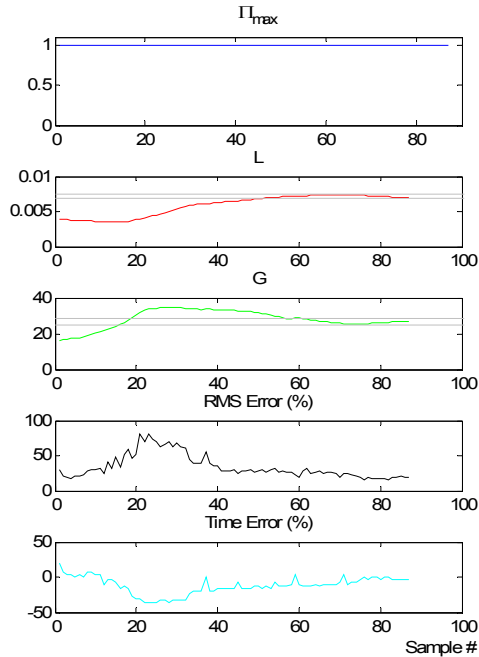


Figure 5-7 – Evolution of parameters G and L during self-tuning through repeated runs of 30% relative activity over 30 s. The start point is the manual fit of the curve, while the stop point was determined when change to the parameters was relatively small (n=87).

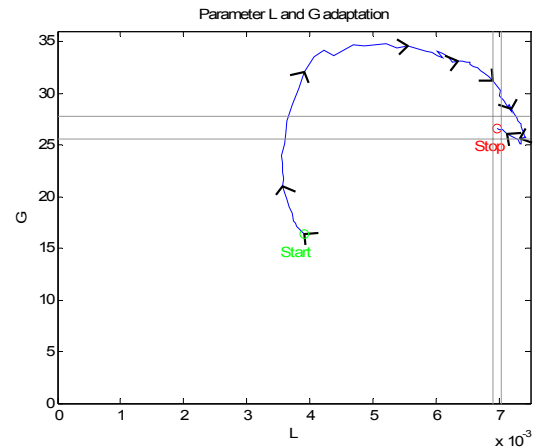


Figure 5-8 – Evolution of parameters G and L during a 30% relative activity over 30 s training session. The grey lines define the region of model parameter variation over 17 subsequent elutions.

The above training process involved 87 repeated elutions, which in a typical clinical setting would require several weeks to complete. Although a clinical system is not expected to be in a parameter state that is so far from the nominal values, this slow learning indicates that the self tuning algorithm will be very slow to accommodate changes in the system. The system learning parameters,  $\gamma_L$  and  $\gamma_G$ , can be increased in order to speed up the learning process - suggested values could be 0.1 and 0.05 respectively.

#### *Variation in Valve Model Parameters with Requested Elution Parameters*

In the above training set, the parameters are optimized for the specific requested profile (30% relative activity over 30 s). It is expected that these parameters should remain valid over other profiles as well (different durations and relative activities), but in practice this may not be true as the self-tuning mechanism corrects for measured activity rate errors regardless of what their source is. Over a set of elutions with variable relative activities this suspicion was confirmed in the sense that changing the relative activity seemed to result in conflicting parameter adjustments.

One reason for the conflicting L parameter adjustments is the two different scenarios through which this parameter may be adjusted. To illustrate this, Figure 5-9 (bottom) shows an example activity rate error vs. desired flow ratio. Since more than 4 data points exist for the higher flow ratio region ( $r_t < r < 1$ ), parameter L is adjusted based on the slope of the line fit to this region (dotted line), referred to as slope rule. As the slope is negative in this case, the adjustment of L is positive (0.00021). However, if less activity was requested, less than 4 data points might be measured in the higher flow ratio region, and the mean error in the lower flow ratio region ( $r < r_t$ ) would be used to adjust L, referred to as a mean error rule. Since the mean error is clearly negative, the slope would be decreased, to increase the duty-cycle in this range. Figure 5-9: top shows the valve response that corresponds to the range of desired flow ratios that were used during the elution and the cut-off between the lower and higher range of the response,  $r_t$ .

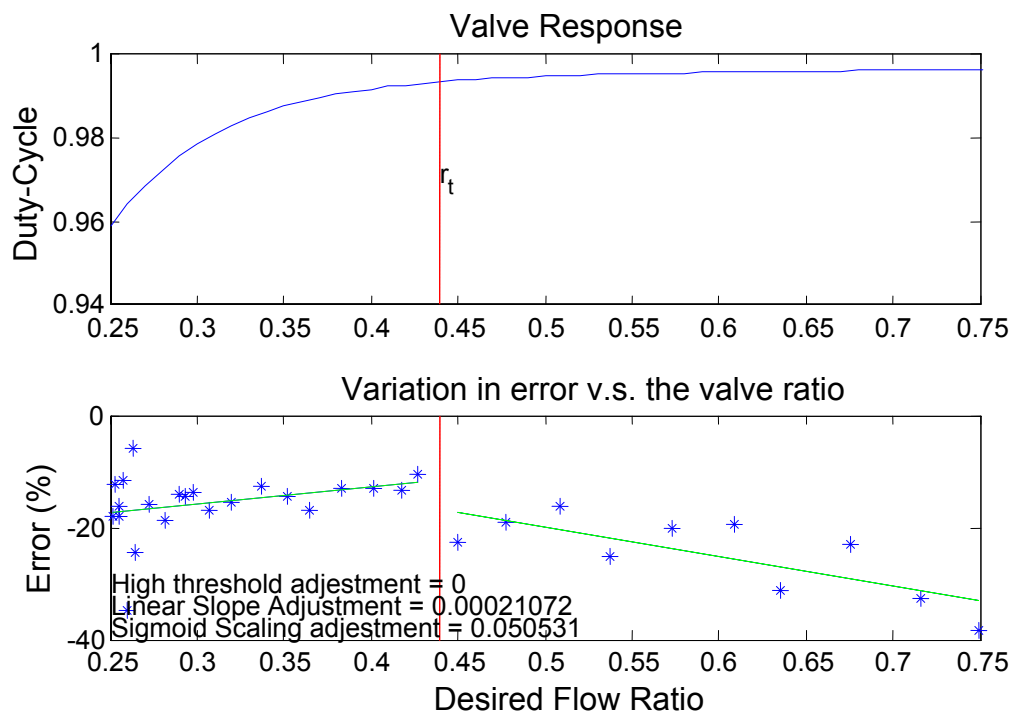


**Figure 5-9 – Example activity rate error measurements used for valve response model parameter tuning to illustrate conflicting adjustments based on how the data are treated.**

With this adjustment conflict in mind, it is interesting to know what values parameter L would converge to with each adjustment scenario. This was attempted through repeated runs of 50% relative activity over 30 s but was aborted as a second problem with the L parameter adaptation law was revealed (Figure 5-10).

If a high relative activity is requested, the generator bolus activity may be exhausted before the end of the elution, resulting in large negative error at very high valve flow ratios. Adjusting parameter L based on the slope rule, results in producing constant-activity rate elutions with a bias. This is a result of the slope rule ‘attempting’ to achieve a constant level of error throughout the range of valve flow ratios. Since negative errors are inevitable if the bolus activity is exhausted, the end result is negative errors throughout the range of valve flow ratios.

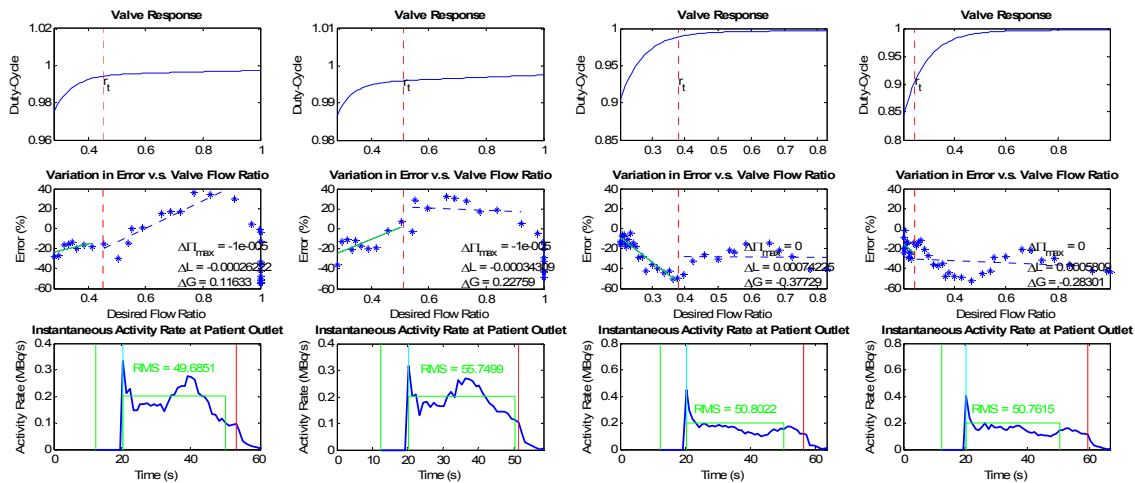


**Figure 5-10 – Adaptation of parameter L over a repeated sequence of 50% relative activity over 30 s elutions revealed that the adaptation law is flawed. The resulting elution curves become flat, but biased due to exhaustion of the generator activity.**

This issue does not occur when the alternate (mean error) rule is used since the lower range, which spans most of the elution time, is always driven to achieve zero error. With the mean error rule, the L parameter is a product of two concurrent processes: driving the average lower range error to zero and adjusting the upper valve saturation point,  $\Pi_{max}$ . It is expected that maintaining the mean error rule as the only adaptation rule for parameter L will yield better self-tuning characteristics; however this was not tested within the scope of this work.

### Analysis of Tuned Valve Response

Comparing the valve response curves produced with manually estimated parameters and self-tuned parameters (Figure 5-11) reveals some interesting issues. The response graph generated with self-tuned parameters (dashed line) follows the measured response less closely than the manual estimate (dotted line). The region of operation of the valve is

$\sim 0.25 < r \leq 1.0$  which corresponds to very small changes in the duty-cycle,  $\sim 0.97 < \Pi < 0.9975$ . The response in this range caused very large changes in flow ratio due to very fine duty-cycle changes, an unfavourable response.

### Valve Response Correction Curve

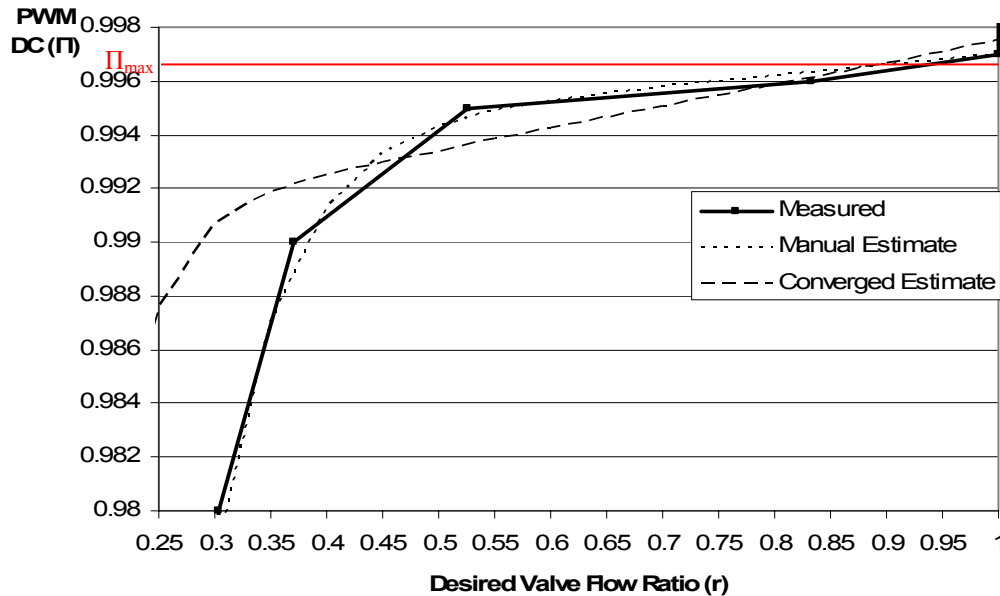


Figure 5-11 – Valve response correction curve used to determine the PWM duty-cycle (DC) required to achieve a desired valve flow ratio. The measured curve (shown in heavy line) is followed more closely by the manually estimated fit (dotted line) than by the automatically tuned fit (dashed line).

The discrepancy between the self-tuned valve response and the measured response is partially due to the self-tuning algorithm adjusting the valve response parameters to decrease the overall activity rate errors. These errors are not caused solely by modeling of the valve response, but also through imperfect system modeling, prediction of activity concentration, and possibly other unknown factors. The self-tuned valve response by its nature will try to correct for these error sources.

A potential limitation in the design of the self-tuning algorithm is that the error analysis does not take into account that errors in the valve response also contribute to activity concentration prediction errors. Even if the system model (and prediction algorithm) were perfect, errors in the valve response model would lead to erroneous prediction of the effective volume through the generator leading to a false activity concentration prediction,  $C_{M..}$ . As a result, activity concentration errors may accumulate as the elution progresses. It is

the role of the corrective algorithm to compensate for errors during the elution, and also reduce prediction error, but some degree of error is inevitable.

Since the elution begins with a high activity concentration from the generator as the bolus portion of the activity curve is eluted, the valve flow ratio during the beginning of the elution is kept low. During the later portion of the elution the valve flow ratio increases if a high relative activity was requested. Since more prediction error is expected as the elution progresses, the activity rate at higher ranges of valve flow ratios ( $r_t < r$ ) is associated with more prediction error than the activity rate associated with the lower range of valve flow ratios ( $r < r_t$ ). For this reason the error measurements associated with the lower valve flow ratio range must be weighted more heavily for adjustment of the model parameters.

Both the theoretical analysis and experimental analysis point to a stable and converging self-tuning model of the valve response over repeated elutions with the same requested profile. However some variation in ideal parameter values is expected between requested profiles. The amount of variation cannot be estimated with the available data, but could be addressed by future research. The experience to date is over a relatively short time period and in a well monitored environment. Furthermore, these results were measured using a single generator. In a clinical setting, generators will be replaced every 2 months approximately, the system will be used without tracking of the parameters, and if the elution profiles worsen it is unlikely that the technologists will be capable of readjusting the parameters. Ultimately, clinical trials will shed light on the long term performance and reliability of the self-tuning algorithm.

## **5.6 Elution Tests**

With the system tuned in both the HC-TC and PCC-PWM control modes, comparisons were performed to determine a preferred method. In a typical clinical application elutions are 30 s long and the activity is matched to the physical size of the patient. Typical relative activities range from 10% for a small patient and a hot generator to 70% for a large patient and a cold generator.

The control algorithms were compared through ten sets of 30 s elutions of 10, 30, 50, and 70% relative activity. Both HC-TC control and PCC-PWM were assessed for comparison. For each run the elution time error was defined as the difference between the actual elution time (required to reach the requested activity) and the requested time (32). In addition, the RMS error relative to the requested activity rate was calculated as an indication of the accuracy of the algorithm in maintaining a constant-activity rate (33). The time error is an indication of the average activity rate throughout the elution, while the RMS error is a measure of deviation of the activity profile from the ideal rectangular form. Typical elution profiles using both control modes are demonstrated in Table 5-4.

$$\text{Elution Time Error} = \hat{T}_{\text{Elution}} - T_{\text{Req}} \tag{32}$$

$$\text{Error RMS} = \frac{\sqrt{\sum (\hat{A}_C - \dot{A}_C)^2} / \hat{T}_{\text{Elution}}}{\dot{A}_C} \cdot 100\% \tag{33}$$

**Table 5-4 – Typical constant-activity elution profiles for various relative activities and over 30 s.**

Relative Activity	HC-TC	PCC-PWM
10%		
30%		
50%		
70%		

Table 5-5 and Figure 5-12 compare the activity rate RMS error and the elution time error over the range of relative activities. The requested elution time is typically achieved using HC-TC but fluctuations cause a >40% RMS error. The PCC-PWM control significantly reduces the RMS error over most of the range of relative activities, except in at the upper extreme of generator activity (70% relative activity).

**Table 5-5 - Comparison of Performance measures for HC-TC and PCC-PWM 30 s Elutions [n=10]**

Requested Dose (% relative activity)	RMS Error $\pm$ SD (%)			Elution Time Error $\pm$ SD (%)			Modeling Accuracy $\pm$ SD		
	HC-TC	PCC-PWM	P-value	HC-TC	PCC-PWM	P-value	HC-TC	PCC-PWM	P-value
10	43.6 $\pm$ 2.7	10.6 $\pm$ 1.4	<0.001	-1.0 $\pm$ 2.3	-3.3 $\pm$ 3.1	0.220	1.10 $\pm$ .08	1.01 $\pm$ .03	0.005
30	54.3 $\pm$ 3.8	12.9 $\pm$ 2.5	<0.001	-1.7 $\pm$ 2.3	0.7 $\pm$ 2.6	0.089	1.14 $\pm$ .03	1.08 $\pm$ .06	0.014
50	42.8 $\pm$ 7.2	13 $\pm$ 3.2	<0.001	3.0 $\pm$ 5.1	3.3 $\pm$ 2.2	0.85	1.02 $\pm$ .03	1.08 $\pm$ .06	0.053
70	45.3 $\pm$ 5.3	41.2 $\pm$ 8.5	0.120	9.0 $\pm$ 4.7	-0.7 $\pm$ 5.2	0.002	.96 $\pm$ .03	.95 $\pm$ .03	0.352

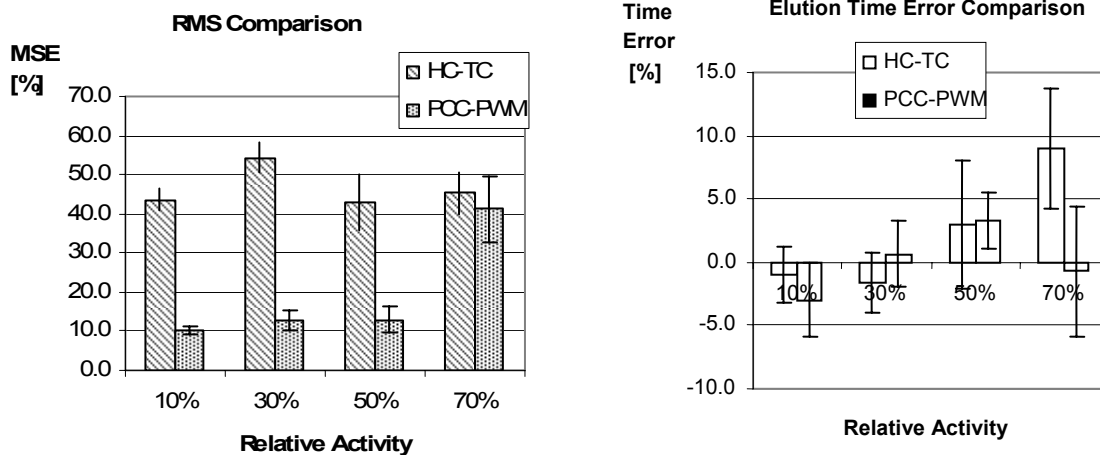


**Figure 5-12 - Comparison of performance measures of elutions [n=10] over 30 s at 10, 30, 50, and 70% relative activity. The root mean square (RMS) activity rate error shown on left is an indication of instantaneous precision, while the elution time error on the right is an indication of global precision.**

The activity rate is measured at the activity counter and is used to predict the activity rate at the patient outlet. To ensure that this prediction is accurate, a comparison with the dose calibrator was made and a modeling accuracy factor (Table 5-5) was calculated for each relative activity (relating to flow rates 5-25 ml/min). The modeling accuracy was calculated as the ratio between the integrated rate of activity based on both activity counter and dose calibrator readings (34) demonstrated by Figure 5-13. The activity counter readings were corrected for transport delay to the patient outlet while the calibrator readings were

deconvolved with the <sup>82</sup>Rb decay curve to convert accumulated activity readings to activity rate measurements. Ideally the area ratio should be equal to 1 indicating perfect modeling. As Table 5-5 shows, using both HC-TC and PCC-PWM resulted in model accuracy  $\approx 1$  throughout the entire range of relative activities, with a significant improvement with PCC-PWM in the 10-30% relative activity range. The PCC-PWM results indicate modeling error that is typically less than 10% with a slight underestimation of activity at the patient outlet in the 30-50% relative activity range.

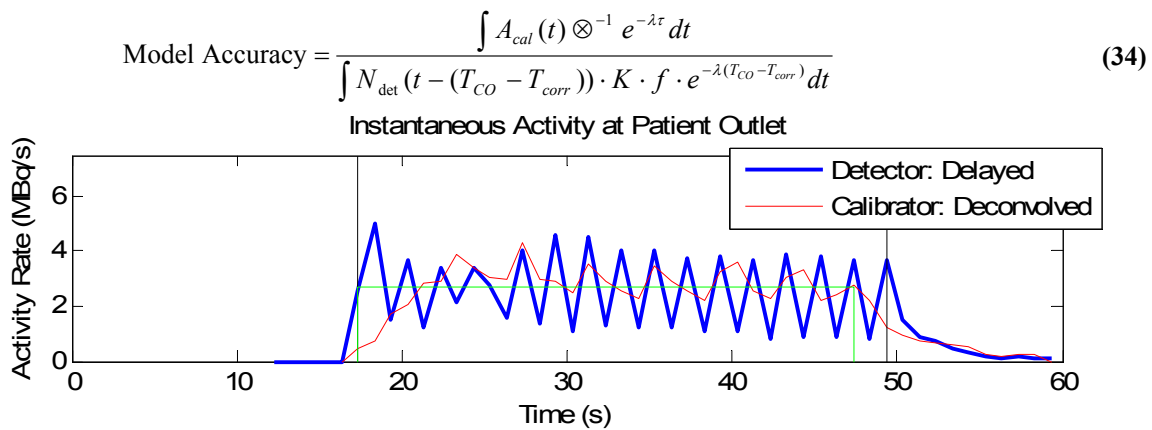


**Figure 5-13 – Activity rate at patient outlet calculated based on the activity counter readings (blue) and dose calibrator readings (red). The ratio of integral activity over the elution time (black lines) is used to assess the accuracy in predicting activity rate at the patient outlet based on activity counter readings.**

The high RMS error of the PCC-PWM control at 70% relative activity is partly a result of the initial overshoot which is not discarded as with lower relative activity elutions. The initial activity portion cannot be removed, as the generator activity will be insufficient to achieve the requested activity without it. The source of this overshoot is an initial rise in activity at high flow rates that is too fast for the system to respond to. The magnitude of the peak varies significantly based on whether the rise of activity is sampled early enough to afford the prediction algorithm time to respond. In most cases the rise is not sampled early enough, leading to an overshoot in activity rate of approximately 100% over approximately 2 s as is shown in the lower right figure in Table 5-4.

Over a 30 s elution a 100% initial overshoot over 2 s would result in a 26% RMS error even if no additional error is experienced over the remaining 28 s of the elution. However, the integrator component of the corrective mechanism attempts to correct for this overshoot by reducing the activity rate over the remainder of the elution resulting in an even higher RMS error. To make matters worse, the activity rate from the generator decreases

below the set point as the bolus of activity is exhausted. This is seen in the decrease of activity rate in the final ~5 s of the elution in the mentioned figure. Since the generator valve is already fully opened at this point, nothing more can be done to increase the activity rate. These reasons combine to set the upper limit of relative activity that can be expected from a constant-activity elution.

At 70% relative activity the mean elution time error achieved by PCC-PWM is less than with HC-TC ( $p=0.002$ ). However, the variability of elution time error is similar for both control modes ( $p>0.45$  for 10,30,70%) with exception of 50% relative activity ( $p=0.022$ ). At 70% relative activity PCC-PWM seems to experience more variability in the elution time error compared to lower relative activity elutions. This is partially due to late registration of the activity rise phenomenon as discussed above.

Due to the higher saline flow rate ( $>20$  ml/min) used in high relative activity rate elutions, a fast rise of activity over time results as the bolus is flushed from the generator. Detection of a rise in activity is needed to synchronize the prediction algorithm with the actual eluted volume (by solving for  $V_s$ ). If this rise is not sampled early enough for the prediction algorithm to take effect, an initial overshoot results which will lead to early stopping of the elution. If the rise is detected early enough to avoid the overshoot, as with most cases at low flow rates, the total elution time to reach the same activity may be longer, thus introducing a variation in elution time error. With the current implementation the variation in early rise detection is a fundamental limit.

### *Range of Relative Activities as a Function of Elution Duration*

Although 30 s elutions are the norm, there may be reason to believe that longer elutions may permit more accurate measurement of perfusion [18,27,28]. Since this issue is being addressed through a current study at the UOHI it was deemed necessary to assess the system characteristics at various elution durations.

A second set of elutions was aimed at determining the minimum and maximum relative activities that can be eluted from the generator as a function of the elution duration. Elutions of 15, 30, 60, 120, and 240 s were used as a test set in which the maximum relative activity was determined empirically. The success of each elution was evaluated by testing for no significant drop in activity recorded at the end of the elution due to insufficient activity in

the generator, and that both the RMS error and elution time error remained unchanged from the 30 s elutions.

As the results in Figure 5-14 show, the performance between HC-TC and PCC-PWM is similar for short elution durations (15-60 s), however at longer durations (120 and 240 s) the HC-TC method has difficulty controlling low relative activities. At durations of 240 s the PCC-PWM method can perform elutions using as low as 36% relative activity elutions, while HC-TC can only achieve relative activities where activity was at least 69%. The measured maximum relative activities were almost identical throughout the entire range of durations. The HC-TC method was not capable of achieving low activity rates leading to premature elution of the requested activity. Pump flow rates were set in the same manner for both control algorithms to avoid bias; however it may be that by better adjusting the saline flow rates this short coming of the HC-TC method could be overcome.

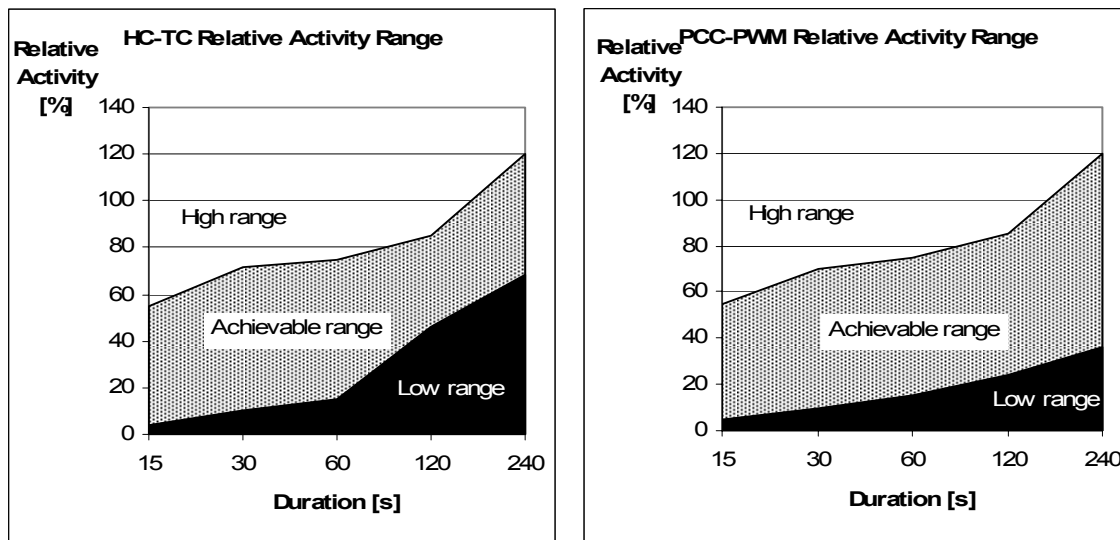


Figure 5-14 – Range of relative activities that can be achieved using the HC-TC method (left) and the PCC-PWM method (right) without significantly influencing the precision. The high range indicates that the requested activity is higher than can be provided by the generator, while the low range indicates activity that is too low for the control algorithm to generate.

## 5.7 Generator Life Span

In order to increase the cost effectiveness of  $^{82}\text{Rb}$  generators, one would like to perform as many scans as possible between reloading of the generator. This issue has only been addressed in the context of the range of relative activities that can be eluted to patients (Chapter 1). However, several other factors must also be taken into account.

### Breakthrough Sr Activity

Elution of <sup>82</sup>Sr and <sup>85</sup>Sr isotopes (half-life of 25 and 65 days respectively) to the patient is undesired, as Sr tends to accumulate in the bone marrow, which is particularly radiation sensitive [15]. Of concern to us was premature Sr breakthrough, due to the pulsating flow of saline through the generator as the valve is cycled.

Daily calibration samples are used to test for the breakthrough of Sr activity; if significant Sr activity is detected, the generator cannot be used on humans. The specifications of our generator permit 20 L of saline to be eluted before Sr breakthrough should be experienced. We continued to use the generator on the development system past the specifications and experienced first breakthrough after approximately 40 L were eluted through the generator. Once breakthrough appeared, it was tracked over two months. The measured breakthrough activity reached a maximum around the 40<sup>th</sup> day. However, if the activity is corrected for <sup>82</sup>Sr decay it becomes clear that the breakthrough (<sup>82</sup>Sr to <sup>82</sup>Rb activity ratio) continues to increase as shown in Figure 5-15.

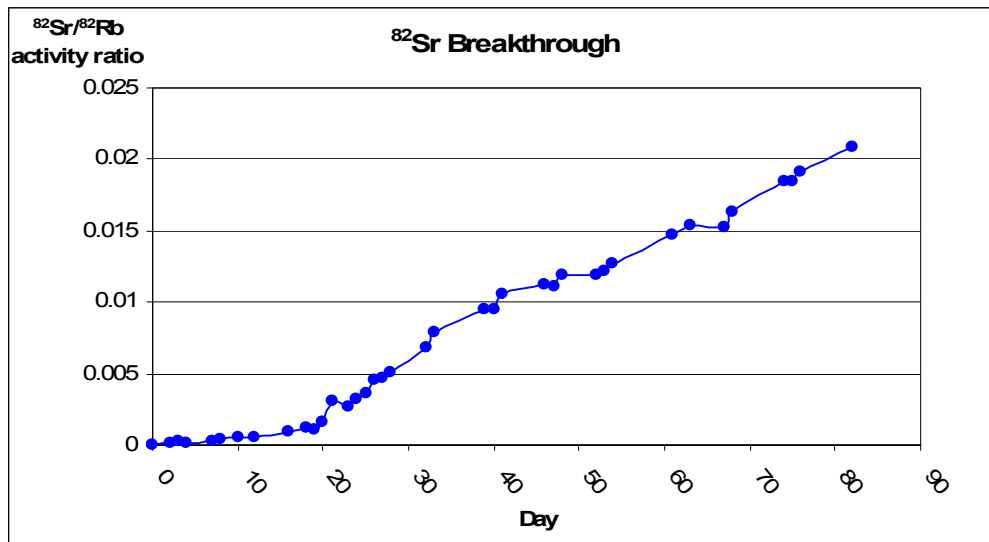


Figure 5-15 - Breakthrough ratio progression over time as measured and corrected for <sup>82</sup>Sr decay.

We have no data to suggest premature breakthrough due to the cycling valve. However, testing on additional generators is required to determine whether breakthrough is accelerated or not. Sr breakthrough does not appear to be a safety concern as it changes slowly and is tested for on a daily basis as part of the daily protocol.

### Activity Curves

The activity rate vs. volume curve collected during the daily calibration run is used to predict the activity concentration from the generator as part of the prediction algorithm. A question that arises is whether these curves change over the life time of the generator. It is clear that their amplitude decreases as the  $^{82}\text{Sr}$  in the generator decays (Figure 5-2: bottom), but the shape of the curves had not been investigated.

Calibration curves over the life of the generator were normalized by their peak activity rate and plotted on the same graph with the colours varying (blue to orange) in order of date (Figure 5-16). This graph reveals that over the life of the generator, the bolus volume becomes smaller, evident as a narrower peak. This may be a result of the Sr migration along the generator column resulting in less delay and dispersion of the solution as it travels through a smaller volume to the generator outlet. These curves follow the model described by (1), but the model parameters vary with time (or total eluted volume).

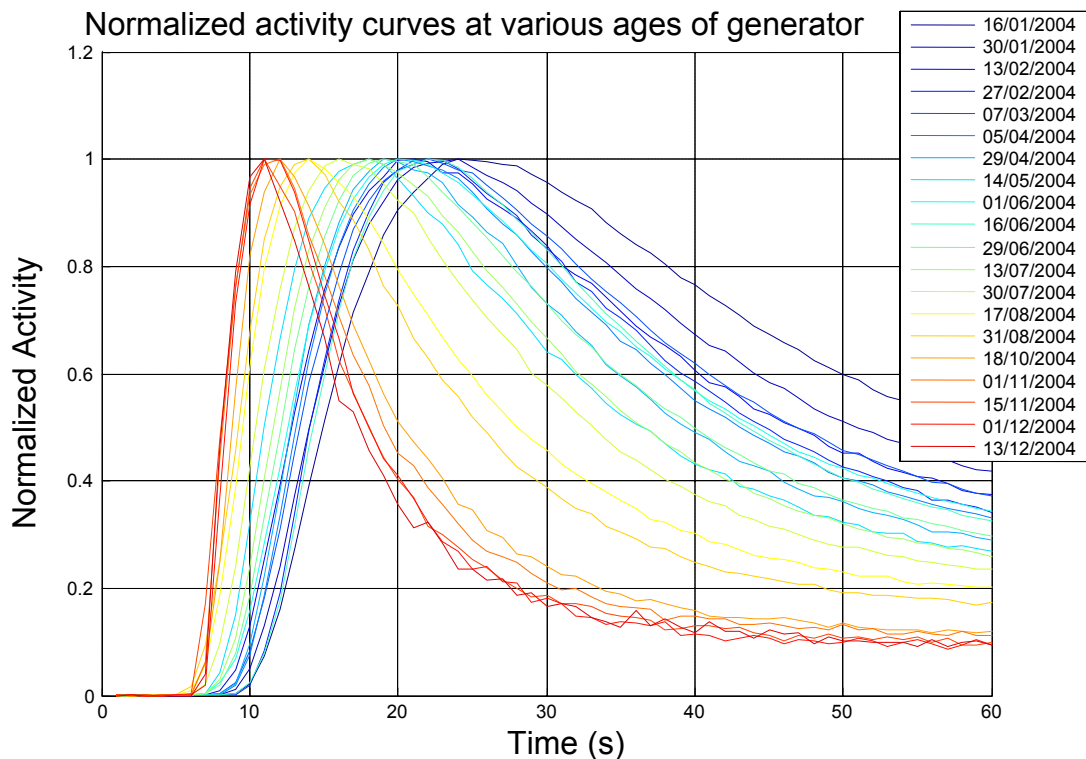


**Figure 5-16 - Normalized activity rate vs. time curves measured during calibration runs over the life span of a generator.**

The significance of these results is that the prediction mechanism is expected to perform better with a new generator than with an old one. In the case of an old generator, a

small error in the volume through the generator will manifest itself as a large error in the predicted activity concentration, and therefore a larger error in the predicted valve flow ratio. Since all of the constant-activity elution measurements in this work were performed within the last two months of the generator on the research system, it is expected that the elution performance measures may improve once a newer generator is obtained for research use. Replacement of this generator was not scheduled until late January 2005; therefore this hypothesis could not be tested.

The life span of  $^{82}\text{Sr}/^{82}\text{Rb}$  generators has been determined until now by the risk of  $^{82}\text{Sr}$  breakthrough and minimum patient activity ( $\sim 2000$  MBq). The results of Figure 5-16 pose yet another constraint on the life span of the generator, the bolus width which limits the accuracy of constant-activity elutions. Fortunately, these constraints do not contradict each other. As the Sr isotopes migrate along the tin-oxide column they not only increase the risk of Sr breakthrough, but also make constant-activity elution harder to achieve.

### **5.8 Benefits of $^{82}\text{Rb}$ Constant-Activity Elutions**

Since this project was started, the RbES has been used in several studies which are in their initial phase. Some of the relevant initial results are included here to demonstrate the benefits of the constant-activity rate  $^{82}\text{Rb}$  elutions. All the studies mentioned within have been conducted with approval of the University of Ottawa Heart Institute Research Ethics Board.

#### ***Comparison of $^{82}\text{Rb}$ and $^{13}\text{N}$ -ammonia for Measurement of Perfusion in 3D PET***

With the RbES capable of producing constant-activity elutions, one can address the larger issue: “Do constant-activity elutions of  $^{82}\text{Rb}$  enable perfusion measurements with similar quality to those obtained using  $^{13}\text{N}$ -ammonia?” Although this question is not addressed fully within the scope of this work, some indication can be seen from preliminary results of ongoing studies using the RbES.

Of the patients that underwent  $^{82}\text{Rb}$  perfusion scans at the UOHI Cardiac PET Center, 14 subjects participated in a comparative study of  $^{82}\text{Rb}$  and  $^{13}\text{N}$ -ammonia perfusion measurement. These (normal) volunteers have low risk of cardiac disease and were scanned

using both tracers and under similar conditions of rest and dipyridamole induced stress of the heart. Dipyridamole increases myocardial blood flow through dilation of the coronary arteries. The study is planned to continue with additional normal volunteers, as well as subjects with coronary artery disease (CAD).

As the tracer is introduced to the patient through an injection into the hand, it passes through the right ventricle of the heart, the lungs, and to the left ventricle of the heart. Dynamic imaging of the left ventricle blood cavity allows measurement of the blood activity before significant tracer uptake is experienced in the myocardium. If the blood activity curves in the LV cavity using both tracers have a similar shape it can be concluded that the tracers were introduced at a similar rate and that the subsequent perfusion measurement is conducted under similar conditions for both tracers.

The subjects were scanned on two occasions less than two weeks apart. On each occasion either a <sup>13</sup>N-ammonia or <sup>82</sup>Rb (constant-activity using HC-TC) perfusion scan was conducted under rest and stress condition. In total, four scans were performed on each patient with 220 MBq introduced over 30 s. The studies were performed with a Siemens/CTI ART 3D scanner using a dynamic protocol with time frames as shown in Table 5-6. The <sup>13</sup>N-ammonia acquisition was over a longer time since the slower decay permits longer uptake measurements.

**Table 5-6 - Dynamic scan time frame durations for <sup>82</sup>Rb and <sup>13</sup>N-ammonia perfusion measurements.**

	<sup>82</sup> Rb dynamic scan time frames	<sup>13</sup> N-ammonia dynamic scan time frames
	12 x 10 s	12 x 10 s
	2 x 30 s	2 x 30 s
	1 x 60 s	1 x 60 s
	1 x 120 s	1 x 120 s
	1 x 240 s	1 x 240 s
		2 x 300 s
Total Scan Time	10 min	20 min

Figure 5-17 gives results from a representative study, showing a comparison of blood activity vs. time curves under both rest (left) and stress (right) conditions. The curves are shift corrected to minimize the mean-squared-error and are corrected for the activity decay of each tracer. In addition, the curves are normalized by the peak activity. The blood curves in this case are similar in shape and magnitude.

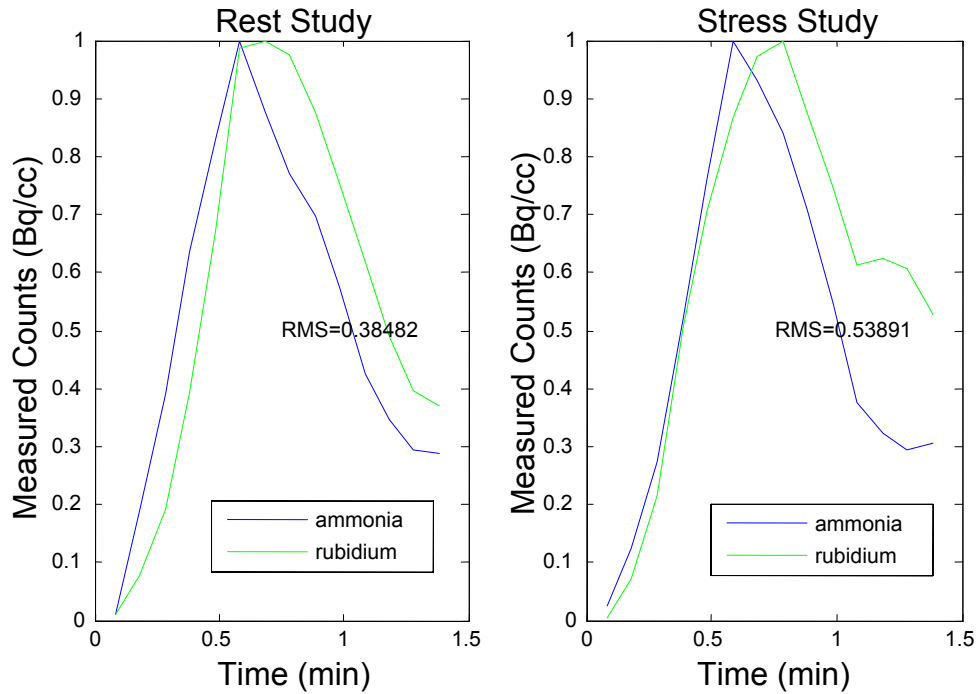


**Figure 5-17 – Representative graph of  $^{82}\text{Rb}$  and  $^{13}\text{N}$ -ammonia activity concentration in the blood over time for the same patient show similar curves. Left is under rest condition, while Right is under dipyridamole induced stress condition.**

The variation in blood activity vs. time curve shapes using constant-activity  $^{82}\text{Rb}$  is similar to intra-patient variations for repeated ammonia studies. The key benefit appears to be that the intra-patient blood activity curve with constant-activity  $^{82}\text{Rb}$  studies is less variable than with constant-time elutions. The reason is that the activity rate profiles using constant-activity elution are similar regardless of the generator age.

### *Optimized Perfusion Measurements*

A second study being performed at UOHI aimed to create more controlled experimental conditions by performing the studies in dogs. PET images of dogs are higher quality than those of humans as the small tissue mass introduces less attenuation and scatter. The entire procedure is carried out with the dog under full anaesthesia and respiratory monitoring. As with the human study, perfusion scans were conducted under rest and dipyridamole induced stress condition using constant-activity  $^{82}\text{Rb}$ .

During a rest study the activity (40-300 MBq) and the duration (15-240 s) of the PCC-PWM elutions were varied in order to assess the variation in perfusion measurements. If the tracer kinetic model is accurate, one would expect similar perfusion measurements

regardless of these parameters. The results in Table 5-7 confirm this expectation as the standard deviation in perfusion measurements (average across entire LV) is 8.1%. These results are well within range of typical test-retest variability (~15%) using constant-time elutions.

Variable Activity (time = 30 s)			Variable Time (Activity = 150 MBq)	
Activity (MBq)	Relative Activity	Median Perfusion (ml/min/g) [n=2x576]	Time (s)	Median Perfusion (ml/min/g) [n=2x576]
40	9.1%	0.57	15	0.68
75	17.0%	0.60	30	0.63
150	34.0%	0.64	60	0.60
300	68.0%	0.64	120	0.59
			240	0.67

**Table 5-7 – Rest study results comparing perfusion measurements in a dog at varied <sup>82</sup>Rb constant-activity elution time durations and activities show that similar results are obtained regardless of these elution parameters.**

### 5.9 Critical Analysis and Future work

Although experience with the system instilled confidence in its design, the self-tuning algorithm seems to be the potential weak point in the entire PCC-PWM control concept. The main concern is that repeated elutions at a given relative activity rate may result in model parameters that are not suited to other relative activity rates. While there is no evidence to suggest that this is the case, the system has not been used over a long period needed to reach a firm conclusion. Several alternatives to the self-tuning algorithm may be considered in the future:

1. Abandoning the PCC-PWM algorithm in favour of the simpler but less precise threshold comparison algorithm.
2. Removal of the self-tuning algorithm, leaving maintenance of the model parameters at the hands of the operators.
3. Continued research into development of an improved model and tuning algorithm.
4. Seeking of a variable flow ratio valve that better meets the requirements for this problem. Namely the valve must be fast, robust, accurate, and simple to integrate with the system.

Of these options, a decision for future steps must be made based on various considerations and how they are weighed. If precision is a crucial factor, reverting to the threshold comparison controller is unacceptable as the comparison of the two approaches clearly indicates that the PCC-PWM has more desirable characteristics. Whether or not precision is crucial remains to be determined as the comparative perfusion study continues.

Replacing the self-tuning algorithm with free parameters that can be set by the operator is an unlikely option, as this would entail thorough understanding of the system by the technologists. A poor selection of model parameters could result in undesirable activity profiles.

In order to improve precision while maintaining complete automatic tuning of the system, it is most likely that further research is required. First and foremost this research would need to better assess the automatic-tuning performance of the current implementation. Part of this assessment should be selection of the learning parameters  $\gamma_L$ ,  $\gamma_G$ , and  $\gamma_R$  to improve the learning rate while maintaining a reasonable immunity to abnormal elution results. Further experience with the existing system will indicate if additional development is required, and would also serve as a benchmark to which other improvements could be compared.

Other models and tuning techniques could also be considered. Further research could look at a model that better describes the valve response than the sigmoid-linear model does. Alternatively, a simpler model that can be tuned with fewer parameters (even if less characteristic of the true response) can be sought. Since the desired flow ratios typically fall within the 25-100% range, there is no need to model the entire dynamic range of the valve.

A final possibility is searching for or developing a valve that can accurately control the valve flow ratio directly. If this were the case, modeling and tuning of the valve response could possibly be avoided or simplified. Such a valve would require a fast response time enabling to fully open and close within a fraction of a second. In addition, the valve would have to be sufficiently precise so that fine changes in flow ratio could be generated. Finally the valve would have to be simple enough in design so as to ensure a high degree of reliability while making integration into the current system easily achievable.

Of these considerations it seems that the most benefit could be gained for the least effort by reevaluating the range of readily available flow control valves. However, if an alternative to the current two-way pinch valve is still not feasible, it appears that further research and development of the valve response model and its self-tuning algorithm is the most promising route for future improvement of the RbES.

## Chapter 6: Conclusion

This thesis describes the development of the  $^{82}\text{Rb}$  Elution System (RbES) as a complete system to automatically administer precise amounts of  $^{82}\text{Rb}$  activity from a  $^{82}\text{Sr}/^{82}\text{Rb}$  generator for use as a perfusion tracer in PET. This work describes the system hardware, which for the most part was handed down from previous work [18,20], and the complete development of the software. Much of the work focuses on development of a control system that can directly administer a constant rate of activity to the patient despite variation in activity concentration from the  $^{82}\text{Sr}/^{82}\text{Rb}$  generator as a function of time and eluted volume.

Analysis of the system model is based on comparison to an external dose calibrator. Both calibration results and elution tests confirm that the system model is sufficiently accurate for predicting the activity delivered to the patient based on the on-board positron counter readings. This result is important not only to patient safety but also to system precision.

The RbES has matured to the point where it can be routinely used in clinical studies. This is reflected both by meeting of the design requirements, behaviour verification, and system characterization. The testing includes not only functionality of the system under ordinary conditions, but also in abnormal situations. The system is sufficiently automated that no user intervention other than monitoring is required during an elution process.

Constant-activity elutions are implemented by controlling saline flow through the generator or its bypass line (using an on/off solenoid valve) using two methods, which are compared in chapter 5. The first method, hysteresis corrected threshold comparison (HC-TC), modifies the previously published threshold comparison method [18] by correcting for valve hysteresis. The second method cycles the solenoid valve and modulates the pulse-width (PWM) in order to simulate a variable flow valve. A predictive-corrective control (PCC) algorithm determines the desired flow ratio through the valve, which a valve response model translates to a corresponding pulse-width.

The measured results demonstrate that the RbES using PCC-PWM can dramatically improve the precision of constant-activity elutions over HC-TC if the valve response model

is properly tuned. This is noted in the reduction of RMS error, as well as in reduction of performance variability as the requested elution parameters change. However, this work does not clearly determine if the proposed self-tuning algorithm is reliably effective during routine clinical use. A clinical setting entails routine use of the system as desired by the clinical application and does not include ad-hoc training sessions intended for tuning of the valve response model. In this work, the training sessions span the entire dynamic range of achievable relative activities forcing the self-tuning algorithm to converge to global nominal values without biasing towards a specific range of relative activities. The risk of biasing the model parameters is very real in a clinical setting as repeated elutions within a limited relative activity range are likely.

Future work should focus on assessing long term reliability of the current implementation. In particular the focus should be on the performance of the self-tuning algorithm proposed in this work as well as potential alternatives. In addition, the sigmoid-linear model used to describe the valve response may prove to be overly complicated with too many degrees of freedom. However, the need for a valve response model and self-tuning algorithm may be completely avoided by seeking or developing a more suitable flow ratio control mechanism. For example, a new valve may be found with linear response. If it is also fast acting, simple to integrate and cost effective the problem can be significantly simplified. For this reason, it is the recommendation of the author that a first step to future improvement be research into a possible replacement for the generator valve that exhibits faster transition response than the current model.

Additional work should concentrate of preparing the system for distribution to external facilities by improving robustness and protection of intellectual property. This would include transporting the software to a proven real-time operating system in place of Microsoft Windows 98. In addition, the software should be compiled to binary code, which would both hide the source code and simplify the system. Byte code would eliminate the use of both the virtual machine and interpreter in the current application; thus reducing the consumption of computer resources, and potentially improving the robustness of the system. In contrast, the current market does not seem to justify the development of new hardware components, confirming the decision to utilize off-the-shelf components.

Current theories suggest that constant-activity elutions may indeed have a favourable effect on quantitative perfusion measurement using PET. Preliminary studies at UOHI in a dog demonstrate that similar measurements are obtained regardless of the amount of tracer activity and elution duration in this mode. In a second experiment comparing  $^{13}\text{N}$ -ammonia and  $^{82}\text{Rb}$  as perfusion tracers in humans (both introduced at constant-activity rates), preliminary results indicate that there is no significant difference in quantitative perfusion measurements obtained using either tracer. If these results are confirmed through future work, constant-activity  $^{82}\text{Rb}$  elutions may serve as a cost effective alternative to  $^{13}\text{N}$ -ammonia for quantitative perfusion measurement using PET, which could offer cheaper state-of-the-art diagnosis to a wider population.

---

## List of References

---

1. S. R. Bergmann, B. E. Sobel, "Positron Emission Tomography of the Heart", Futura Publishing Inc., 1992.
2. I. Koike, M. Ohmura, M. Hata, N. Takahashi, T. Oka, I. Ogino, J. Lee, T. Umezawa, K. Kinbara, K. Watai, Y. Ozawa, T. Inoue, "FDG-PET scanning after radiation can predict tumor regrowth three months later", *Int. J. of Radiation Oncology Biology Physics*, Vol. 57, No. 5, p 1231-1238, 2003.
3. J. N. Talbot, Y. Petegnief, K. Kerrou, F. Montravers, D. Grahek, N. Younsi, "Positron emission tomography with [<sup>18</sup>F]-FDG in oncology", *Nucl. Inst. and Meth. in Phys. Res., Section A: Accelerators, Spectrometers, Detectors and Associated Equipment*, Vol 504, No. 1-3, pp. 129-138, 2003.
4. K. Mah, C. B. Caldwell, Y. C. Ung, C. E. Danjoux, J. M. Balogh, S. N. Ganguli, L. E. Ehrlich, R. Tirona, "The impact of <sup>18</sup> FDG-PET on target and critical organs in CT-based treatment planning of patients with poorly defined non-small-cell lung carcinoma: a prospective study", *Int. J. of Radiation Oncology Biology Physics*, Vol. 52, No. 2, pp. 339-350, 2002.
5. R. S. Beanlands, "Positron emission tomography in cardiovascular disease", *Can. J. Cardiology*, Vol. 12, No. 10, pp. 875-883, 1996.
6. M. R. Costanzo, S. Augustine, R. Bourge, et al., "Selection and treatment of candidates for heart transplants", *Circulation*, Vol. 92, pp. 3593-612, 1995.
7. H. Schelbert, R. Bonow, E. Geltman, J. Maddahi, M. Schwaiger, "Position statement. Clinical use of cardiac positron emission tomography", Position paper of the Cardiovascular Council of the Society of nuclear Medicine., *J. Nucl. Med.*, Vol. 34, pp. 1385-8, 1993.
8. K. Baete, J. Nuyts, W. Van Paesschen, P. Suetens, P. Dupont, "Anatomical-based FDG-PET reconstruction for the detection of hypo-metabolic regions in epilepsy", *IEEE Trans. on Med. Imag.*, Vol 23, No. 4, pp. 510-519, 2004.

9. J. S. Lee, D. S. Loo, S. K. Kim, S. K. Lee, J. K. Chung, M. C. Chul, K. S. Park, "Localization of epileptogenic zones in F-18 FDG brain PET of patients with temporal lobe epilepsy using artificial neural network" IEEE Trans. on Med. Imag., Vol. 19, No. 4, Apr, pp. 347-355, 2000.
10. C. K. Yen, Y. Yano, T. F. Budinger, R. P. Friedland, S. E. Derenzo, R. H. Huesman, H. A. O'Brien, "Brain tumor evaluation using Rb-82 and positron emission tomography", J. Nucl. Med., 23(6), pp. 532-537, 1982.
11. T. Jones, "Clinical Uses of  $^{82}\text{Sr}/^{82}\text{Rb}$  Generators", Appl. Radiat. and Isot., Vol 38, No 3, pp. 171-173, 1987.
12. R. D. Finn, D. J. Schyler, "Production of Radionuclides for PET, Principals and Practice of Positron Emission Tomography", Lippincott Williams and Wilkins, p1:15, 2002.
13. M. A. Green, "The potential for generator-based PET perfusion tracers", J. Nucl. Med., Vol 31(10), pp. 1641-1645, 1999.
14. M. R. Cackette, T.J. Ruth, J.S. Vincent, " $^{82}\text{Sr}$  production from metallic Rb targets and development of an  $^{82}\text{Rb}$  generator system", Appl. Radiat. Isot., Vol. 44, No. 6, pp. 917-922, 1993.
15. Y. Yano T. F. Budinger, G. Chiange, H. A. O'Brien, P. M. Grant, "Evaluation and application of alumina-based Rb-82 generators charged with high levels of Sr-82/85", J. Nucl. Med., Vol 20, pp. 961-966, 1979.
16. Y. Yano, "Essentials of a Rubidium-82 generator for nuclear medicine", Appl. Radiat. Isot., Vol 38, No 3, pp. 205-211, 1987.
17. V. Dhawan, "Model for  $^{82}\text{Sr}/^{82}\text{Rb}$  generator elution profiles: A second approach to radiodosimetry", Appl. Radiat. Isot., Vol. 38, No. 3, pp. 233-239, 1987.
18. N. J. Epstein, A. Benelfassi, R. S. Beanlands, R. A. deKemp, "A  $^{82}\text{Rb}$  infusion system for quantitative perfusion imaging in 3D PET", App. Radiat. Isot, Vol. 60, pp. 921-7, 2004.

19. G. P. Gennaro, B. C. Bergner, P. S. Haney, R. H. Kramer, M. D. Loberg, "Radioanalysis of  $^{82}\text{Rb}$  Generator Eluates", *Appl. Radiat. and Isot.*, Vol 38, No 3, pp. 219-225, 1987.
20. N. J. Epsein, "Modeling and simulation of a rubidium-82 infusion system", Internal document at University of Ottawa Heart Institute Cardiac PET Unit, August 2001.
21. K. L. Gould, "PET perfusion imaging and nuclear cardiology", *J. Nucl. Med.*, Vol.32, pp. 579-606, 1991.
22. L. Golanowski, R. A. deKemp, R. S. Beanlands, T. D. Ruddy 2000, "Variance and covariance of  $^{82}\text{Rb}$  kinetic parameters: computed simulations and dynamic PET studies", *Proceeding of the 22<sup>nd</sup> annual EMBS International Conference*, pp. 1096-99, 2000.
23. W. J. Lin, R. R. Sciacca, R. L. Chou, A. F. Laine, S. R. Bergmann, "Quantification of perfusion in human subjects using  $^{82}\text{Rb}$  and wavelet-based noise reduction", *J. Nucl. Med.*, Vol 42, pp. 201-208, 2001.
24. K. Yoshida, N. Mullani, K. L. Gould, "Coronary flow and flow reserve by PET simplified for clinical applications using rubidium-82 or nitrogen-13-ammonia", *J. Nucl. Med.*, Vol 37, pp. 1701-1712, 1996.
25. M. L. Beauchesne, T. D. Ruddy, R. A. deKemp, M. T. Aung, N. Levesque, T. Alvarez-Diez, T. K. Vickers, B. A. Aubrey, R. S. B. Beanlands, "Reproducibility of myocardial perfusion measurements with rubidium-82 PET imaging", *abstract Circulation* 98, I-222, 1998.
26. R. A. deKemp, T. D. Ruddy, T. Hewitt, M. M. Dalipaj, R. S. B. Beanlands, "Detection of serial changes in absolute myocardial perfusion with  $^{82}\text{Rb}$  PET", *J. Nucl. Med.*, Vol 41, pp. 1426-1435, 2000.
27. R. R. Raylman, J. M. Caraher, G. D. Hutchins, "Sampling requirements for dynamic cardiac PET studies using image-derived input functions", *J. Nucl. Med.* Vol 34, pp. 440-447, 1993.
28. D. L. Bailey, H. Young, P. M. Bloomfield, S. R. Meikle, D. Glass, M. J. Myers, T. J. Spinks, C. C. Watson, P. Luk, A. M. Peters, T. Jones, "ECAT – ART a continuously

- rotating PET camera: performance characteristics, initial clinical studies, and installation considerations in a nuclear medicine department”, *Eur. J. Nucl. Med.*, Vol 24(1), pp. 6-15, 1997.
29. Y. Yano, J. L. Cahoon, T. F. Budinger, “Precision flow-controlled Rb-82 generator for bolus or constant-infusion studies of the heart and brain”, *J. Nucl. Med.*, Vol 22:11, pp. 1006-1010, 1981.
  30. T. M. Alvarez-Diez, R. A. deKemp, R. S. Beanlands, J. Vincent, “Manufacture of strontium-82/rubidium-82 generators and quality control of rubidium-82 chloride for myocardial perfusion imaging in patients using positron emission tomography”, *Appl. Radiat. Isot.*, Vol. 50, pp. 1015-1023, 1999.
  31. G. F. Knoll, “Radiation detection and measurement”, Second Edition, 1989 by John Wiley and Sons, Inc. ISBN 0-471-81504-7.
  32. Matlab 6.5.1 User Manual: Real-Time Windows Target: Introduction: Real-Time Kernel.
  33. A. P. Johnson, M. W. S. Macauley, “High precision timing within Microsoft Windows: Threads, scheduling and system interrupts”, *Microprocessors and Microsystems*, Vol 25, No 6, pp. 297-307, 2001.
  34. University of Ottawa Heart Institute Investigator’s Report, 2003
  35. Capintec CRC-15R User Manual, Capintec Inc.
  36. “The American Heritage Dictionary of the English Language”, 3<sup>rd</sup> Edition, 1992 by Houghton Mifflin Company. Provided through Microsoft Bookshelf, 1999.
  37. T. Imaizumi, O. Oyama, Yoshimitsu T., “Study of pneumatic servo system employing solenoid valve instead of proportional valve by keeping the solenoid valve plunger to be floating”, *Flucom Symposium Proceedings*, article 076, 2000.
  38. E. Kreyszig, “Advanced engineering mathematics” 8<sup>th</sup> edition, 1999, by John Wiley and Sons, Inc. ISBN 0-471-15496-2.
  39. K. J. Astrom, B. Wittenmark, “Adaptive Control”, 2<sup>nd</sup> edition, Addison Wesley, 1995.
  40. K. S. Narendra, A. M. Annaswamy, “Stable Adaptive Systems”, Prentice Hall, 1989.

## Appendix A: Test Cases

Merge into here the report from the TestList Database.